Subsurface geology and oil and gas potential of Estancia Basin, New Mexico

This book is dedicated
to the memory of
Lucille Pipkin,
pioneering New Mexico
oil woman and gracious benefactor
of geology students
and to
Arthur L. Bowsher,
petroleum geologist extraordinaire.

Bulletin 157

New Mexico Bureau of Mines & Mineral Resources

A DIVISION OF
NEW MEXICO INSTITUTE OF MINING & TECHNOLOGY

Subsurface geology and oil and gas potential of Estancia Basin, New Mexico

by Ronald F. Broadhead
New Mexico Bureau of Mines and Mineral Resources, Socorro, New Mexico 87801

SOCORRO 1997

Original Printing

Published by Authority of State of New Mexico, NMSA 1953 Sec. 63-1-4
Printed by University of New Mexico Printing Services, June 1997

Available from New Mexico Bureau of Mines & Mineral Resources, Socorro, NM 87801 Published as public domain, therefore reproducible without permission. Source credit requested.

Contents

Tables

Figures

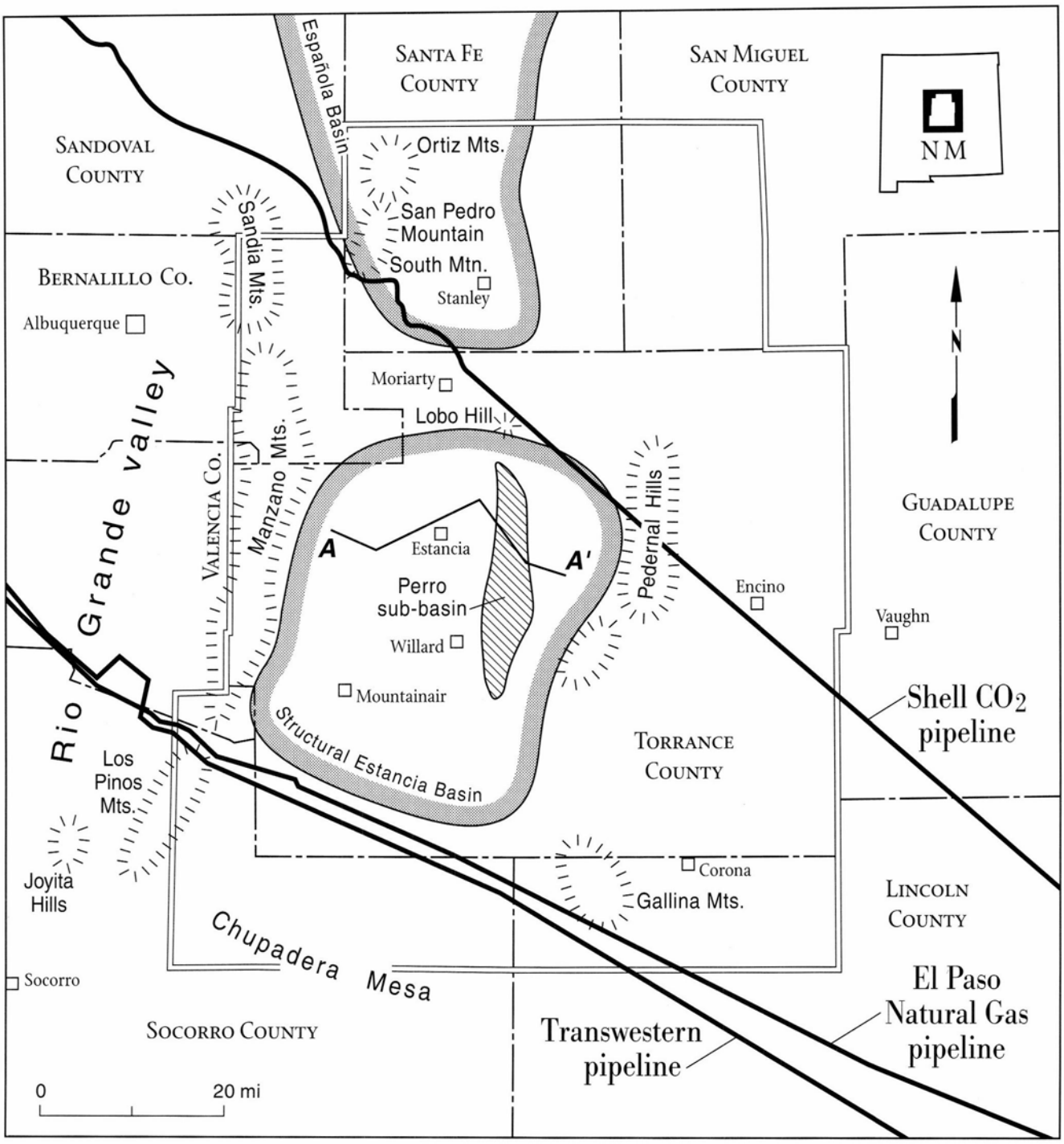

FIGURE 1—Location of Estancia Basin and bordering geomorphic elements, central New Mexico, and natural gas pipelines that cross the basin.

Abstract

The Estancia Basin of central New Mexico is an asymmetric, north—south-trending structural depression that originated during the Pennsylvanian. The present-day basin covers 1,500 mi^2 and is defined approximately by the Estancia Valley. It is bounded on the east by the late Paleozoic Pedernal uplift, on the west by the Tertiary-age Sandia, Manzano, and Los Pinos Mountains, on the north by the Española Basin, and on the south by Chupadera Mesa. Depth to Precambrian basement ranges from more than 8,500 ft in a narrow graben (Perro sub-basin) in the eastern part of the basin to less than 1,000 ft on a shelf to the west.

Basin fill consists primarily of Pennsylvanian and Wolfcampian sandstones and shales in the Perro sub-basin and sandstones, shales, and marine limestones on the shelf. In the Perro sub-basin, reservoirs are fine- to coarse-grained sandstones with relatively low permeabilities and porosities. On the shelf, reservoirs are mostly fine- to coarse-grained sandstones with porosities that range from 0 to 16% and average approximately 10%. Most limestones on the shelf have less than 5% porosity and are poor reservoirs; however, algal grainstones and recrystallized lime mudstones appear locally to form good reservoirs with porosities that can exceed 20%.

Mature to marginally mature dark-gray to black Pennsylvanian shales are probable source rocks. Thermal Alteration Index ranges from 2.0 to 3.2. Shales become thermally mature with depth in the Perro sub-basin. On the western shelf, shales become mature to the west as a result of increased heating from the Rio Grande rift. Total organic carbon exceeds 0.5% in many shales, sufficient for hydrocarbon generation. Kerogen types are mixed algal, herbaceous, and woody, indicating that gas, or possibly gas mixed with oil, was generated. Kerogens in the shales of the Perro sub-basin are entirely woody, gas-prone types. In limestones and shales of the western shelf, kerogens have mixed marine and continental provenance, indicating that both oil and gas may have been generated on thermally mature parts of the shelf.

Forty-three exploratory wells have been drilled in the basin. Only 17 of those wells have been drilled to Precambrian. Density of wells that penetrate the lowermost Pennsylvanian is less than one well for every three townships. Most of the wells were drilled before 1950 and lacked modern logs and testing apparatus with which to evaluate fully the drilled section. In spite of this, numerous shows of oil and gas have been reported; many of these shows are well documented by modern logs and tests, especially from wells drilled since 1970. During the 1930s and 1940s, carbon dioxide gas was produced commercially from two small fields on the western flank of the basin.

Introduction

The Estancia Basin of central New Mexico (Fig. 1) is a structural depression that initially developed during Early Pennsylvanian (Morrowan) time. The present-day structural basin covers 1,500 mi^2 and is defined by the Estancia Valley. It is bounded on the east by the late Paleozoic Pedernal uplift and on the west by the Sandia, Manzano, and Los Pinos Mountains. The Lobo Hill structure separates it from the Espanola Basin to the north. The Estancia Basin merges gradationally southward with Chupadera Mesa, a topographic upland that was a shallow shelf during the Pennsylvanian. Depth to Precambrian ranges from less than 1,000 ft on the western flank of the basin to more than 8,500 ft near the town of Willard in the eastern part of the basin.

Surface elevation of the Estancia Valley ranges from 6,100 ft to 6,400 ft. To the east Pedernal Peak is 7,580 ft. On the west, Manzano Peak is 10,120 ft. The crest of the Manzano and Sandia Mountains exceeds 9,000 ft in most places.

The Estancia Basin contains a Precambrian igneous and metamorphic basement complex overlain by sedimentary rocks of Pennsylvanian, Permian, Triassic, and Quaternary age. Pre-Pennsylvanian Paleozoic strata have not been reported in the subsurface. Strata exposed at the surface are mostly Pennsylvanian, Lower Permian, and Quaternary. Middle Permian and Triassic strata are present only as erosional remnants in the basin (Figs. 2, 3). The Upper Cretaceous section has been removed by Laramide and/or post-Laramide erosion. Major structural development of the basin occurred from Morrowan (Early Pennsylvanian) through Wolfcampian (Early Permian) time, but the present western, northern, and southern boundaries of the basin were defined by Laramide uplift and middle to late Tertiary uplift associated with development of the Rio Grande rift.

The Estancia Basin is a frontier exploration area that has not produced oil and hydrocarbon gases to date. Carbon dioxide (CO2) gas was produced commercially from Lower Pennsylvanian sandstones in two small fields west of the town of Estancia during the 1930s and 1940s. A total of 43 exploration wells have been drilled in the basin; 155 wells have been drilled in the area covered by this report (Fig. 4; Table 1, in appendix). Only 17 of the 43 wells in the basin have been drilled to Precambrian basement. Density of wells that penetrate the lowermost Pennsylvanian is less than one well for every three townships. Many of the wells were drilled before 1950, have no geophysical logs, and did not test reported shows. The only information on these wells are drilling records and/or drill cuttings. Without a suite of modern logs and without adequate tests of reported shows, these wells represent an incomplete evaluation of the section they penetrated. Therefore, the effective drilling density of the basin is significantly less than one well for every three townships.

The purpose of this report is to describe and analyze the subsurface structure and stratigraphy of the Estancia Basin for purposes of characterizing reservoirs, source rocks, and hydrocarbon occurrences. Most data used in the study are from petroleum exploration wells. Structural analyses were synthesized from drill-hole data, reflection seismic profiles, gravity and aeromagnetic maps, and published surface geologic maps. Data relating to stratigraphy and reservoirs were obtained from geophysical logs, drill cuttings, scout reports, and descriptions of drill cuttings on file at the New Mexico

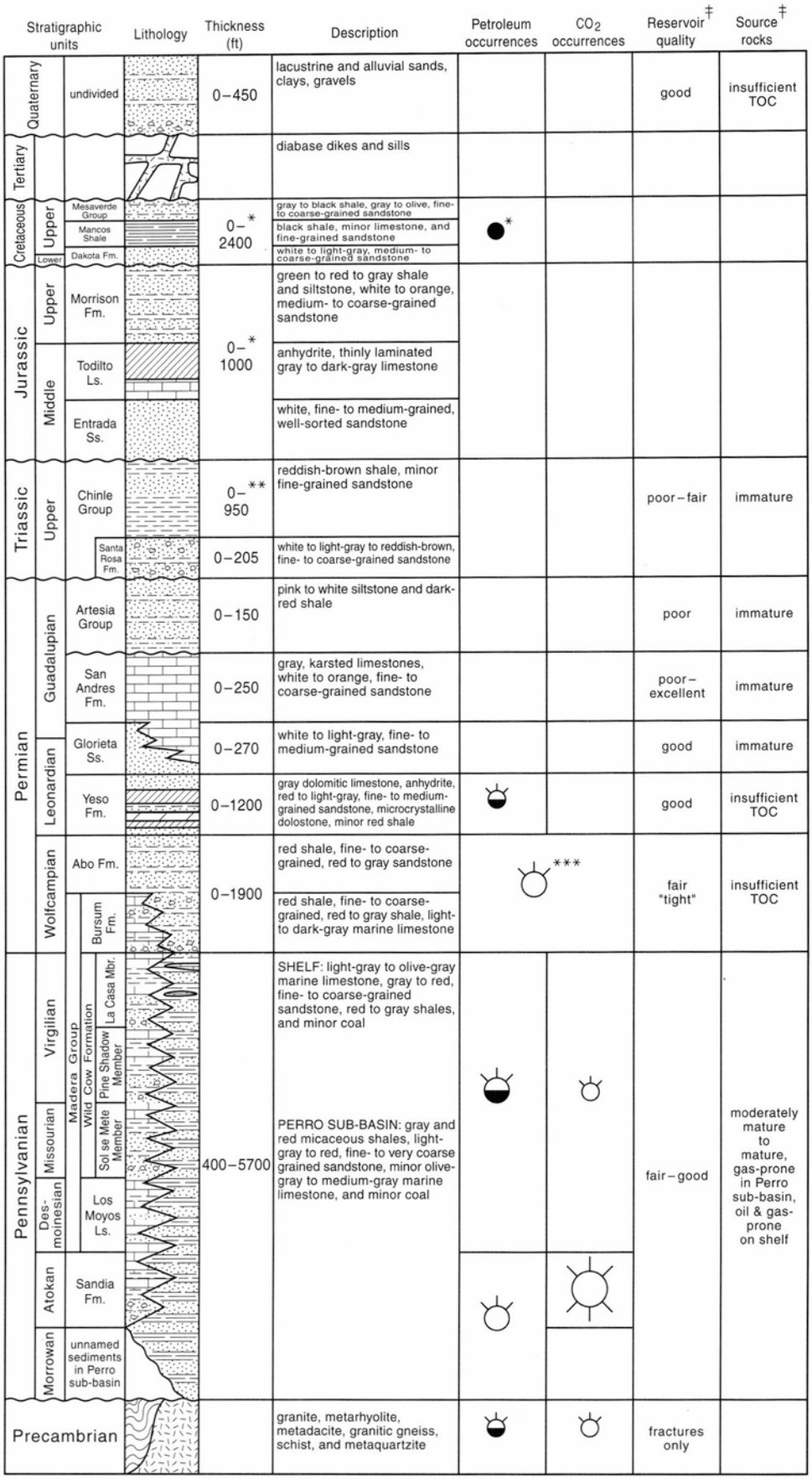

FIGURE 2—Stratigraphic chart of Phanerozoic sedimentary units in the Estancia Basin and summary of hydrocarbon occurrences, reservoir quality, and petroleum potential.

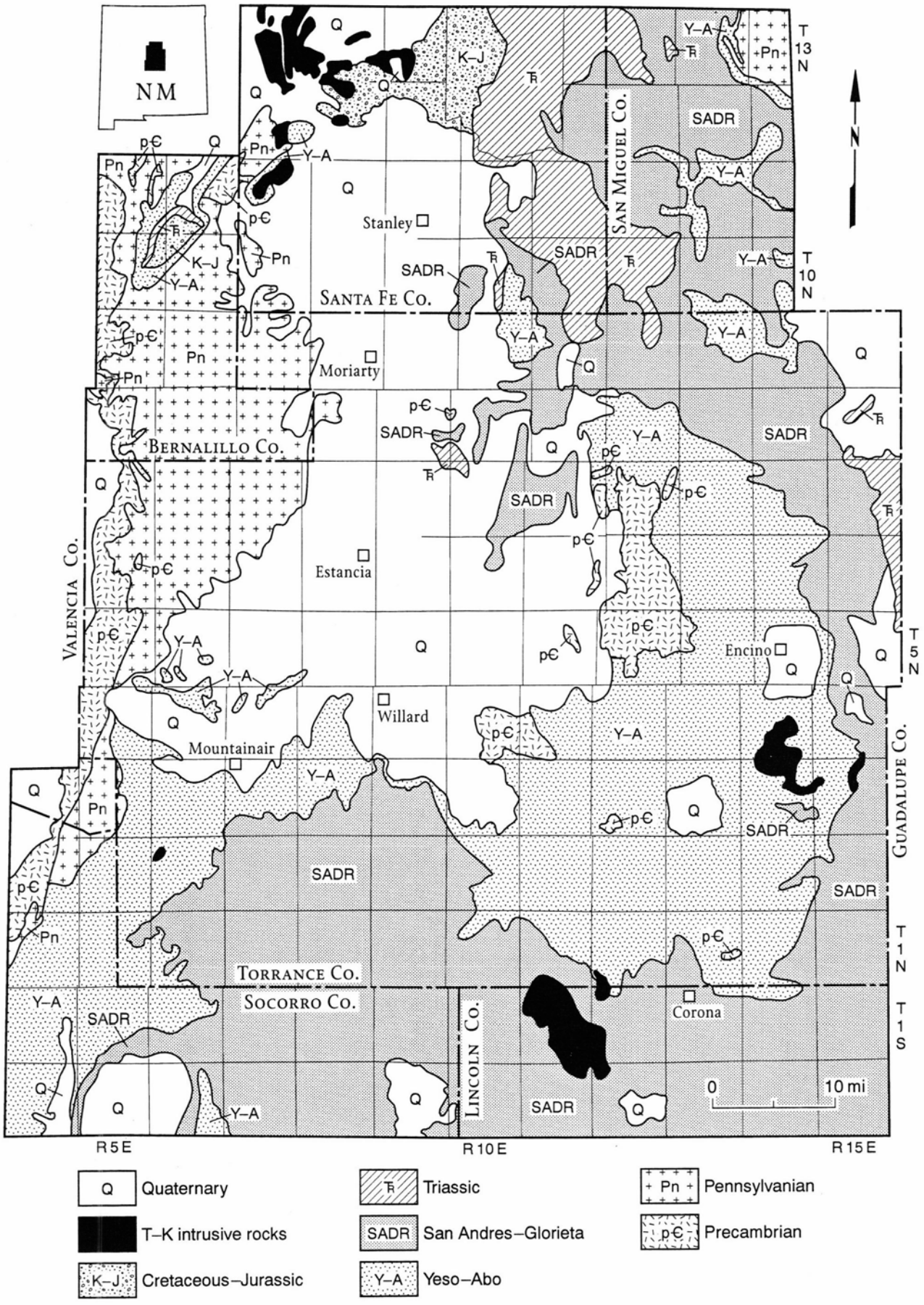

FIGURE 3—Generalized surficial geologic map of Estancia Basin area. Simplified from Dane and Bachman (1965). Outcrop patterns of Precambrian and Cretaceous–Tertiary intrusives simplified compared to Figs. 5, 6, 10, and 13.

Bureau of Mines and Mineral Resources.

Acknowledgments—Charles E. Chapin, Director of the New Mexico Bureau of Mines and Mineral Resources and State Geologist of New Mexico supported this study. Ben Donegan, George Scott, Shari Kelley, Randy Keller, and Charles Chapin offered stimulating discussion and shared their extensive knowledge of the Estancia Basin. Paul Bauer graciously provided descriptions of cores of Precambrian rocks from the Pedernal Hills. Jack Ahlen, Charles Chapin, and Frank Kottlowski reviewed the manuscript and provided helpful insight into its preparation. Jane Love and Nancy Gilson edited the manuscript. Lynne Hemenway and Terry Telles provided word processing. Rebecca Titus drafted the illustrations.

Structure

The Estancia Basin (Fig. 1) is an asymmetric structural depression that has existed as a depositional basin from Morrowan (Early Pennsylvanian) through Recent time. The basin has undergone three major stages of tectonic deformation (Chapin, 1971; Chapin and Cather, 1981; Beck and Chapin, 1991, 1994; Barrow and Keller, 1994; Broadhead, 1994): 1) late Paleozoic (Pennsylvanian-Early Permian) deformation associated with formation of the ancestral Rocky Mountains; 2) Laramide deformation from the Late Cretaceous through the Eocene; and 3) multiphase extensional deformation, beginning in the Oligocene, associated with formation of the Rio Grande rift.

The Estancia Basin can be defined as either a structural basin or as a Quaternary depositional basin. The geologic definitions of the structural basin and the Quaternary depositional basin are discussed below. In this report, the Estancia Basin is regarded as a structural basin and not as a Quaternary depositional basin.

The structural Estancia Basin is bordered on its western side by the Sandia, Manzano, and Los Pinos Mountains; these three mountain ranges separate the Estancia Basin from the Albuquerque Basin segment of the Rio Grande rift. The structural basin is bordered on the east by the Pedernal Hills, which are a topographic expression of the Pedernal uplift of the ancestral Rocky Mountains. The Pedernal Hills separate the Estancia Basin from the Rowe-Mora Basin to the east. The northern boundary of the Estancia Basin is defined by a reversal of structural dip at the approximate location of Lobo Hill (Fig. 1). South of this boundary, Paleozoic strata dip into the Estancia Basin. The southern boundary of the structural Estancia Basin is indistinct. The basin merges to the south with Chupadera Mesa between Mountainair and the Socorro-Torrance County line.

The Quaternary depositional Estancia Basin is defined by the areal extent of Quaternary valley-fill sediments within the Estancia Valley (Fig. 3). The Quaternary depositional basin has a larger extent than the structural basin. The northern limit of preservation of Quaternary sediments within the Estancia Valley is approximately 16 mi north of the Torrance-Santa Fe County line and approximately 24 mi north of Lobo Hill, the northern limit of the structural basin. The southern boundary of the depositional basin is defined by the northern edge of Chupadera Mesa. On the east and the west, the boundaries of the depositional basin lie within the confines of the Estancia Valley and the structural basin.

Two structure-contour maps were prepared for this study. One map (Fig. 5) depicts the structure of the top of the Precambrian surface, and the other (Fig. 6) depicts the structure of the top of the Abo Formation (Permian). These maps were prepared using several sources of data. Well data were the primary control for subsurface mapping. Formational (stratigraphic) tops were determined from geophysical logs for wells drilled after approximately 1950; these determinations of formational tops were confirmed with descriptions of drill cuttings. Many of the wells in the basin were drilled before 1950 and consequently have no geophysical logs. When available, descriptions of drill cuttings were used to determine formation tops in these older wells. The presence of varied igneous and metamorphosed sedimentary rocks within the Precambrian made the use of sample logs and drill cuttings especially useful for the determination of the top of the Precambrian.

Surface geologic maps were also used as control for map contouring. Especially important control elements are the major faults and fold axes that have been mapped at the surface (shown as solid lines on Figs. 5, 6). Main sources of map data are Read et al. (1944), Wilpolt et al. (1946), Bates et al. (1947), Kelley (1972), Kelley and Northrop (1975), Titus (1980), and Hawley (1986). Structures in the Sandia, Manzano, and Los Pinos Mountains have been mapped by Reiche (1949), Stark (1956), Myers (1967, 1969, 1977), Myers and McKay (1970, 1971, 1972), and Myers et al. (1981). The Precambrian of the Pedernal Hills has been mapped by several workers, including Gonzales (1968) and Bauer and Williams (1985).

Seismic reflection profiles were indispensable to the construction of the subsurface structure-contour maps. Barrow and Keller (1994) provided an integrated picture of gravity, magnetic, and reflection seismic data within the basin. Of particular importance were the seismic reflection profiles provided to Barrow and Keller by Mobil Exploration and Production. Along with the wells analyzed and correlated for this study, the interpretation of the seismic profiles by Barrow and Keller provide a constrained three-dimensional view of the basin.

Regional aeromagnetic (Fig. 7A) and gravity (Fig. 7B) maps can also be used to define the structure of Precambrian basement in the Estancia Basin. The location of Precambrian outcrops and the location of major basement faults are fairly well defined by the residual aeromagnetic intensity map (Figs. 5, 7A). Particularly well defined is the location of the Pedernal uplift and its distinction from the Estancia Basin to the west and the Rowe-Mora Basin to the east. The Perro sub-basin is apparent but not defined exactly by the aeromagnetic map; well data and seismic data are needed to define its location and geometry exactly, although its presence is indicated by a north-south-trending negative anomaly. The Tertiary intrusions that form the Ortiz and San Pedro Mountains are also readily apparent.

The regional gravity map (Fig. 7B) is not as useful as the aeromagnetic map for defining structure of the Precambrian basement. The general location of the Estancia Basin is apparent, but the Pedernal uplift, the Perro sub-basin, and the Rowe-Mora Basin are poorly

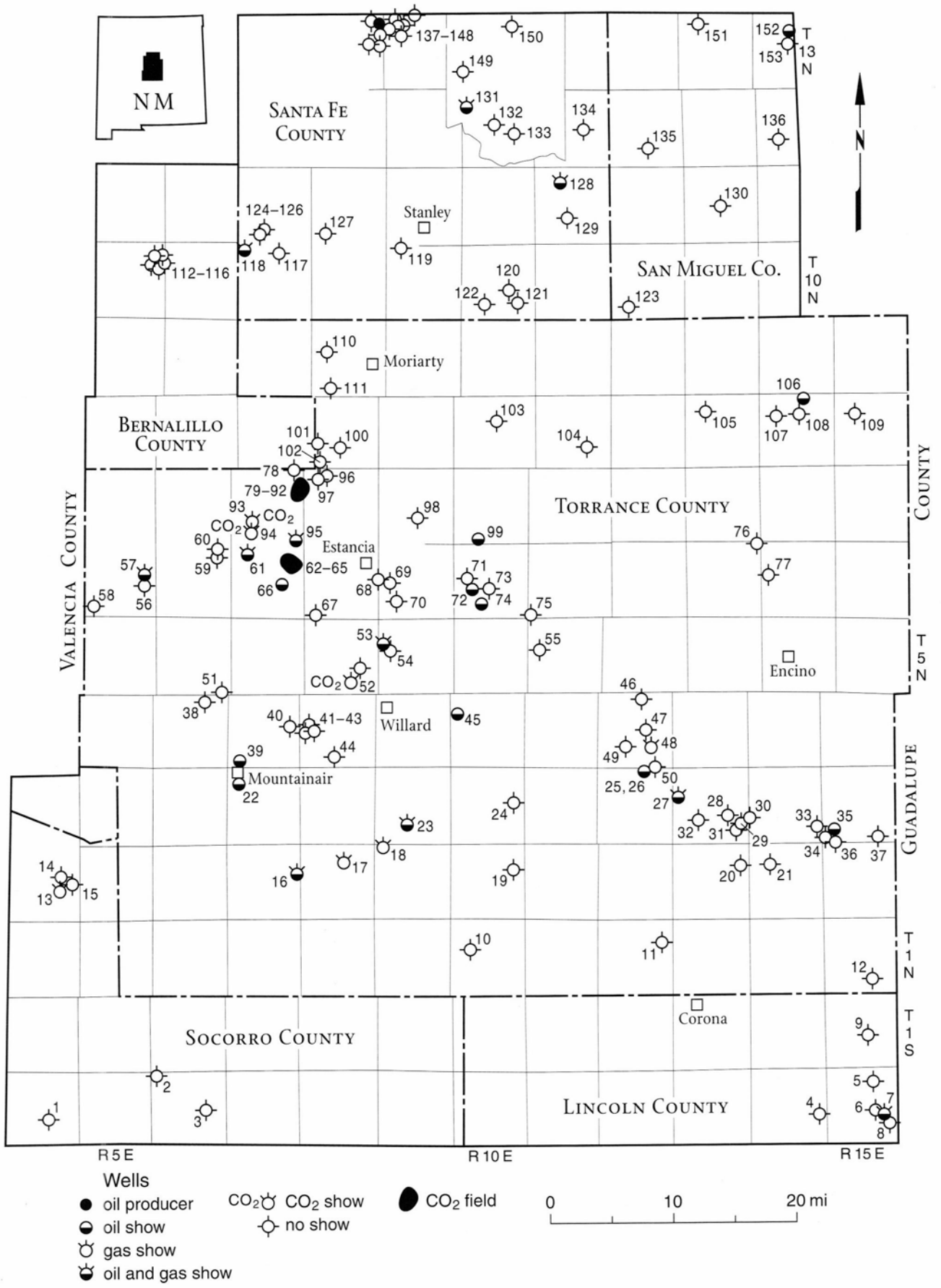

FIGURE 4—Petroleum exploration wells drilled in Estancia Basin and adjoining areas. Numbers correspond with listing in Table 1.

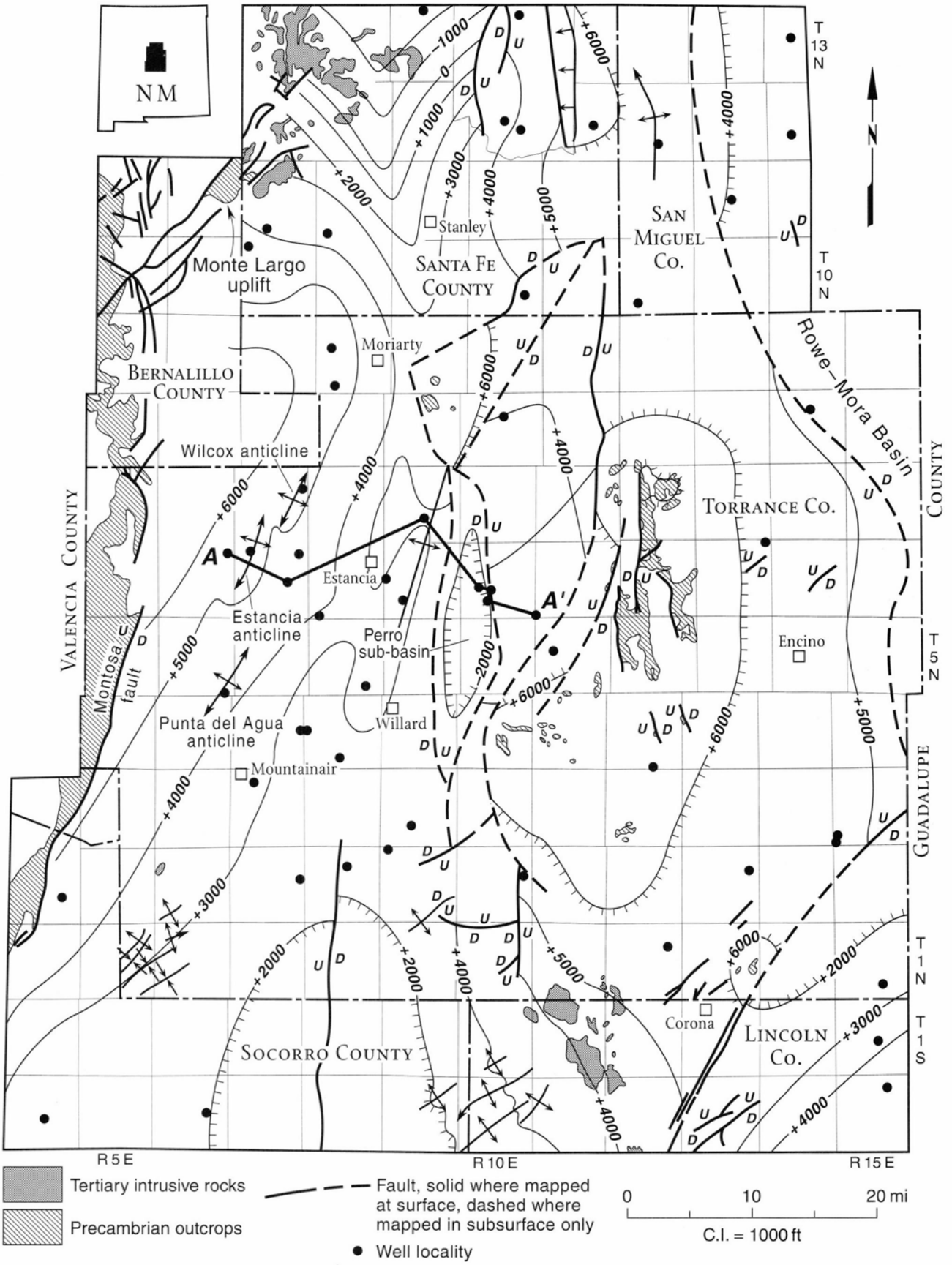

FIGURE 5—Structure-contour map of Precambrian basement, Estancia Basin. See text for discussion of contouring methods. Contour interval is 1,000 ft. Datum is sea level. Outcrops of Precambrian and Tertiary intrusives from Kelley (1972), Wilpolt et al. (1946), Reiche (1949), Stark and Dapples (1946), Myers (1967, 1969, 1977), Myers and McKay (1970, 1971, 1972), and Myers et al. (1981).

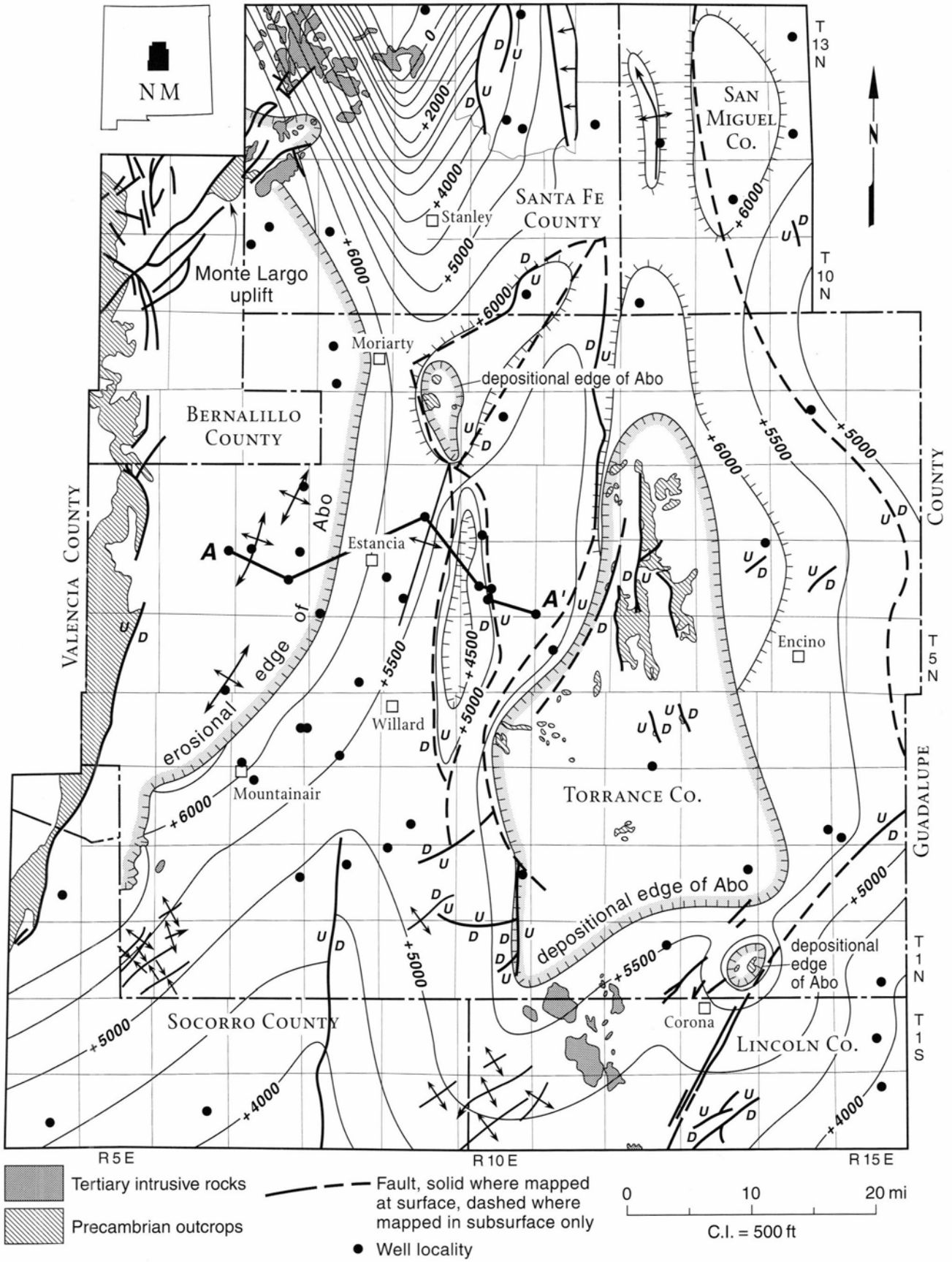

FIGURE 6—Structure-contour map on top of Abo Formation (Permian), Estancia Basin. See text for discussion of contouring methods. Contour interval is 500 ft. Datum is sea level.

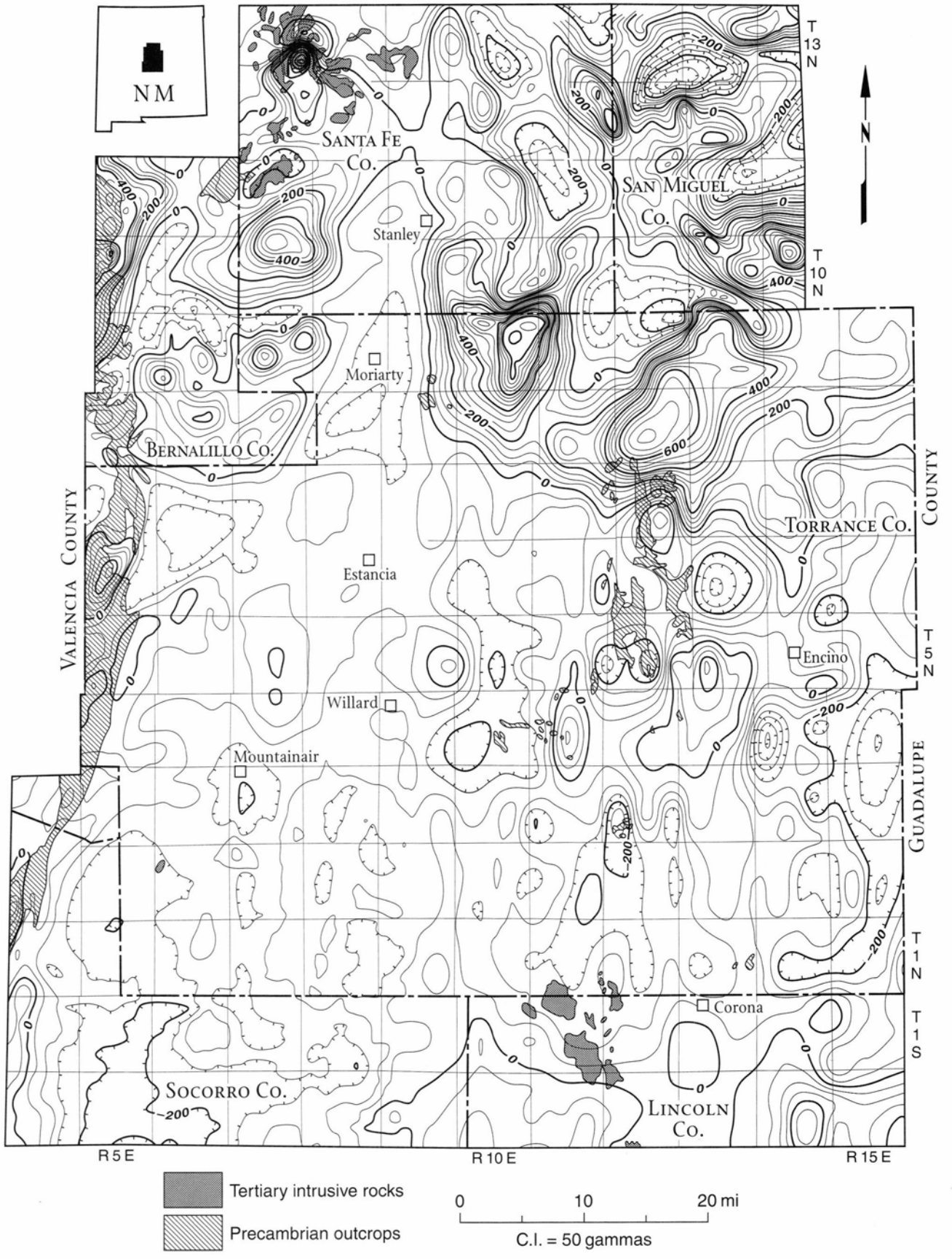

FIGURE 7A—Composite residual total intensity aeromagnetic map of the Estancia Basin area. Contour interval is 50 gammas. From Cordell (1983).

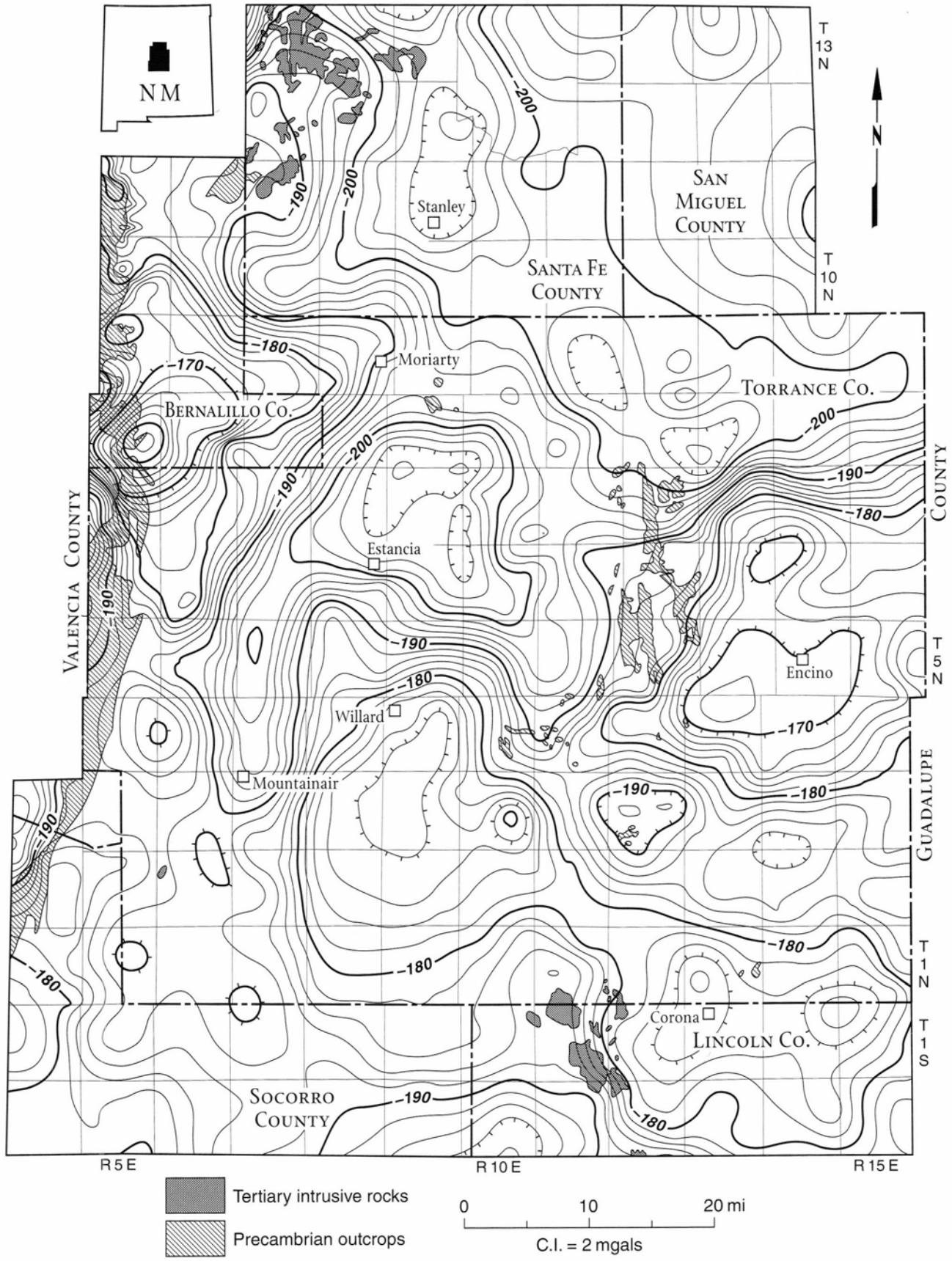

FIGURE 7B—Bouguer gravity anomaly map of the Estancia Basin area. Contour interval is 2 milligals. From Keller and Cordell (1983).

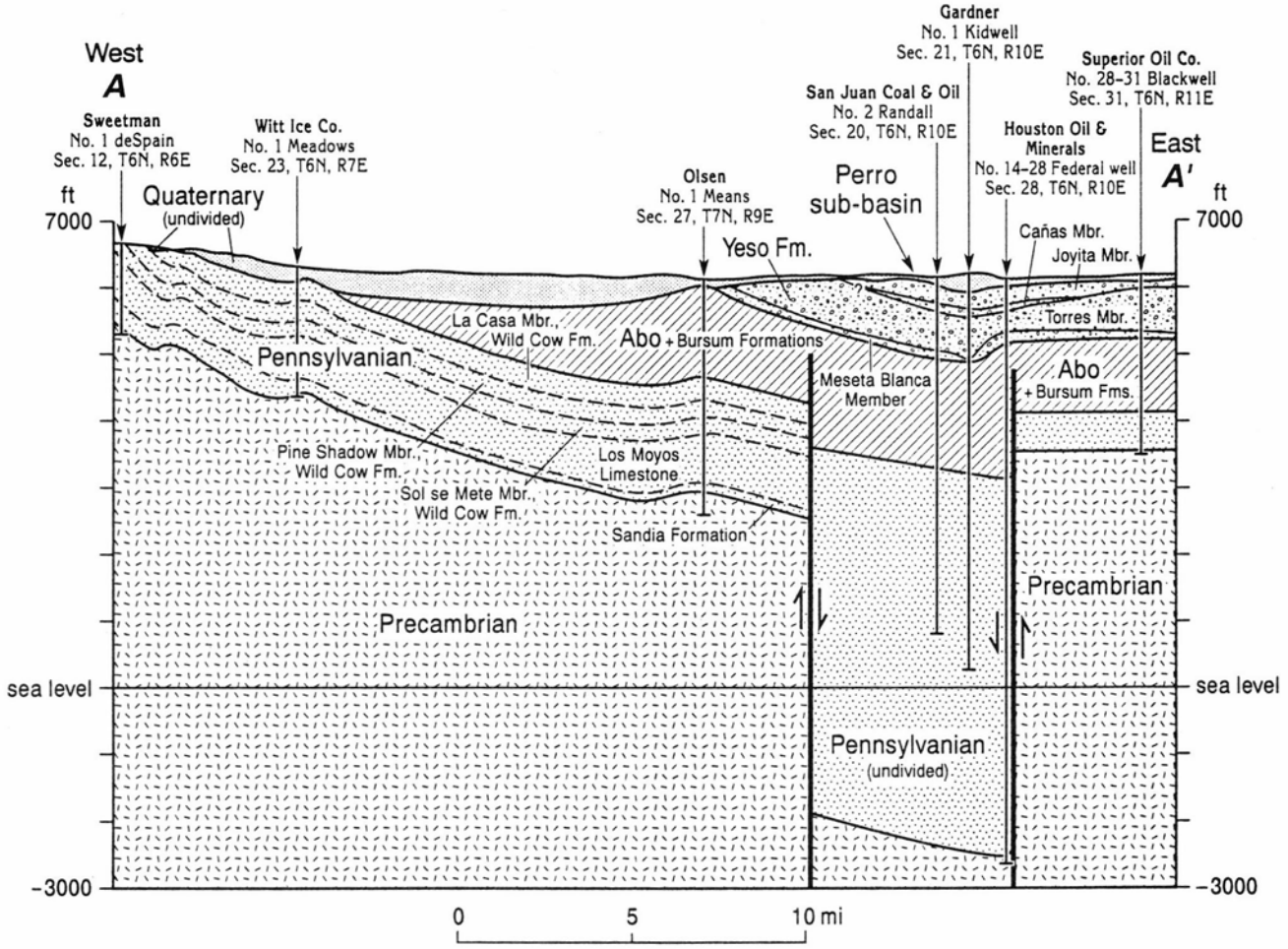

FIGURE 8—East–west structural cross section A–A′ through Estancia Basin. Datum is sea level.

defined as are the Tertiary intrusions that form the Ortiz and San Pedro Mountains. Perhaps thick sections of low-grade metamorphosed sediments or the presence of granitic intrusions within the Precambrian (Barrow and Keller, 1994) have contributed to the vagueness of the gravity map. At any rate, the aeromagnetic map is better suited for defining basement structure than the gravity map.

The main basin-forming structures are north- to north-east-trending high-angle faults. In most cases, these faults are not exposed at the surface. Very few of these faults offset the upper surface of the Abo, although they do offset strata in the lower Abo (Fig. 8). Major faults on the east side of the basin form down-to-the-west stairstep blocks that are bounded on the east by the Precambrian highlands of the Pedernal Hills. These faults offset the entire Pennsylvanian section and part of the Abo (Permian) Formation and are thought to be similar to the ancestral Rocky Mountain faults described by Beck and Chapin (1991) in the Joyita Hills of central New Mexico (Figs. 1, 9); the Joyita Hills are a surface expression of the late Paleozoic Joyita uplift, a tectonic element of the ancestral Rocky Mountains. The Pennsylvanian section and the Abo thicken westward into the basin (Fig. 10). These relationships indicate that major fault movement occurred from the Early Pennsylvanian until the

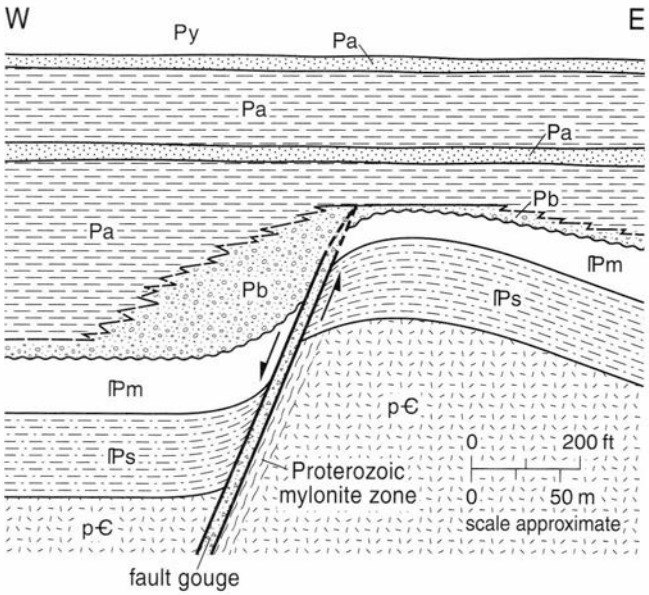

FIGURE 9—Generalized east–west cross section normal to a north-striking normal fault of the ancestral Rocky Mountains, Joyita Hills, central New Mexico. The fault does not offset Abo strata and is, therefore, pre-Abo in age. **Py**, Yeso; **Pa**, Abo; **Pb**, Bursum; **IPm**, Madera; **IPs**, Sandia; **p€**, Precambrian basement. From Beck and Chapin (1991).

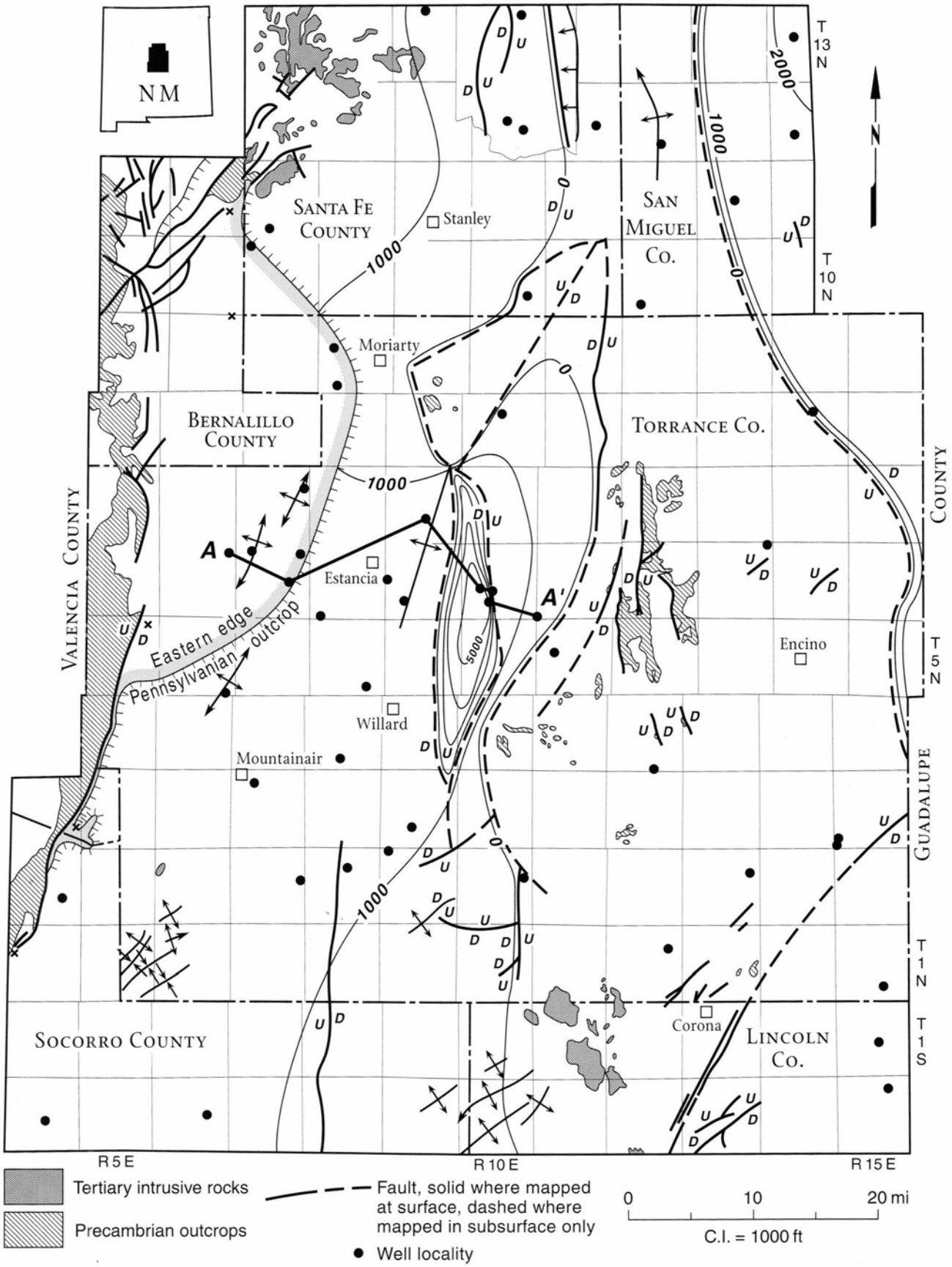

FIGURE 10—Isopach map of Pennsylvanian strata, Estancia Basin. Contour interval is 1,000 ft.

Wolfcampian (Early Permian). In places, these faults are exposed at the surface and may have been reactivated during Laramide deformation and during formation of the Rio Grande rift (see Barrow and Keller, 1994).

Perhaps the most striking structural feature of the Estancia Basin is the narrow north—south-trending graben (the Perro sub-basin) in T4-7N R9-10E (Figs. 5, 8). This graben is bounded on the east and west by high-angle normal faults. Maximum vertical offset of the Precambrian surface is approximately 6,000 ft along the eastern fault and 4,500 ft along the western fault. On the basis of reflection seismic profiles, Barrow and Keller (1994) concluded that the eastern fault is associated with flower structures and underwent strike-slip movement. As discussed elsewhere in this report, the sedimentary fill within this graben is of Morrowan (Early Pennsylvanian) through Wolfcampian (Early Permian) age. Most of the graben fill appears to be of Morrowan and Atokan (Early Pennsylvanian) age. Therefore, vertical displacement along the graben-bounding faults occurred mostly during the Early Pennsylvanian but persisted into the Wolfcampian. Barrow and Keller (1994) have discussed evidence for reactivation of the eastern fault during the Laramide (Late Cretaceous—early Tertiary) and believe it may have been active during the Proterozoic as well. Laramide displacement was minor compared to late Paleozoic movement. The extent of Proterozoic movement is unknown.

At the surface, the Perro sub-basin is characterized by the presence of numerous playa lakes. Smith (1957) described and characterized these lakes. The Perro sub-basin is named for the largest of the lakes, Laguna del Perro (English translation is "Dog Lake").

A structural high forms Lobo Hill and separates the Estancia Basin from the Espanola Basin (Fig. 5). Available data indicate Lobo Hill is bounded on its west, north, and east sides by high-angle normal faults. These faults are part of the fault system that forms the intrabasin graben (Perro sub-basin) to the south.

Beck and Chapin (1991, 1994) analyzed similar late Paleozoic, high-angle normal faults in the Joyita Hills (Figs. 1, 9) and concluded that late Paleozoic deformation in central New Mexico was the result of left-oblique (sinistral) wrench faulting along a north—south-trending structural zone that stretched from the late Paleozoic Orogrande Basin in southern New Mexico to the west side of the Peñasco uplift in northern New Mexico. General spacial location, time of formation, orientation, and form suggest the faults that form the Perro sub-basin may be broadly related to this structural zone and therefore have undergone left-oblique slip during the Pennsylvanian and Early Permian.

West of the Perro sub-basin, Pennsylvanian and Permian strata rise gently to the west as they climb onto the eastern dip slopes of the Sandia, Manzano, and Los Pinos Mountains. Average dip of strata in this area is approximately 240 ft per mile (2.6°) east—southeast. Superposed on this monoclinal slope are relatively small folds and faults. The fold axes trend northeast and form an en echelon pattern. One of these folds, the Wilcox anticline (Fig. 5), appears to form a trap for CO2 gas in basal Pennsylvanian sandstones. The Wilcox anticline has an estimated closure of 60-80 ft, and the Estancia anticline has closure of at least 100 ft (Winchester, 1933). Similarly oriented anticlines in T1-2N R5-6E are associated with Tertiary-age diabase dikes; field observations indicate that these anticlines were formed by arching of strata over the dikes and that folding was caused by dike intrusion (Bates et al., 1947).

The east flank of the Sandia and northern Manzano Mountains is cut by many northeast- and north-trending normal faults (Titus, 1980). These faults appear to have mostly normal and strike-slip displacement. Fault density is highest near the crests of the mountain ranges and decreases to the east. Northeast-trending strike-slip faults form the Monte Largo uplift (Fig. 5) in northeast Bernalillo County (Kelley and Northrop, 1975).

To the south, the east-dipping upper Paleozoic strata are truncated against the Precambrian core of the Los Pinos and southern Manzano Mountains by large reverse faults. These are the Palomas and Montosa faults, which are thought to have been active during compressional Laramide uplift that formed the Los Pinos and Manzano Mountains (Bates et al., 1947; Russell and Snelson, 1994). They were later reactivated with a normal sense of movement during formation of the Rio Grande rift (Bates et al., 1947; Russell and Snelson, 1994).

Stratigraphy and reservoir geology

Strata in the Estancia Basin range from Precambrian to Quaternary in age (Fig. 2). These strata were analyzed using wireline logs, drill cuttings, and petrographic thin sections of drill cuttings. Cores were not utilized because few have been taken in the basin and apparently none have been preserved. Descriptions of logs and cuttings were integrated with published studies of outcrops in the Sandia, Manzano, and Los Pinos Mountains in order to provide a comprehensive summary of stratigraphic characteristics.

Reservoir geology was evaluated using wireline logs, descriptions of drill cuttings, and petrographic analyses of thin sections. Reports of oil and gas shows compiled from drill records on file at the New Mexico Bureau of Mines and Mineral Resources were also used to evaluate reservoir geology. Most thin-section samples were impregnated with blue epoxy in order to facilitate study of pore systems. Reservoir evaluation was hampered because many of the wells in the basin were drilled before the advent of wireline logs. Also, some of the more recent wells were drilled by independent operators with limited budgets who could not afford a comprehensive suite of modern logs. As a result, many of these wells are represented only by one or two types of logs, often of somewhat dated technology. These older logs can be used to evaluate reservoirs but are not as useful as modern logs.

Precambrian

Igneous and metasedimentary rocks constitute the Precambrian of the Estancia Basin and adjoining uplifts. On the east, Precambrian rocks are exposed in the Pedernal Hills, where they consist primarily of granite, metarhyolite, metadacite, granitic gneiss, quartzite, and schist (Gonzales, 1968; Gonzales and Woodward, 1972; Armstrong and Holcombe, 1982; Bauer and Williams, 1985). Paul Bauer examined cores from several shallow mineral exploration holes in the Pedernal Hills and deter-

mined that the Precambrian is predominantly a fine- to medium-grained quartzofeldspathic gneissic rock with well-developed sub-horizontal foliation that is probably representative of high strain; the protolith is thought to be a fine-grained granite or aplite (P. Bauer, pers. comm. 1995). Also present in the cores is a fine-grained, quartz-rich feldspathic schist with relict feldspar grains and well-developed foliation; Bauer believes the protolith is a felsic volcanic rock. On the west, the Precambrian of the Sandia Mountains consists of granite, metaquartzite, schist, gneiss, and greenstone (Kelley and Northrop, 1975). The Precambrian of the Manzano Mountains consists primarily of metaquartzite, schist, metarhyolite, granite, and greenstone (Reiche, 1949; Stark, 1956). In the Los Pinos Mountains, the Precambrian consists of metaquartzite, schist, metarhyolite, and granite (Stark and Dapples, 1946).

Wells studied for this report indicate that the Precambrian within the Estancia Basin consists of schist, quartzite, metapsammites, and granite. Both dark-colored biotite schists and light-colored muscovite schists are present. The metapsammites are foliated and consist of either biotite or chlorite in a groundmass of fine- to coarse-grained quartz. In some of the metapsammites the groundmass is arkosic.

The schists, quartzites, and metapsammites appear to be present everywhere except the Perro sub-basin. On the western shelf, the Olsen No. 1 Means well penetrated a sequence of quartzite overlain by schist; 302 ft of schist was drilled, and then 186 ft of quartzite was drilled. The well reached total depth in the quartzite. In the Stevens Operating Corp. No. 1 Hobbs well, 380 ft of interlayered schists and metaquartzites was drilled in the Precambrian. In other wells on the western shelf, Pennsylvanian sediments rest unconformably on Precambrian schist, metaquartzite, or metapsammite. Insufficient Precambrian was drilled to determine the vertical sequence of metasediments. Although data are limited, the metasediments appear to form a layered sequence. Only one well, the Houston Oil and Minerals No. 14-28 Federal, was drilled deep enough to penetrate the Precambrian in the Perro sub-basin; in that well, the mud log indicates the Precambrian consists of granitic rocks.

An in-depth discussion of the Precambrian of the Estancia Basin is beyond the scope of this report. Interested readers are referred to the studies cited above.

Mississippian

Strata correlatable with the Mississippian System have not been positively identified within the Estancia Basin. Erosional remnants of the Espiritu Santo Formation of the Arroyo Peñasco Group (Mississippian: Osagean) are present near Placitas at the north end of the Sandia Mountains and are also present in the Manzano Mountains (Armstrong, 1955, 1967; Kelley and Northrop, 1975). In the Sandia Mountains, the Espiritu Santo unconformably overlies the Precambrian and consists of upward-shallowing carbonate tidal sequences. Maximum thickness is 73 ft. The carbonates are mostly dolostones, dedolomites, and minor lime mudstones. A thin section of sandstones and conglomerates, known as the Del Padre Sandstone Member, is locally present at the base of the Espiritu Santo and attains a maximum thickness of 7 ft.

The Log Springs Formation, also of Mississippian age, unconformably overlies the Espiritu Santo Formation in the Sandia Mountains (Armstrong et al., 1979). At Placitas, it is 5-6 ft thick. The Log Springs is nonmarine and consists of a basal red hematitic shale that is overlain by arkosic to conglomeratic, argillaceous, crossbedded, red to orange sandstone (Armstrong and Mamet, 1974). The Log Springs contains eroded clasts from the Arroyo Peñasco Group, as well as from the Precambrian igneous and metamorphic basement complex.

Throughout most of the subsurface of the Estancia Basin, strata correlatable with lithostratigraphic units of the Mississippian System are not present, and strata of Pennsylvanian age rest unconformably on Precambrian basement. Strata that may be correlatable with the Arroyo Peñasco Group are present, however, in the northern part of the study area in the southern Espanola Basin. In the Bar-S-Bar Ranch No. 1 Fee well in the southern Espanola Basin, Precambrian granite was encountered at a depth of 2,380 ft. The interval from 2,360 ft to 2,380 ft consists of fine- to coarse-grained, moderately sorted sandstones and may be the Del Padre Sandstone Member. The overlying strata from 2,320 ft to 2,360 ft are dominantly limestone composed of lime mudstones and bioclastic wackestones; bioclasts are fragments of brachiopods, crinoids, and algae. Examination of well cuttings with a low-power binocular microscope revealed trace amounts of euhedral dolomite crystals. This interval may be correlatable with the Espiritu Santo Formation. Strata above 2,320 ft consist of sandstones, shales, and limestones correlatable with the Pennsylvanian. The presence of fusulinids from 2,110 ft to 2,120 ft indicates a Pennsylvanian age, rather than a Mississippian age. The Log Springs Formation has not been identified in the subsurface of the Estancia Basin, but it is possible that it is present but unrecognized because of its thinness and its gross similarity to the overlying Pennsylvanian section.

Pennsylvanian

Pennsylvanian strata are present throughout the subsurface of the Estancia Basin and attain a maximum thickness of 5,700 ft in the Perro sub-basin; the thickest closed contour on the isopach map is 5,000 ft (Fig. 10). The Pennsylvanian section within the basin is Morrowan to Virgilian in age. It is a syntectonic basin fill and is coeval with the major stage of basin development. Strata in the subsurface can be correlated with the Pennsylvanian in mountain ranges to the west of the basin. Myers (1967, 1969, 1977), Myers and McKay (1970, 1971, 1972), and Myers, McKay, and Sharps (1981) have mapped the Manzano Mountains extensively. Based on his work, Myers (1973, 1982) summarized the litho-stratigraphy and biostratigraphy of Pennsylvanian and Lower Permian strata in the Manzano Mountains. This report extends Myers' stratigraphy eastward into the subsurface of the Estancia Basin.

Pennsylvanian in Los Pinos, Manzano, and Sandia Mountains

The Pennsylvanian and Lower Permian strata of the Manzano Mountains consist of four formations (ascending; Fig. 11): Sandia Formation (Atokan), Los Moyos Limestone (Desmoinesian to early Missourian), Wild Cow Formation (Missourian—Virgilian), and Bursum Formation (Wolfcampian). The Los Moyos Limestone, Wild Cow Formation, and Bursum Formation constitute

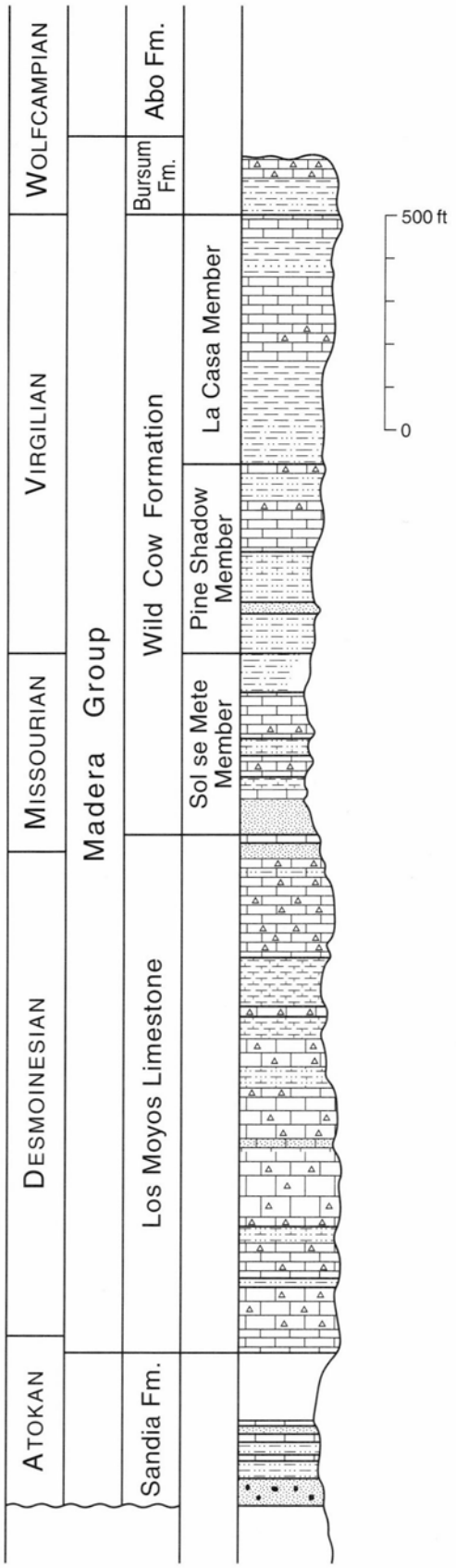

FIGURE 11—Stratigraphic section of Pennsylvanian and Lower Permian strata, Manzano Mountains. Modified from Myers (1982).

the Madera Group. The Wild Cow Formation is subdivided into three members (ascending): Sol se Mete Member (Missourian), Pine Shadow Member (Virgilian), and La Casa Member (Virgilian). The Pennsylvanian—Permian boundary is placed at the contact between the Wild Cow and the Bursum by most workers; however, Myers (1982) concluded that the uppermost parts of the Wild Cow (La Casa Member) of the northern Manzano Mountains may be chronostratigraphically equivalent to the Bursum of the southern part of the Manzano Mountains.

The Sandia Formation is 50-300 ft thick in the Manzano Mountains, where it consists of shale, siltstone, sandstone, conglomerate, and minor limestone (Myers, 1982). The lowermost beds are conglomerates and coarse-grained sandstones that grade upward into sandstones, siltstones, and shales that are locally carbonaceous and coaly. These in turn grade upward into sandstones, silt-stone, and minor thinly bedded marine limestone and carbonaceous shale. The upper 60 ft of the Sandia Formation consists of shale, sandstone, siltstone, and limestone; marine fossils are common in the upper 30 ft. Studies of fusulinids indicate the Sandia Formation is Atokan in age (Myers, 1982).

The Los Moyos Limestone is approximately 600 ft thick in the Manzano Mountains, where it consists of thickly bedded, cliff-forming, cherty, gray limestones (Myers, 1973). The limestones are intercalated with thinly bedded, dark shales and orange siltstones, sandstones, and conglomerates. The lower 80-100 ft of the Los Moyos is olive to gray, cherty calcarenites. Fusulinids indicate the Los Moyos is Desmoinesian and early Missourian in age (Myers, 1973, 1982). As such, it is time equivalent to Strawn and lower Canyon strata of the Permian and Tucumcari Basins and north-central Texas.

The Wild Cow Formation overlies the Los Moyos Limestone without major unconformity. The Wild Cow consists of three cyclic sequences of arkosic sandstone and conglomerate that grade upward into shales. The shales, in turn, grade upward into cliff-forming, gray limestones. Each of the three sequences has been defined and mapped as a member (ascending): Sol se Mete Member, Pine Shadow Member, and La Casa Member.

The Sol se Mete Member has an average thickness of approximately 200 ft in the Manzano Mountains (Myers, 1973). Thickness varies from 150 ft to 300 ft. The Sol se Mete Member consists of a basal clastic unit overlain by shale. Studies of fusulinids indicate it is Missourian in age (Myers, 1973). The basal clastic unit is 15-100 ft thick and consists of conglomerate, fine- to coarse-grained sandstone, and siltstone. The sandstones are arkosic, and the conglomerates contain angular to subrounded rock fragments of the metamorphic basement complex. In places, petrified logs have been described from the basal clastic unit. The basal clastic unit grades upward into a unit of calcareous, gray shale. Red beds are present locally at the top of this unit. This shale unit is overlain by 3060 ft of cherty, gray limestone. This upper limestone unit grades southward into siltstone and fine-grained sandstone in the southern part of the Manzano Mountains.

The Pine Shadow Member of the Wild Cow Formation is 180-250 ft thick in the Manzano Mountains (Myers, 1973). The Pine Shadow Member consists of a basal, coarse-grained clastic unit, a middle unit of fine-grained clastics, and an upper unit of limestone. The Pine Shadow Member contains fusulinids of early Virgilian age (Myers,

1973). The basal, coarse-grained clastic unit is 5-100 ft thick in the Manzano Mountains. It consists of arkosic conglomerate, yellow to brown micaceous siltstone, and fine-grained sandstone. The conglomerates contain cobble-size clasts of metamorphic rocks and fragments of fossilized wood. The overlying fine-grained clastic unit consists of thinly bedded yellow to gray siltstone and minor shale. The uppermost unit is 50-130 ft thick and consists of limestone and minor amounts of sandstone, siltstone, and calcareous shale.

The La Casa Member of the Wild Cow Formation is 250-350 ft thick in the Manzano Mountains (Myers, 1973). It consists of a basal clastic unit overlain by a carbonate unit. Fusulinids indicate most of the La Casa Member is from middle to late Virgilian in age; the uppermost beds are locally Wolfcampian in age (Myers, 1973, 1982). The basal clastic unit is 30-120 ft thick in the Manzano Mountains (Myers, 1973). At Priest Canyon in the southern part of the mountain range, this basal clastic unit is approximately 120 ft thick and consists of siltstones and shales. This is overlain by 100 ft of light-gray limestones that are, in turn, overlain by red and gray shales and yellowish-green sandstones. The upper part of the La Casa Member is 30 ft thick and consists of light olive-gray limestones. To the north in the central and northern Manzano Mountains, the basal clastic unit consists of 30-50 ft of arkosic sandstones that are locally conglomeratic. The overlying limestones grade northward into interbedded limestones, sandstones, siltstones, and shales.

Pennsylvanian in subsurface of Estancia Basin

The Pennsylvanian section is 400-5,700 ft thick in the subsurface of the Estancia Basin (Fig. 10). The Pennsylvanian is thickest in the structurally deep, downfaulted Perro sub-basin. It is absent from the Pedernal uplift and Lobo Hill. In the northeast part of the area covered by this report, the Pennsylvanian attains a thickness of approximately 2,000 ft in a south-trending projection of the late Paleozoic Rowe-Mora Basin. On the shelf west of the Perro sub-basin, the Pennsylvanian varies in thickness from 1,000 ft to 1,600 ft. Thickness variations in this area are not coincident with axes of the north-northeast-trending anticlines, indicating that the folds are post depositional and therefore post-Pennsylvanian in age. The thicker areas of Pennsylvanian strata may define intrashelf basins, but this has not yet been documented with stratigraphic or facies studies. To the east, the Pennsylvanian section thins against the western flank of the Pedernal uplift (Fig. 10). These thickness trends may represent both syndepositional thickening into fault-bounded grabens and post-depositional (but pre-Permian) erosional truncation and removal of the Pennsylvanian from upthrown fault blocks.

Pennsylvanian lithostratigraphic units mapped by Myers in the Manzano Mountains (Fig. 11) can be correlated eastward into the subsurface of the Estancia Basin (Fig. 8). Correlation is based on the cyclic nature of these units; each has a basal clastic facies that fines upward. A marine facies dominated by limestones forms the upper part of each unit. Lateral continuity of these limestones enables correlation between widely spaced wells; however, these limestones do not extend into the Perro sub-basin. Therefore, Pennsylvanian strata in the sub-basin can not be correlated lithostratigraphically with Pennsylvanian strata on the shelf to the west with present subsurface control.

Approximate ages of the Pennsylvanian on the western shelf can be determined from the biostratigraphic studies by Myers in the Manzano Mountains. Similar ages can be expected for these units in the subsurface to the east. Notably, strata of Morrowan age appear to be absent from the western shelf, as well as from the mountain ranges to the west.

The lowermost Pennsylvanian in the Perro sub-basin was deposited earlier than on the shelf to the west. Evidence for this is mainly based on palynologic studies in the Houston Oil and Minerals No. 14-28 Federal well, which indicate that the lowermost Pennsylvanian in the Perro sub-basin is Morrowan in age (letter dated December 10, 1984, from Ann Reaugh of Geochem Laboratories, Inc., to Ben Donegan of Leonard Minerals Co.). Ann Reaugh identified pollen in cuttings from 8,370 ft to 8,740 ft as Early Pennsylvanian and probably Morrowan in age. The Precambrian top is at 8,660 ft, so the cuttings from 8,660 ft to 8,740 ft were almost certainly cavings from the overlying section. If this age determination is correct, then the Pennsylvanian in the lower part of the well is older than the oldest Pennsylvanian sediments on the western shelf and in the Manzano Mountains, which are Atokan. The top of the Morrowan section is undetermined. If this is so, then the Precambrian metasediments of the Pedernal highlands east of the sub-basin and the shelf west of the sub-basin were exposed during the Early Pennsylvanian. During this time, the Perro sub-basin was being filled with sediments derived from erosion of these areas. Support for this hypothesis comes from the petrography of many of the sandstones and shales in the Perro sub-basin. A large percentage of these sediments contain large detrital grains of muscovite and biotite, which may have been derived from the muscovite- and biotite-rich metasediments on the western shelf and in the Pedernal highlands. Large grains of these fragile minerals can not survive long distances of transport and must have been locally derived.

Pennsylvanian lithofacies reflect tectonic controls on sedimentation and proximity to sources of sediment. The Pennsylvanian is subdivided into three major lithofacies in the subsurface of the Estancia Basin (Fig. 12).

Pedernal facies—The Pedernal facies consists primarily of red shales and fine- to very coarse grained, gray to red sandstones. Minor amounts of gray shales and limestones are also present. The Pedernal facies has been encountered only in shallow strata on the west flank of the Pedernal uplift in Torrance County, and there only in one well, the Superior Oil Co. No. 28-31 Blackwell. The granitic and metamorphic rocks of the Precambrian core of the Pedernal uplift were the source of clastic sediments of the Pedernal facies.

Sandstones in the Pedernal facies are gray to red and fine to very coarse grained; some are conglomeratic, and others are argillaceous. The percentage of clay matrix is generally low, near zero, but is as high as 20% in some samples. The sandstones are subarkosic arenites composed dominantly of quartz with subsidiary amounts of detrital plagioclase and potassium feldspar. Sand-size fragments of red shale and siltstone typically compose 0-20% of the sandstones in the Pedernal facies. A small percentage of detrital muscovite and biotite are present within most of the sandstones. Trace amounts of calcite and hematite cement are common but do not completely

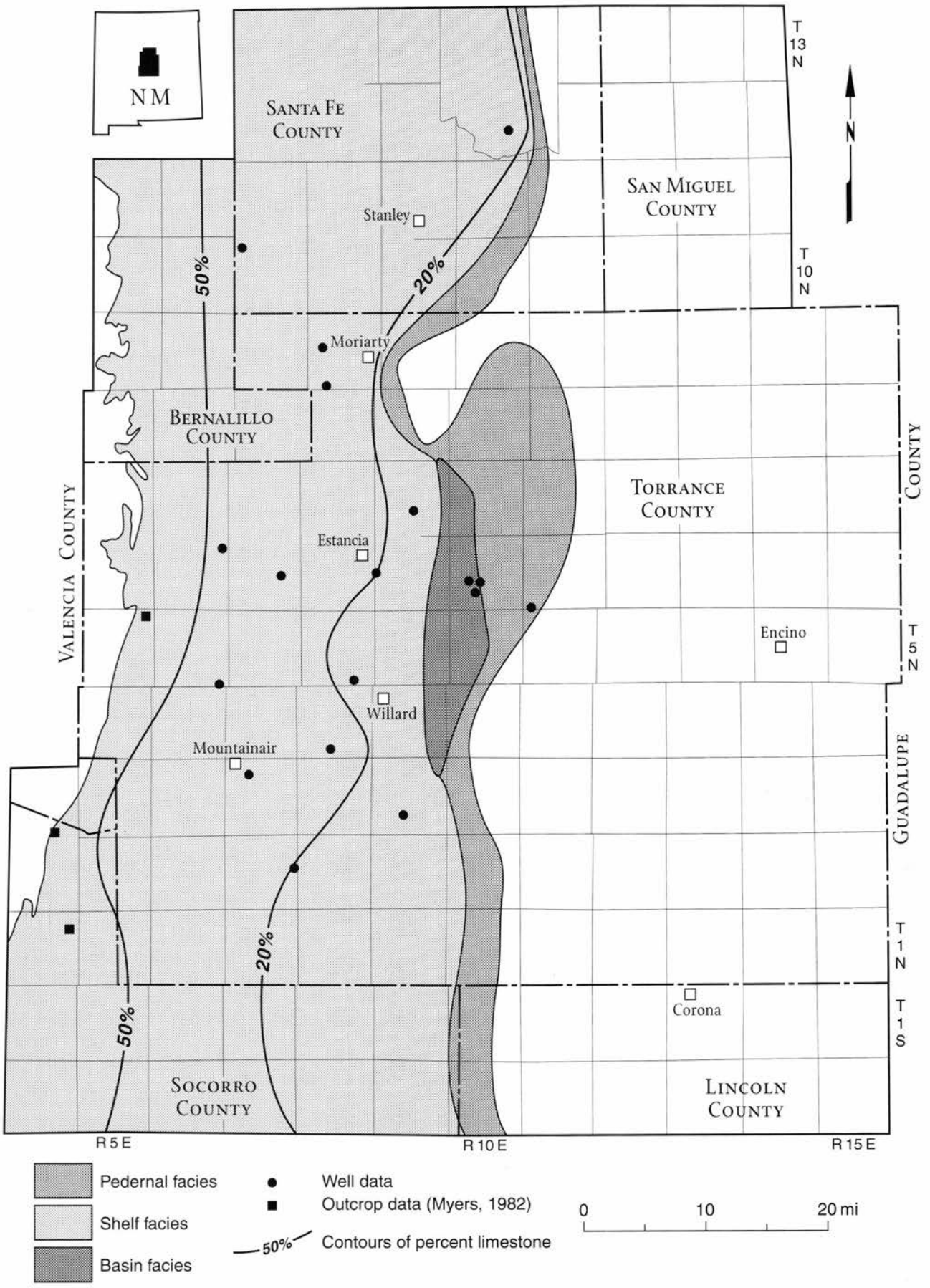

FIGURE 12—Lithofacies map of Pennsylvanian strata and percentage of limestone in Pennsylvanian section, Estancia Basin. See text for definition of lithofacies.

occlude porosity. Most of the sandstones have from a trace to 10% visual intergranular porosity and are good reservoirs. Porosity is primary. Most of the sandstone beds are less than 10 ft thick.

Shales in the Pedernal facies are red to gray. Red shales predominate and are grayish red to dusky red, sandy, silty, micaceous and noncalcareous. Gray shales are light gray to grayish black, silty, micaceous, and calcareous to noncalcareous. The gray shales contain abundant brachiopods and wood fragments.

Limestones in the Pedernal facies are dark gray and argillaceous. Observed samples were crinoidal brachiopodal wackestones. Micrite matrix has generally been recrystallized to microspar. Limestones are present as thin beds in the upper 200 ft of the Madera Group in the Superior No. 28-31 Blackwell.

Basin facies—The Pennsylvanian basin facies consists mostly of dark-gray shales, red shales, and fine- to very coarse grained, white to gray sandstones. Minor limestones and trace amounts of coal are also present. The basin facies is restricted to the Perro sub-basin. Limited drilling within the sub-basin indicates that it is filled entirely with the basin facies (Fig. 12). As discussed above, Pennsylvanian strata in this graben are predominantly Morrowan and Atokan in age and are older than the bulk of the Pennsylvanian strata that are present on the shelf to the west of the graben. The Precambrian rocks of the western shelf and the Pedernal uplift were the source of many of the Pennsylvanian sediments deposited in the graben.

Sandstones in the basin facies are light-gray to grayish-red, fine- to very coarse grained quartz arenites and subarkosic arenites. Some are conglomeratic. Sorting is moderate to poor; red clay matrix constitutes 0-20% of the rock. The sandstones consist predominantly of rounded to subangular quartz and feldspar, granitic rock fragments, and minor mica and calcite cement. The red clay matrix is detrital in some sandstones; in other sandstones it is a pseudomatrix of squashed fragments of red shales. Calcite cement is 0-50% of the rock. Where it is more than 10%, the calcite has a blocky texture and replaces framework grains; visual porosity is zero. Where it is less than 10%, the sandstones contain visual porosity and are fair to good reservoirs. Most sandstone beds in the basin facies are 1-6 ft thick. Maximum observed bed thickness is 22 ft.

Both gray and red shales are present in the basin facies. Gray shales are light gray to grayish black to black. The lighter-colored varieties are generally silty, micaceous, and calcareous. The darker-colored varieties generally contain less silt and mica and are not calcareous; trace amounts of disseminated pyrite are present in most of the darker-colored shales. Many of the dark-gray to black shales have a waxy luster. Some gray shales bear a brachiopod fauna. Kerogens are dominantly nonmarine woody types.

Red shales in the basin facies are pale reddish brown to grayish red to dusky red. Most are silty and micaceous but not calcareous. A few of the red shales contain fine- to medium-grained quartz sand.

Limestones in the basin facies are olive-gray to medium-gray lime mudstones and bioclastic wackestones. Lime mudstones predominate. Many are argillaceous, and some are sandy. Most appear to have been recrystallized to microspar. Beds have a maximum thickness of 2-3 ft. Most of what appears to be lime mudstones in cuttings may actually be pedogenic nodules of calcite in red shale. Bioclasts in the wackestones have been recrystallized into spar and microspar. The limestones in the basin facies have no visual porosity and are poor reservoirs. Limestones constitute 3-8% of this facies as measured in vertical section.

Coal is present as thin beds in the basin facies. Examination of drill cuttings from two wells (San Juan Coal & Oil No. 2 Randall, Gardner Petroleum No. 1 Kidwell) and the mud log from a third well (Houston Oil & Minerals No. 14-28 Federal) revealed the presence of coal in all three wells.

Shelf facies—The shelf facies consists of interbedded marine limestones, gray shales, red shales, fine- to coarse-grained sandstones, and minor coal. Limestones are more abundant in this facies than in either the Pedernal facies or the basin facies. The shelf facies is the most areally extensive of the Pennsylvanian lithofacies in the Estancia Basin. It occupies the basin west, northwest, and southwest of the Perro sub-basin. It is also present in the Espanola Basin in the northern part of the study area.

Sandstones in the shelf facies are light-gray to medium-gray to grayish-red, fine- to very coarse grained subarkosic arenites and quartz arenites. Many are conglomeratic. They are composed primarily of quartz and feldspars. Most contain trace amounts of granitic rock fragments and detrital muscovite and biotite. Most feldspars have been partially altered to clays. Cements are anhedral patches of blocky calcite, subhedral to anhedral microcrystalline hematite, and early-stage syntaxial quartz overgrowths. Sorting is generally poor. A large percentage of the fine-grained sandstones contain as much as 20% clay matrix. The coarser-grained sandstones contain from zero to a trace of clay matrix.

Reservoir quality of sandstones in the shelf facies is variable. Sandstones with a large percentage of cement or clay matrix have only a trace or no visual porosity and are poor reservoirs; wireline porosity logs indicate 0-2% porosity for these sandstones. Sandstones with little or no cement and clay matrix, however, are fair to good reservoirs. In many cases, they have been disaggregated into individual sand grains in the drill cuttings, indicating a low level of cementation and good reservoir quality. In these sandstones, wireline logs indicate that porosity averages approximately 10% and typically ranges from 6% to 14%. Porosity is as high as 16% in some of the sandstones.

Limestones of the shelf facies are mostly light-gray to olive-gray to dark-gray lime mudstones and bioclastic wackestones. The percentage of limestone increases to the west (Fig. 12). Bioclastic packstones and grainstones are present but less common. Fauna in the wackestones include brachiopods, bryozoans, ostracods, and crinoids and more rarely calcareous algae, fusulinids, foraminifera, and gastropods. Oolites are sometimes present. Visual porosity is absent in most of the limestones. Algal grainstones in cuttings at depths of 2,130-2,150 ft in the MAR Oil & Gas No. 1 Estes well have a maximum visual porosity of 15%. In the Navajo Oil No. 1 Manzano well, lime mudstones at depths of 1,160-1,236 ft have been recrystallized to microspar with intercrystalline porosity; porosity estimated visually by the Archie method ranges from 17% to 22%. Neutron porosity logs and density porosity logs indicate that limestones of the shelf facies have an average porosity of only 2% and a typical range of 0-5%. The highest porosity obtained from wireline logs

was 8%. Geophysical logs were not run for the Navajo Oil No. 1 Manzano well (drilled in 1937), and the only logs available for the MAR No. 1 Estes well are an old gamma-ray-neutron log (neutron reading in API units) and an induction-electric log, so porosities were not estimated from logs for the zones described in these two wells.

Both red and gray shales are present in the shelf facies. Red shales are grayish red to reddish brown to dusky red and are silty. A large percentage are micaceous, and a small percentage are sandy. Most are not calcareous. The gray shales are medium gray to grayish black and silty. A large percentage are calcareous. A small percentage of the gray shales are micaceous. A faunal assemblage of brachiopods and bryozoans is commonly present in the gray shales. Many of the gray shales contain fragments of wood.

Both red and gray shales are present in the Pennsylvanian in any single well; however, the relative percentage of each varies vertically within a well and also varies areally among wells. In general, gray shales are more prevalent than red shales in the western part of the Estancia Basin and in the southern part of the Espanola Basin (Fig. 12). Gray and red shales are present in approximately equal amounts in the area between Willard and Estancia. Red shales are dominant south and east of Mountainair.

Permian

Bursum and Abo Formations

The Bursum and Abo Formations conformably overlie Pennsylvanian strata in the Estancia Basin. In the southern Manzano Mountains, the Bursum is approximately 100 ft thick and gradationally overlies the La Casa Member of the Wild Cow Formation (Myers, 1973, 1982). The Bursum Formation consists of lenticular, red, arkosic sandstones, red and green shales, and greenish-gray limestones. It grades northward into the lower part of the Abo Formation in the central Manzano Mountains. As previously mentioned, the uppermost beds of the La Casa Member of the Wild Cow Formation in the northern Manzano Mountains may be temporally equivalent to the lower part of the Bursum Formation of the southern Manzano Mountains (Myers, 1973, 1982). Fusulinids indicate the Bursum is Wolfcampian in age (Thompson, 1954; Myers, 1982).

The Abo Formation conformably overlies the Bursum Formation in the southern Manzano Mountains, where it is approximately 900 ft thick (Myers, 1973, 1982). In the northern Manzanos, the Bursum has been laterally replaced by the lower Abo, which rests on the La Casa Member of the Wild Cow Formation. In the Manzano Mountains, the Abo consists of nonmarine, red, hematitic, arkosic conglomerates, crossbedded sandstones, siltstones, and shales.

The age of the Abo in the Manzano Mountains has been the subject of considerable debate (Hunt, 1983). Lateral equivalence with the Bursum Formation suggests a Wolfcampian age for the lower Abo. Kottlowski (1963), Hatchell et al. (1982), and Hunt (1983) have summarized the biostratigraphy of Abo flora. These flora indicate that the Abo is mostly of Wolfcampian age but that the uppermost Abo may be Leonardian.

For this report, the Bursum and Abo Formations have been mapped as a single unit in the subsurface of the Estancia Basin (Fig. 13). Their lateral equivalence and intergradational nature, as well as the absence of closely spaced wells, make separation of these units difficult and uncertain.

The Bursum and Abo Formations have a combined maximum thickness of 1,900 ft (Fig. 13). These units are thickest in the Perro sub-basin, and they pinchout eastward against the Pedernal uplift and on the flanks of Lobo Hill. To the west, the Abo and Bursum have been erosionally truncated on the dip slope of the Manzano and Sandia Mountains. In the southern Espanola Basin, the Abo thins eastward over the crest of the Pedernal uplift but does not appear to pinchout in this area. The Bursum is identifiable as a separate stratigraphic unit in the Perro sub-basin, where it is 1,100 ft thick. It is not present east of the sub-basin. On the western shelf, the Bursum is identifiable as far north as Willard, where it is 1,020 ft thick in the Mountainair No. 1 Veal well in T4N R7E and 701 ft thick in the Eidal No. 1 Mitchell well in T4N R8E. To the north, it grades into the lower part of the Abo Formation. To the southwest, it thins to 290 ft in the Skelly No. 1 Goddard well in T2S R4E. As noted above, the Bursum is only 100 ft thick in the southern Manzano Mountains. This westward and southwestward thinning appears to be caused by gradation of the Bursum into the lower part of the Abo Formation.

Lateral gradation of the Bursum into the lower Abo is also present within the Perro sub-basin. In the Gardner No. 1 Kidwell well in sec. 21 T6N R10E, Bursum limestones are lime mudstones and bioclastic wackestones; most beds appear to be 2-3 ft thick. One mile to the west in the San Juan Coal & Oil No. 2 Randall well in sec. 20 T6N R10E, these limestones are micritic, nonfossiliferous, and nodular and are finely interbedded with red shales. It is unknown whether they are a marine or nonmarine deposit. They are very different from the limestones in the Gardner well, which appear to be a marine facies.

Sandstones in the Bursum and Abo Formations are pale red to grayish red to light gray and are very fine to very coarse grained. Beds are typically 3-12 ft thick. The fine-grained sandstones are generally well sorted. The coarse-grained sandstones are moderately to poorly sorted, and many are conglomeratic. The sandstones are subarkosic arenites and quartz arenites and are composed mostly of quartz and feldspar framework grains. They contain 0-10% rock fragments, which are usually intraformational siltstones and shales. The red color is imparted by a coating of hematite and clay on the framework grains. Anhydrite, gypsum, and calcite are present as intergranular cements. Cement is typically 0-20% of the sandstones but in rare cases may constitute 60% of the rock. Calcite cement is generally present in blocky patches that partially replace framework grains.

Most Abo and Bursum sandstones are "tight" and have only a trace or no visual porosity when examined in thin section. Depositional porosity has generally been occluded by cements and the clay—hematite matrix. A few sandstones have been disaggregated into individual sand grains in the drill cuttings and may have significant porosity. Neutron porosity logs and density porosity logs indicate that porosity averages 12% and typically ranges from 12% to 16%. Much of the porosity may be in a micropore system within the clay—hematite matrix. Furthermore, the clay minerals in the sandstones may cause the logs to indicate a higher porosity than is actually present. Overall, Abo and Bursum sandstones are

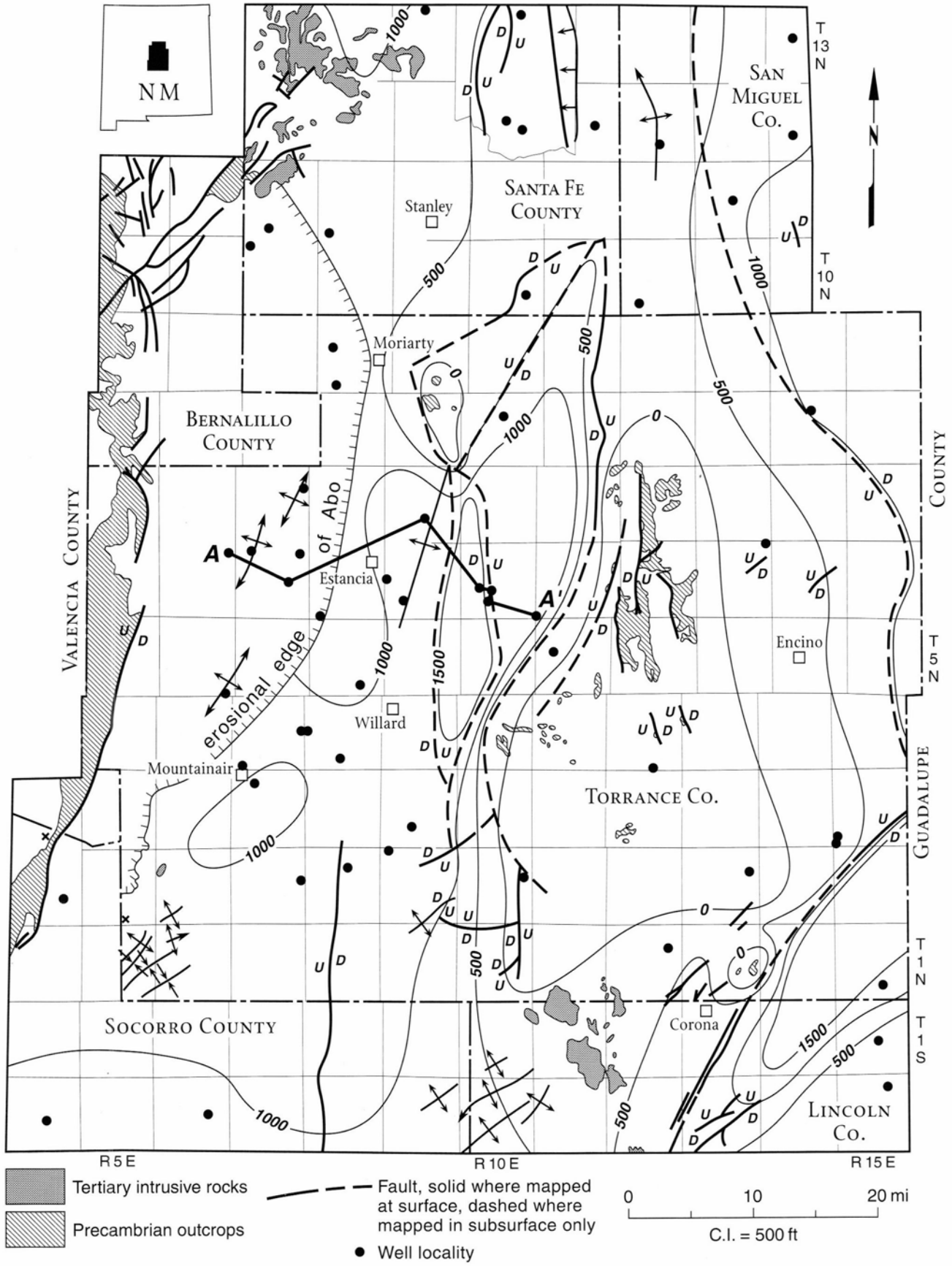

FIGURE 13—Isopach map of combined Abo and Bursum Formations (Permian), Estancia Basin. Contour interval is 500 ft.

poor reservoirs; however, they are lithologically similar to the low-permeability sandstone reservoirs in the Pecos Slope Abo gas pool of Chaves County, New Mexico (Broadhead, 1984; Bentz, 1992), and could conceivably be tight gas reservoirs.

Shales in the Abo and Bursum Formations are red to gray. More than 90% of the shales are red. The red shales are grayish red to dusky red to dark reddish brown. Almost all of the red shales are silty. Most are micaceous. They are not calcareous or appear to contain only small amounts of calcite. Some of the red shales contain rounded microcrystalline calcite nodules that may be pedogenic features.

Gray shales in the Abo and Bursum are light gray to medium gray to black. Most are silty, and they are generally not calcareous. Gray shales are present mostly in the Bursum, where they are still generally less than 10% of the drill cuttings.

The presence of limestones differentiates the Bursum from the Abo Formation. The Abo-Bursum contact is placed at the top of the highest marine limestone, which is included in the Bursum. Bursum limestones are light gray to medium gray to olive gray. Many are argillaceous lime mudstones and contain wisps, streaks, and clasts of red shale. Others are bioclastic wackestones that contain a sparse, poorly preserved, recrystallized fauna. Bursum limestones have no visual porosity and are poor reservoirs.

Yeso Formation

The Yeso Formation overlies the Abo Formation in the eastern part of the Estancia Basin. It has been eroded from the western part of the basin. Myers (1982) described the Abo-Yeso contact as gradational in the Abo Pass area at the juncture between the Manzano and Los Pinos Mountains. In the subsurface of the Estancia Basin, this contact appears to be sharp in drill cuttings and on wireline logs. If it is gradational in the subsurface, the zone of gradation is only 1-2 ft thick. East of the basin in the Pedernal Hills, Yeso shoreline sediments rest unconformably on Precambrian basement (Kottlowski, 1985).

Maximum thickness of the Yeso is 1,200 ft in the Estancia Basin. Throughout most of the basin, the Yeso is overlain unconformably by Cenozoic lacustrine and alluvial deposits; however, erosional remnants of the Glorieta Sandstone (Permian: Leonardian) overlie the Yeso in the northern part of the Estancia Basin, in the southern part of the Espanola Basin, and on Chupadera Mesa. Kelley (1972) concluded that the Yeso-Glorieta contact is disconformable but may appear gradational where the two units are composed of similar rock types.

The Yeso Formation has been subdivided into four members (ascending) in central New Mexico (Needham and Bates, 1943; Kelley and Wood, 1946; Wood and Northrop, 1946): Meseta Blanca Member, Torres Member, Cañas Gypsum Member, and Joyita Sandstone Member. Hunter and Ingersoll (1981) summarized the stratigraphy and lithology of the Yeso Formation in central New Mexico. The four members are recognizable in the subsurface of the Estancia Basin but are not correlatable to the north in the subsurface of the Espanola Basin.

Meseta Blanca Member—The Meseta Blanca Member is 30-260 ft thick in the Estancia Basin. Maximum thickness of 260 ft is in the southwest part of the basin in the Bruce Wilson No. 1X Judd well in sec. 6 T3N R7E. From there, it thins to the south, east, and north. To the west, it has been removed by erosion. In the Blue Quail Energy No. 1 Addison well in sec. 13 T2N R7E, the Meseta Blanca is only 150 ft thick. In the Abernathy and Jones No. 1 Dean well in sec. 28 T3N R9E, it is 140 ft thick. In the Perro sub-basin, it is 30-170 ft thick.

The Meseta Blanca is composed almost entirely of sandstones with a few thinly interbedded red shales. The sandstones are orange to pale red to light gray, very fine to medium grained, moderately sorted, and generally silty. They are subarkosic arenites composed mostly of quartz and feldspars. Grain-size distribution of some sandstones is bimodal with coarse clasts floating in a matrix of fine- to very fine grained sand. Meseta Blanca sandstones have 0-10% visual porosity, and reservoir quality is highly variable. Cements that occlude porosity are first-generation early-stage hematite, which imparts the red and orange colors, and later-stage syntaxial quartz overgrowths and blocky calcite.

Torres Member—The Torres Member conformably overlies the Meseta Blanca Member and is 550-930 ft thick in the Estancia Basin. It is composed of interbedded limestones, dolostones, anhydrites, shales, and sandstones. These rock types define horizontally and vertically complex facies within the Torres. The limestones are light gray to dark gray, microcrystalline, and generally dolomitic, anhydritic, and silty. Texture is compact micro-crystalline to sucrosic microcrystalline. Most of the limestones have less than 2% visual porosity. A few limestones have as much as 20% pinpoint and vugular porosity.

Dolostones in the Torres Member are yellowish brown to brownish gray and microcrystalline. They generally have a sucrosic texture. Nodules and fracture fillings of anhydrite are common. Visual porosity ranges from 0 to 10%.

Anhydrites in the Torres Member are white to light gray and are microcrystalline to macrocrystalline. The gray anhydrites are generally dolomitic; some are argillaceous. Others have very thin, alternating white and light-gray laminations.

Sandstones in the Torres Member are light brown to orange to pale red. They are fine to very coarse grained and moderately to well sorted. Most Torres sandstones are fine- to very coarse grained, silty, argillaceous, angular arkosic arenites and arkosic wackes; only trace amounts of visual porosity are present. Other sandstones are well-rounded quartz arenites that have been disaggregated into individual sand grains in drill cuttings. The rounded, disaggregated nature indicates that they probably have a large percentage of porosity and are good to excellent reservoirs. A small percentage of Torres sandstones are cemented by anhydrite and have little or no porosity.

Cañas Member—The Cañas Member of the Yeso Formation conformably overlies the Torres Member and is 0-120 ft thick in the Estancia Basin. It is thickest in the Perro sub-basin and thins to approximately 80 ft to the south and southwest. It pinches out to the east as it onlaps the Pedernal uplift.

The Callas Member is composed dominantly of anhydrite in the subsurface. In outcrops, the anhydrite has been converted to gypsum. Minor, thin-bedded, pale-red to grayish-red shales, medium-gray microcrystalline dolostones, dark-brown microcrystalline limestones, and pale-red to orange, fine-grained sandstones are also present.

Joyita Member—The Joyita Member of the Yeso Formation conformably overlies the Cañas Member and is 50-270 ft thick in the Estancia Basin. It is thickest in the Perro sub-basin. The Joyita Member is composed dominantly of white to grayish-orange to pale-red, fine- to medium-grained arkosic sandstones. Minor silty red shales and anhydrites are also present.

Glorieta Sandstone

The Glorieta Sandstone is 100-270 ft thick in the Estancia Basin. It is thickest in the southern part of the basin. The Glorieta consists of white to light-gray, fine- to medium-grained, well-sorted quartz arenites. Visual porosity ranges from 0 to 10%. The Glorieta is exposed mainly in arroyos that cut the mesas capped by the overlying San Andres. Like the overlying San Andres, it has been eroded from most of the central and western parts of the basin. Although it has good reservoir properties, the Glorieta is too shallow and crops out in too many places to form an oil and gas reservoir; however, it is one of the principal aquifers in the basin (Smith, 1957; White, 1994).

San Andres Formation

The San Andres Formation is 0-250 ft thick in the Estancia Basin. It is thickest in the southern part of the basin and thins to the north. It has been removed by Laramide and post-Laramide erosion from the central and western parts of the basin. On Chupadera Mesa the San Andres forms the caprock on many of the mesas that characterize this area. In the Estancia Basin, the San Andres consists primarily of medium-gray limestones and white to medium-gray to orange, fine- to coarse-grained sandstones. A karst topography is present on top of the San Andres (Smith, 1957). Karstic dissolution has rendered the San Andres highly permeable in some areas; however, it is too shallow and crops out in too many places to form a significant reservoir for oil and gas.

Artesia Group

Strata of the Artesia Group (Permian: Guadalupian) are present in San Miguel, easternmost Santa Fe, and northernmost Torrance Counties. The Artesia Group is present mostly east of the Pedernal Hills and northeast of Lobo Hill (Read et al., 1944; Kelley, 1972). Only local erosional remnants are present within the Estancia Basin. As mapped by Read et al. (1944), thickness varies from 0 to 150 ft. In the area covered by this report, the Artesia Group consists of red to maroon, fine-grained sandstones, siltstones, and shales.

Triassic

Triassic strata are preserved as erosional remnants in the northernmost part of the Estancia Basin. A Triassic section is also present north of Lobo Hill in the Espanola Basin and east of the Pedernal uplift in the Rowe-Mora and Tucumcari Basins. In the southern Espanola Basin in the Bar-S-Bar Ranch No. 1 Fee well, located in T12N R10E, 1,155 ft of Upper Triassic strata of the Chinle Group is present. These strata consist dominantly of grayish-red to dark reddish-brown silty shales and minor, light-gray to grayish-red, fine- to medium-grained sandstones. The lowest 205 ft is Santa Rosa Formation and consists dominantly of white to pink, fine- to medium-grained sandstones. The sandstones are poorly cemented and appear to be good reservoirs. Minor red shales are also present in the Santa Rosa. The Bar-S-Bar Ranch well is the southernmost in which Triassic strata were encountered in the Espanola and Estancia Basins.

Post-Triassic strata

Jurassic strata are present within the Espanola Basin **but** are not known to be present within the Estancia Basin. In the Transocean Oil No. 1 McKee well, located in sec. 3 T13N R9E, approximately 1,000 ft of Jurassic strata was drilled. The top of the Morrison Formation is at a depth of 2,364 ft. The top of the Todilto Limestone is at a depth of 3,270 ft. The top of the Entrada Sandstone is at a depth of 3,390 ft.

Upper Cretaceous strata have been preserved in the southern Espanola Basin but not in the Estancia Basin. In T12-13N R8-10E, 2,400 ft of Upper Cretaceous is preserved as a north-dipping wedge within the large north-dipping synclinal feature that forms the southern end of the Espanola Basin. These strata have been erosionally truncated on the southern end of this feature during the Laramide and/or post-Laramide age.

Fifteen wells have been drilled in the northern half of T13N R8E and T13N R9E in pursuit of Cretaceous oil. One well, the Black Oil No. 1 Ferrill, was drilled in 1985 and established production from Niobrara and lower Mancos shales at depths between 2,740 ft and 2,762 ft. As of December 31, 1993, cumulative production was 755 bbls.

The Estancia Basin is covered in most places by a thin veneer of Quaternary sediments. Maximum thickness of this Quaternary fill is approximately 450 ft. The Quaternary is less than 250 ft thick in most places. The Quaternary is composed of sands, gravels, silts, and clays (Smith, 1957). Most of the fill was deposited in a closed lacustrine basin during the Pleistocene. Smith (1957), Bachhuber (1982), and Johnpeer et al. (1987a, b), among others, have discussed the geology of the Quaternary fill.

Petroleum geology

Oil and gas shows

Oil and natural gases have been encountered in Pennsylvanian and Permian strata in several wells that have been drilled in the Estancia Basin (Fig. 4; Table 2, in appendix). Petroleum production has not been established in any of these wells. Carbon dioxide gas has been produced commercially from two small fields on the western flank of the basin (Fig. 4; Table 3) and is discussed separately.

Documentation of shows ranges from simple reports of "show of oil" or "show of gas" in some wells to detailed descriptions of drill-stem tests or production tests through casing perforations. The drill-stem tests and production tests provide better and more reliable documentation of shows, but other types of reports are valuable when examined critically. The report "show of oil" with-

TABLE 3—CO_2 fields in Estancia Basin. Data from Anderson (1959) and Foster and Jensen (1972).

Field	Location	Number productive wells	Average depth to production (ft)	Reservoir	Gas composition	Field status	Initial potential of individual wells, MCFD
Estancia north	secs. 12, 13 T7N R7E, Torrance Co.	7	1,260	Sandia Formation (Pennsylvanian)	98.4–99% CO_2 0.97–1.56% N_2 0.03–0.04% He	abandoned	100–869 MCFD
Estancia south	sec. 36 T7N R7E sec. 12 T6N R7E, Torrance Co.	3	1,690	schist (Precambrian) Sandia Formation (Pennsylvanian)	99% CO_2	abandoned	50–1,000 MCFD*

*Well records at the New Mexico Bureau of Mines and Mineral Resources indicate an initial potential of 50 MCFD for the Lee No. 1 Milbourne well. However, a scout report in the December 17, 1942, issue of the Oil and Gas Journal indicates an initial potential of 12 MMCFD for this well as a result of deepening to a total depth of 2,000 ft from a depth of 1,860 ft. The smaller value is probably the more correct of the two because it is similar to initial potentials for other productive CO_2 wells in the area and because the well was never offset, which would be a reasonable occurrence if a well with a potential of 12 MMCFD was completed.

out documentation of the nature of the show may be just wishful thinking by the operator, or it may be a bona fide show. Shows of oil and gas are discussed below by stratigraphic unit.

Precambrian

Several shows have been reported from Precambrian basement in the Estancia Basin (Table 2). Shows of oil and gas have been reported from schist and granite. Shows of carbon dioxide have been reported from schist. If these reports are accurate, the impermeable nature of both of these rock types indicates that fluids most likely entered the borehole through fractures. If so, then these fluids may have originated in the overlying Pennsylvanian sediments and migrated into the uppermost Precambrian through fractures connected with the Sandia Formation.

Sandia Formation and pre-Sandia Pennsylvanian strata (Pennsylvanian: Morrowan—Atokan)

Shows were reported from the Sandia Formation in the MAR Oil and Gas No. 1 Estes well (Table 2). Slight gas-cut water and carbon dioxide gas were swabbed through casing perforations at depths from 2,582 ft to 2,612 ft. It was also reported that carbon dioxide and nitrogen gas flowed through casing perforations from 2,624 ft to 2,646 ft.

One other well reported significant shows in the Lower Pennsylvanian section. The Houston Oil and Minerals No. 14-28 Federal well, located in sec. 28 T6N R10E, was drilled in the Perro sub-basin to a total depth of 8,759 ft. The top of the Pennsylvanian section (Madera Group) was encountered at a depth of 3,008 ft. The mud log indicates numerous shows of methane from 7,100 ft to 8,750 ft. As discussed in the stratigraphy section of this report, this depth interval is Morrowan to Atokan in age and therefore is Sandia or pre-Sandia in age. Although some of the shows may be merely background gas from the dark-gray to black shales in this part of the section, the mud log also indicates the presence of increased amounts of methane at depths associated with sandstone beds, indicating that the sandstones discharged methane into the drilling mud. The borehole sonic log indicates that porosities of the sandstones typically vary from 4% to 8% and that the sandstones are typically 5-10 ft thick.

Madera Group exclusive of Bursum Formation (Pennsylvanian: Desmoinesian—Virgilian)

More shows have been reported from the Madera Group than from any other stratigraphic unit in the Estancia Basin (Table 2). As is the case with the overlying Abo and Yeso Formations, many of the shows are poorly documented. Some reports are detailed enough to confirm that the shows are bona fide recoveries of hydrocarbons; these reports are discussed below.

In the MAR Oil & Gas No. 1 Estes well, located in sec. 35 T5N R8E, gas-cut water was recovered through casing perforations from 2,100 ft to 2,110 ft and from 2,252 ft to 2,258 ft; carbon dioxide gas was recovered from the deeper interval in addition to the gas-cut water. In the Forty-Eight Petroleum No. 1 Fisher Hill well, located in sec 6 T1ON R7E, a 10-ft flare of gas was reported when drilling at a depth of 1,320 ft, indicating the presence of flammable gas. Less well documented shows of oil and gas were reported from throughout the Madera in this well.

In the Blue Quail Energy No. 1 Addison well and in the Blue Quail Energy No. 1 Shaw well, located in sec. 13 T2N R7E and sec. 6 T2N R9E, crossover of the neutron and density porosity logs ("crossover effect") is present in several sandstones and limestones of the Madera. The sandstones that exhibit this crossover effect are 1-11 ft thick and have log-derived porosities that range from 0 to 15%. Limestones that exhibit crossover effect are 4-15 ft thick and have log-derived porosities that range from 0 to 8%. The magnitude of the crossover can be significant; the density log can read 2-15% more porosity than the neutron log. In many of the sandstones and limestones, the differential in porosity between the two logs is greater than 10%; this may indicate the presence of significant gas saturations. These sandstones and limestones also exhibit separation of the shallow and deep resistivity logs, indicating the presence of significant permeability. Well records do not indicate any attempt to complete depth intervals characterized by crossover effect.

Abo Formation (Permian: Wolfcampian)

No well-documented shows of either oil or gas have been reported from the Abo Formation (Permian: Wolfcampian; Table 2). Tests through casing perforations have either recovered fresh water or have resulted in a

dry swab of the wellbore. In the Blue Quail Energy No. 1 Shaw well, located in sec. 6 T2N R9E, there is crossover of the neutron and density porosity logs in numerous sandstones within the Abo, indicating the presence of gas; without a recovery and analysis of this gas, it is not possible to know whether it is hydrocarbon, nitrogen, carbon dioxide, or perhaps some other compound. The sandstones exhibiting crossover effect are 3-9 ft thick, and log-derived porosities range from 6% to 17%. The magnitude of the crossover can be significant, with the density log indicating 2-7% more porosity than the neutron log. The larger differentials may indicate fairly large gas saturations. These sandstones also exhibit separation of the shallow and deep resistivity logs, indicating the presence of significant permeability. There is no record that the sandstones exhibiting crossover effect were tested with either a drill-stem test or by perforation of casing.

Yeso Formation (Permian: Leonardian)

Numerous shows of oil and gas have been reported from the Yeso Formation (Permian: Leonardian). Most of these shows are poorly documented and therefore questionable. Many of the shows cited in Table 2 have been from shallow wells drilled on the east side of the Pedernal uplift; these wells are not located within the Estancia Basin but are mentioned because of their proximity to the basin. Most wells that have recovered formation fluids from the Yeso through drill-stem tests or casing perforations have recovered water or slight oil- and gas-cut water. Some reports describe the water as salty. The large number of well reports that describe shows in the Yeso suggests that at least some of the reported shows are valid.

Carbon dioxide occurrences

Carbon dioxide gas has been produced commercially from two small fields west of the town of Estancia (Fig. 4, Table 3). The two fields are known informally as the northern Estancia field and the southern Estancia field. The northern field was discovered in 1931 by the Sinoco No. 2 DeHart well, located in sec. 12 T7N R7E. The well was drilled to a total depth of 1,440 ft. Production was obtained from a sandstone in the Sandia Formation at a depth of 1,240 ft. Initial potential was 140 MCFD. Six additional productive wells were drilled between 1934 and 1937. Although well records are sketchy, the reservoirs for the northern field appear to be sandstones of the Sandia Formation (Foster and Jensen, 1972). The produced gas was converted into dry ice at a nearby processing plant (Anderson, 1959).

The discovery well and all other producing wells in the northern field were drilled near the crest of the Wilcox anticline (Fig. 14). This structure has been mapped at the surface as a doubly plunging anticline with 60-80 ft of structural closure (Winchester, 1933). Strata of the Madera Group crop out along the axis of the fold and are faulted at the crest. The trap appears to be structural, but the boundaries of the field were never defined by drilling (Fig. 14). It is not known if there is a stratigraphic component to trapping.

The southern Estancia field was discovered in 1928 by the Wilson No. 1-A Pace well, located in sec. 12 T6N R7E. The well was drilled to a total depth of 2,020 ft. Carbon dioxide was encountered between depths of 1,645 ft and 1,760 ft. Although data are poor, it appears that production was obtained from a sandstone in the Sandia Formation (Foster and Jensen, 1972). In all, three wells produced carbon dioxide from the southern Estancia field (Fig. 15).

The trapping mechanism at the southern Estancia field has not been defined. Existing well records are too generalized to construct local subsurface maps with sufficient detail to identify the trapping mechanism. Furthermore, the producing wells are located in an area where Quaternary sediments at the surface obscure the structure of underlying Pennsylvanian strata.

Carbon dioxide was first produced from the Estancia fields in 1934. In that year, a plant was built to convert the carbon dioxide gas into dry ice (Anderson, 1959). The plant produced dry ice until 1942. Apparently, water seeped through the well casings and limited the amount of gas that could be produced (Anderson, 1959). Cumulative production from the Estancia fields is unknown. As recently as 1963, two wells, the Meyers No. 1 Milbourne and the Meyers No. 1 Smith & Pace, were drilled to develop carbon dioxide resources in the southern Estancia field (Fig. 15). According to Foster and Jensen (1972), both wells discovered additional carbon dioxide resources, but production was never established.

Several water wells that produce from permeable zones in the Madera Group also produce or effervesce CO2 gas (Titus, 1980). These wells are located in T6-7N R7E and are structurally updip from the Estancia CO2

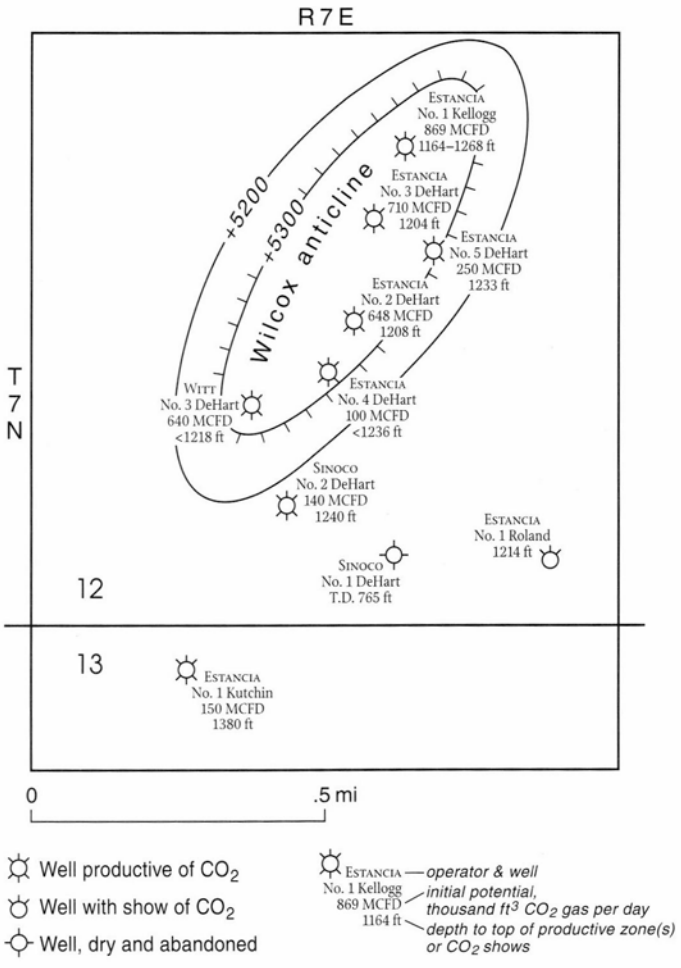

FIGURE 14—Wells in northern Estancia CO_2 field, depths to production and shows, and structure contours on top of main pay sandstone. Contour interval is 100 ft. Datum is sea level.

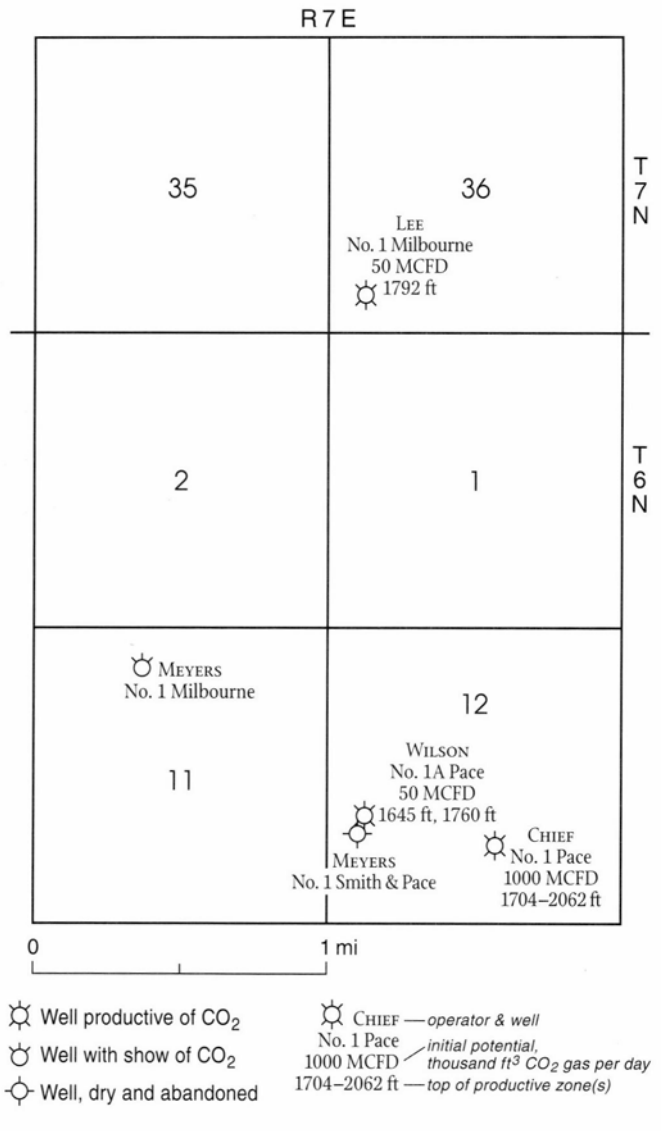

FIGURE 15—Wells in southern Estancia CO_2 field and depths to production and shows.

fields. Water is obtained from depths of 100-300 ft in these wells, more than 1,000 ft shallower than reservoir zones in the Estancia fields. Apparently, CO2-saturated water is characteristic of the Madera in this area. It is not known whether the CO2 recovered from the water wells leaks updip from the reservoirs at the Estancia fields or is hydraulically isolated from those reservoir strata and originates in the strata from which it is produced.

Petroleum source rocks

Source-rock evaluation techniques

A *petroleum source rock* can be defined as any rock that has generated *and* expelled oil and/or gas in commercial quantities (Hunt, 1979). When assessing source-rock potential, four questions must be answered (Dow, 1978; Hunt, 1979; Barker, 1980; Brooks et al., 1987). First, does the rock have sufficient organic matter? Second, is the organic matter capable of generating petroleum and, if so, is it oil prone or gas prone? Third, is the organic matter thermally mature? Fourth, have (generated) hydrocarbons been expelled from the rock?

Petroleum source rocks in the Estancia Basin were evaluated using geochemical source-rock analyses of 15 wells in the Estancia Basin, southern Espanola Basin, and northern Chupadera Mesa (Table 4, in appendix). Source-rock analyses of drill cuttings for these wells are available as open-file reports of the New Mexico Bureau of Mines and Mineral Resources (Table 4). Analyses of eight of the wells were performed for the Bureau as part of the New Mexico Bureau of Mines and Mineral Resources Petroleum Source Rock Project, an effort funded jointly by the state and private industry. Analyses of the other seven wells were performed by independent oil operators and donated to the Bureau for public use.

The analyses done as part of the Source Rock Project were standardized, and the following procedures were performed on each sample of cuttings: 1) lithologic description, 2) total organic carbon (TOC), 3) Thermal Alteration Index (TAI) determined by petrographic analysis of kerogen concentrate, 4) kerogen type determined by petrographic analysis of kerogen concentrate, and 5) Rock-Eval pyrolysis. Cuttings were obtained from the cuttings collection of the New Mexico Bureau of Mines and Mineral Resources Subsurface Library. In order to preserve the integrity of the archived cuttings, analyses were made on composite samples from several vertically continuous 10-ft sample intervals. For most wells, cuttings were sorted and picked under a binocular microscope to exclude nonsource rock types (e.g. sandstone) and to ensure that only one type of possible source rock (e.g. shale or limestone) was analyzed.

Donated analyses were nonstandardized. Most of these analyses were restricted to measurements of TOC and Rock-Eval pyrolysis. As a result, their value for source-

TABLE 5—Qualitative evaluation of source-rock potential as a function of TOC content. From Jarvie (1991).

Source-rock rating	TOC %
Inadequate	0–0.5
Marginal	0.5–1.0
Adequate	>1.0

rock interpretation is more limited than analyses performed as part of the Source Rock Project. In addition, analyses were made on all rock types present within the sampled intervals; nonsource rocks were not excluded. As a result, interpretation is more difficult and less certain.

The question of whether or not the rock has sufficient organic matter to be a source rock can be answered on the basis of TOC measurements. Rocks that have insufficient TOC content can be ruled out as possible source rocks. Jarvie (1991) has recently proposed a modified TOC rating system for screening potential source rocks (Table 5). According to this system, any rock with more than 0.5% TOC is a possible source rock that must be evaluated to answer the other three questions.

For wells analyzed as part of the Petroleum Source Rock Project, interpretation of TOC analyses was fairly straightforward. As discussed above, only cuttings judged to be potential source rocks were analyzed. Therefore, the TOC measurements are considered to approximate the average TOC content of possible source rocks over the sampled interval. For wells that were not part of the Source Rock Project, interpretation of TOC analyses was more difficult. These wells have nonsource rocks, such as sandstones and oxidized red shales, mixed in with source rocks in the samples. Because the non-source rocks contain little or no TOC, the analytical results for the bulk sample will show less TOC than is present within the source rocks alone. For some of these samples, an estimate of percentage of various rock types present within each sample was available. TOC values were corrected using the assumption that the nonsource rocks contain no TOC. This correction results in only a rough approximation of the TOC present within possible source rocks and possibly over estimates TOC because it neglects the small amounts of organic carbon present in the nonsource rocks. If used carefully, however, it probably results in a more appropriate value than the raw TOC measurement. The corrected value of TOC establishes an upper limit for the true TOC content of the rock.

The second question asks what type of organic matter

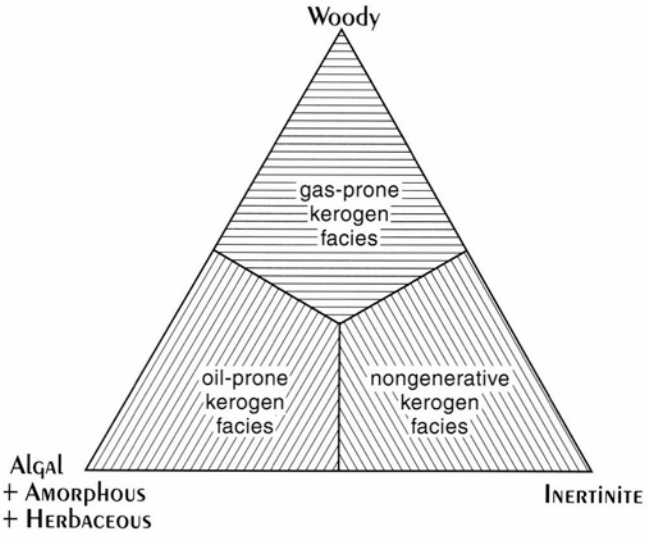

FIGURE 16—Kerogen facies determined from visual petrographic identification of kerogen types.

is present within the rock. The type of organic matter, if present in sufficient quantity, will determine if a source rock will produce principally oil or principally gas upon maturation (Table 6). For this study, identification of organic-matter type was based mainly on the petrographic analyses of kerogen concentrate. Algal, herbaceous, and much amorphous kerogen (kerogen types I and II) will generate oil and associated gas upon maturation (Hunt, 1979; Brooks et al., 1987; Tyson, 1987). Woody kerogen and some amorphous kerogen (kerogen type III) will generate gas and possibly a minor amount of oil or gas condensate upon maturation (Table 6; Hunt, 1979; Brooks et al., 1987; Tyson, 1987). Inertinites are type IV kerogens that have extremely low hydrogen contents and are incapable of generating significant amounts of hydrocarbons. Petrographic analyses of kerogen composition were plotted on a ternary diagram (Fig. 16) with these three endpoints: 1) oil- *and* gas-prone kerogens (algal + amorphous + herbaceous), 2) gas-prone kerogens (woody), and 3) nongenerative kerogens (inertinite). As a first approximation, the ternary diagram can be divided into three *kerogen facies:* 1) an *oil-prone kerogen facies* consisting mostly of algal, amorphous, and herbaceous kerogens; 2) a *gas-prone kerogen facies* consisting mostly of woody kerogens; and 3) a *nongenerative kerogen facies* consisting mostly of inertinite. Recent studies suggest that

TABLE 6—Kerogen types and petroleum products produced upon thermal maturation. Based on summary works of Merrill (1991) and Tyson (1987).

General kerogen type	Kerogen type	Petrographic form	Coal maceral group	Hydrocarbons generated
Sapropelic (oil prone)	I	Algal	Exinite or liptinite	Oil, gas
	II	Amorphous		
		Herbaceous		
Humic (gas prone)	III	Woody	Vitrinite or huminite	Gas, possibly minor oil
	IV	Coaly (inertinite)	Inertinite	None

some woody kerogens can generate significant amounts of oil under the right conditions (Powell and Boreham, 1994; MacGregor, 1994). Although it is possible to differentiate kerogen types I, II, and III on the basis of RockEval pyrolysis (e.g. Tissot and Welte, 1978; Peters, 1986), some type **III** kerogens may be confused with other types of kerogen and result in misleading characterization of kerogen types when using pyrolysis (Tyson, 1987). Also, pyrolysis can not discern the different varieties of kerogens present in samples with mixed kerogen assemblages because the analysis of a single sample results only in one set of measurements. For these reasons, RockEval pyrolysis was used only as reinforcement for petrographically determined kerogen identification.

The relative proportions of organic materials present are also important in determining the oil and gas potential of a source rock (Cornford, 1984; Brooks et al., 1987). For example, a shale with 4% TOC composed of 50% algal matter and 50% woody matter has the equivalent oil-generating potential of a shale with 2% TOC that is entirely algal matter. On the other hand, a shale with 2% TOC that is 95% inertinite and 5% herbaceous matter is equivalent to a shale with only 0.1% herbaceous matter for purposes of oil generation; this is below the 0.5% threshold of TOC thought to be required for source-rock status. Because the inertinite can not generate hydrocarbons (at least not in commercial amounts), this shale is not a source rock, even though it has 2% TOC.

The level of thermal maturity was evaluated using visual kerogen analyses. For the Petroleum Source Rock Project, the color of the kerogen concentrate was analyzed; the kerogen color changes from yellow to orange to brown to black with increasing maturation (Staplin, 1969). Based on calibrated color charts, the sample is then assigned a numerical value (Thermal Alteration Index, abbreviated TAI), which ranges from 1.0 (immature) to 5.0 (metamorphosed; Table 7).

Rock-Eval pyrolysis can also be used to evaluate thermal maturity. The temperature at which the maximum amount of hydrocarbons is generated from the S2 peak (TMAX, °C) has been correlated to thermal maturation of the source rock (Peters, 1986; Table 7). This method, however, does not give as complete an evaluation of maturi

TABLE 7—Correlation of maturation parameters used in this report with zones of hydrocarbon generation. Based on Geochem Laboratories, Inc. (1980), Sentfle and Landis (1991), and Peters (1986).

Maturation level (products generated)	Visual kerogen Thermal Alteration Index (TAI)	Rock-eval TMAX (°C)
Immature (biogenic gas)	1.0–1.7	
Moderately immature (biogenic gas and immature oil)	1.8–2.1	<435
Moderately mature (immature heavy oil)	2.2–2.5	
Mature (mature oil condensate)	2.6–3.5	435–470
Very mature (condensate, wet gas, petrogenic dry gas)	3.6–4.1	
Severely altered (petrogenic methane)	4.2–4.9	>470
Metamorphosed	5.0	

ty as TAI and only places a sample as being within, above, or below the oil zone. Also, the measured value of TMAX is partially dependent upon the type of organic matter present, as well as numerous other factors (Peters, 1986). Furthermore, if the $_{S2}$ peak (the quantity of kerogen that is pyrolyzed to bitumen) is less than 0.2 mg hydrocarbon per gram of rock, values of TMAX will be inaccurate (Peters, 1986); this is the case for many of the Rock-Eval analyses available for the Estancia Basin. Therefore, in this study, thermal maturation was determined mainly from TAI values. Rock-Eval methods were used only in the absence of TAI data and then only with care and only in those samples with a sufficiently large S2 peak.

The fourth question concerns the expulsion of generated hydrocarbons from the source rock. This question is more difficult to answer than the other three questions. For the most part, studies of thermal maturity of source rocks are empirically correlated with the presence of oil in associated reservoirs. It is generally assumed that once hydrocarbons have been generated within the source rock they will be expelled and will migrate into reservoirs. It is also thought that source rocks that are thinly interbedded with reservoirs will expel hydrocarbons at lower levels of maturity than thick source rocks that contain few or no interbedded reservoirs (Leythauser et al., 1980; Cornford et al., 1983). These latter types of rocks may only act as source rocks when they have reached the *mature stage* of generation, whereas rocks thinly interbedded with reservoirs may act as source rocks when they have reached a lower level of maturity, possibly the *moderately mature stage* of oil generation.

Pennsylvanian (Sandia Formation and Madera Group, exclusive of Bursum Formation)

The Pennsylvanian section contains the only identified petroleum source rocks within the Estancia Basin. In several of the analyzed wells, the average measured TOC content of samples from the Pennsylvanian exceeded the minimum requirement of 0.5% necessary for evaluation (Table 4). Maximum TOC values approximate 1% in several wells and approach 2% in several wells, including the Houston Oil and Minerals No. 14-28 Federal, which is located in the Perro sub-basin. In this well, the average measured TOC content is 0.48%, but the average TOC content corrected for the presence of sandstones in the samples is 0.91%, adequate for hydrocarbon generation. Maximum corrected TOC content in the Houston Oil and Minerals well is 2.5%, which is more than sufficient for generation of hydrocarbons in commercial quantities, providing that the rocks are thermally mature. Average corrected TOC values for three wells (Superior No. 28-31 Blackwell, Olsen No. 1 Means, and Gardner No. 1 Kidwell) exceed values from wells with picked and sorted samples by a factor of two or three (Table 4). These corrections are probably too large and result in unrealistically high TOC values; therefore, they are not used in this report. In any case, gray to black shales in the Pennsylvanian contain sufficient TOC to be source rocks, both on the shelf and in the Perro sub-basin.

Both the oil-prone and gas-prone kerogen facies are present within Pennsylvanian strata in the Estancia Basin (Figs. 17, 18). The gas-prone kerogen facies is present within the Perro sub-basin. In the Houston Oil and Minerals No. 14-28 Federal well, woody kerogens are dominant in all samples that were analyzed (Fig 18C).

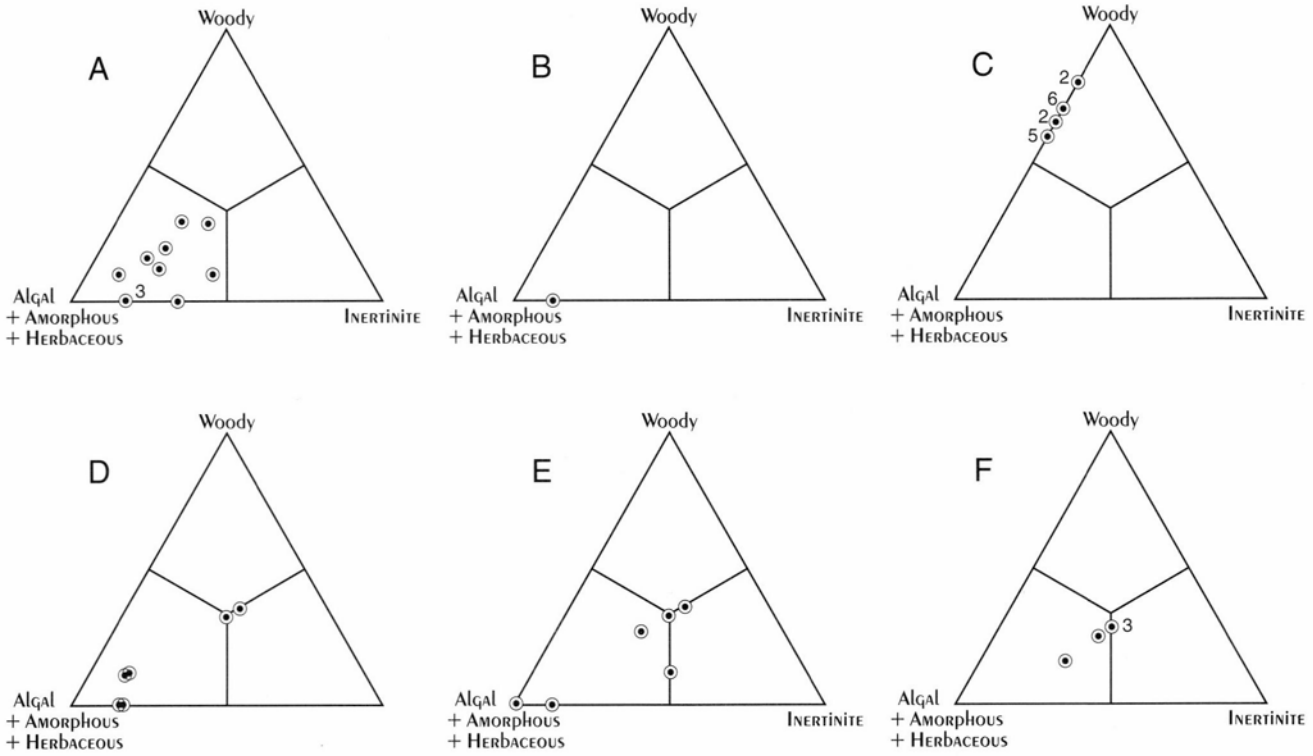

FIGURE 18—Kerogen composition of samples from Pennsylvanian section, Estancia and southern Española Basins. Based on visual petrographic identification of kerogen types. Numbers indicate multiple samples with a given composition. A. Transocean Oil Co. No. 1 McKee well, sec. 4 T13N R9E; B. Bar-S-Bar Ranch No. 1 Fee well, sec. 23 T12N R10E; C. Houston Oil and Minerals No. 14-28 Federal well, sec. 28 T6N R10E; D. Witt Ice Co. No. 1 Meadows well, sec. 23 T6N R7E; E. MAR Oil and Gas No. 1 Estes well, sec. 35 T5N R8E; F. Blue Quail Energy No. 1 Addison well, sec. 13 T2N R7E.

Inertinites are present in trace amounts or are absent completely. The oil-prone fraction is less than one-third of total kerogen in most samples and consists mostly of herbaceous material (cuticle and membranous debris and spores) and only minor amounts of amorphous—sapropelic debris. The dominance of the woody kerogens and almost complete absence of aquatic kerogens, along with the lithologic composition, indicate that Pennsylvanian strata in the Perro sub-basin were deposited in a nonmarine to marginal marine environment (perhaps paludal) or in marine environments characterized by deposition of large amounts of land-derived sediments and kerogens.

The oil-prone kerogen facies is dominant on the shelf areas west and south of the Perro sub-basin (Figs. 17, 18). In wells on the more northerly parts of the shelf in the Estancia and southern Espanola Basins (Bar-S-Bar Ranch No. 1 Fee, Castle and Wigzell No. 1 Kelly Federal, Witt Ice No. 1 Meadows, and Transocean No. 1 McKee), most or all of the samples belong to the oil-prone facies, and in many samples, the kerogens are more than 70% amorphous—sapropelic and herbaceous kerogen (Figs 18A, B, D). In this area, most generated hydrocarbons will be oil and associated gas.

On the southern part of the shelf (Blue Quail Energy No. 1 Addison, MAR Oil and Gas No. 1 Estes, Virgle Landreth No. 1 Panhandle A, and James K. Anderson No. 1 Wishbone Federal; Figs. 17, 18E, 18F), most kerogen samples belong to the oil-prone facies; however, they contain appreciably more woody and inertinitic kerogens than samples on the northern shelf. Many of the samples are borderline between the oil-prone, gas-prone, and nongenerative facies. In this area, any generated hydrocarbons will be primarily oil and associated gas, but significant nonassociated gas may have been generated in strata where a fairly large percentage of woody kerogens are present. In strata where the inertinitic fraction is sufficiently large and the TOC sufficiently low, there may not be sufficient oil- or gas-prone kerogen to generate hydrocarbons in commercial quantities. Overall, however, oil and associated gas would have been generated from thermally mature shales and carbonates in shelf areas of the Estancia Basin.

Thermal maturity of Pennsylvanian strata in the Estancia Basin ranges from moderately immature to mature but is moderately mature to mature in most wells (Figs. 19, 20). The Thermal Alteration Index (TAI) ranges from 1.9 (moderately immature) in the uppermost Pennsylvanian in the MAR Oil and Gas No. 1 Estes well to 3.2 (mature) in the Blue Quail Energy No. 1 Addison well (Table 4). Maximum TAI ranges from 2.3 (moderately mature) to 3.2 (mature) throughout the basin (Fig. 19).

Source rocks are thermally mature (TAI > 2.6) within the deeper parts of the Perro sub-basin and on the western part of the shelf (Figs. 19, 20). Within the Perro sub-basin, thermal maturation is depth dependent; the lowermost 2,000 ft of the Pennsylvanian are thermally mature. In the Houston Oil and Minerals No. 14-28

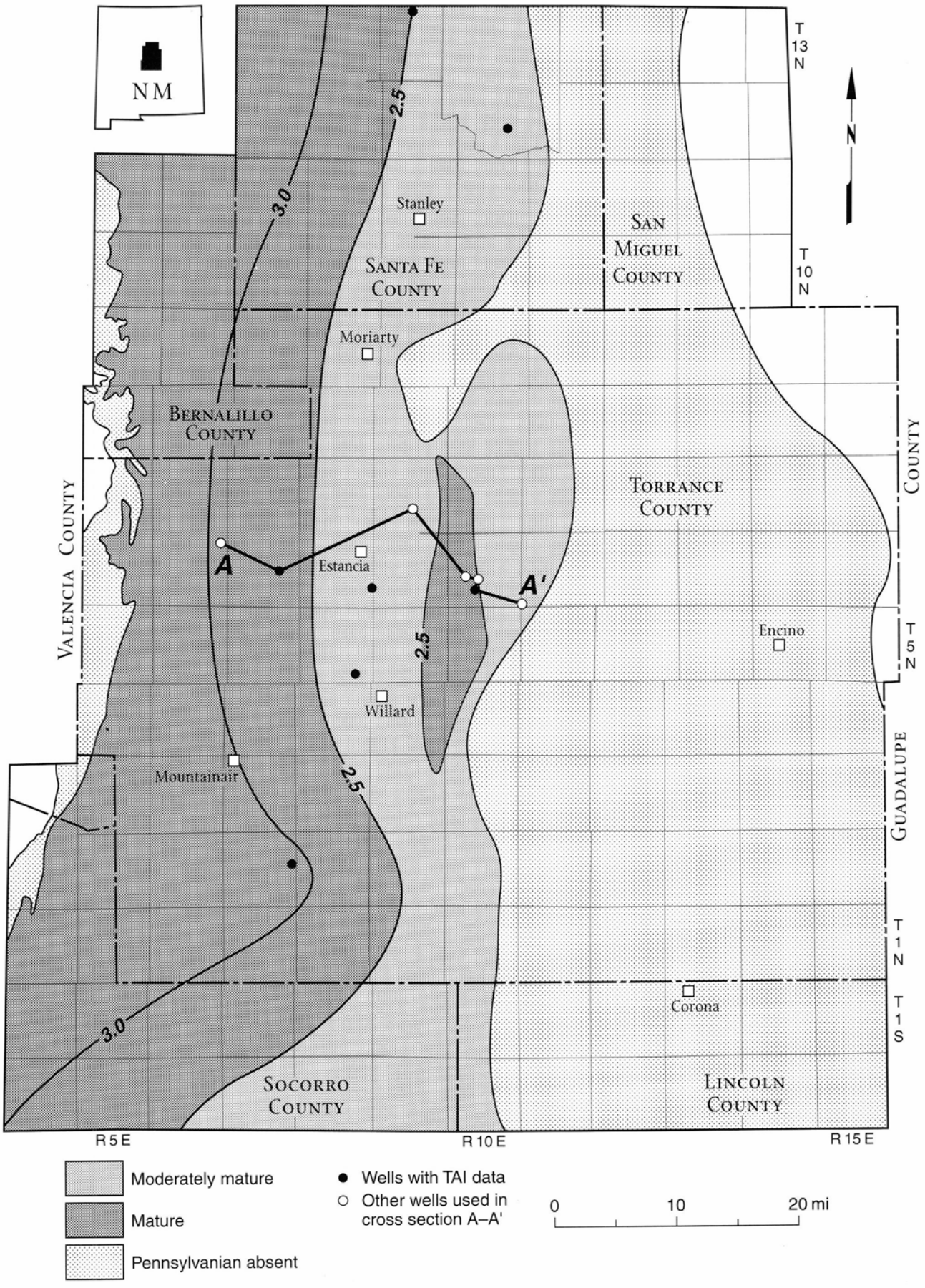

FIGURE 19—Maximum thermal maturity of Pennsylvanian strata, Estancia Basin. Contours are Thermal Alteration Index (TAI).

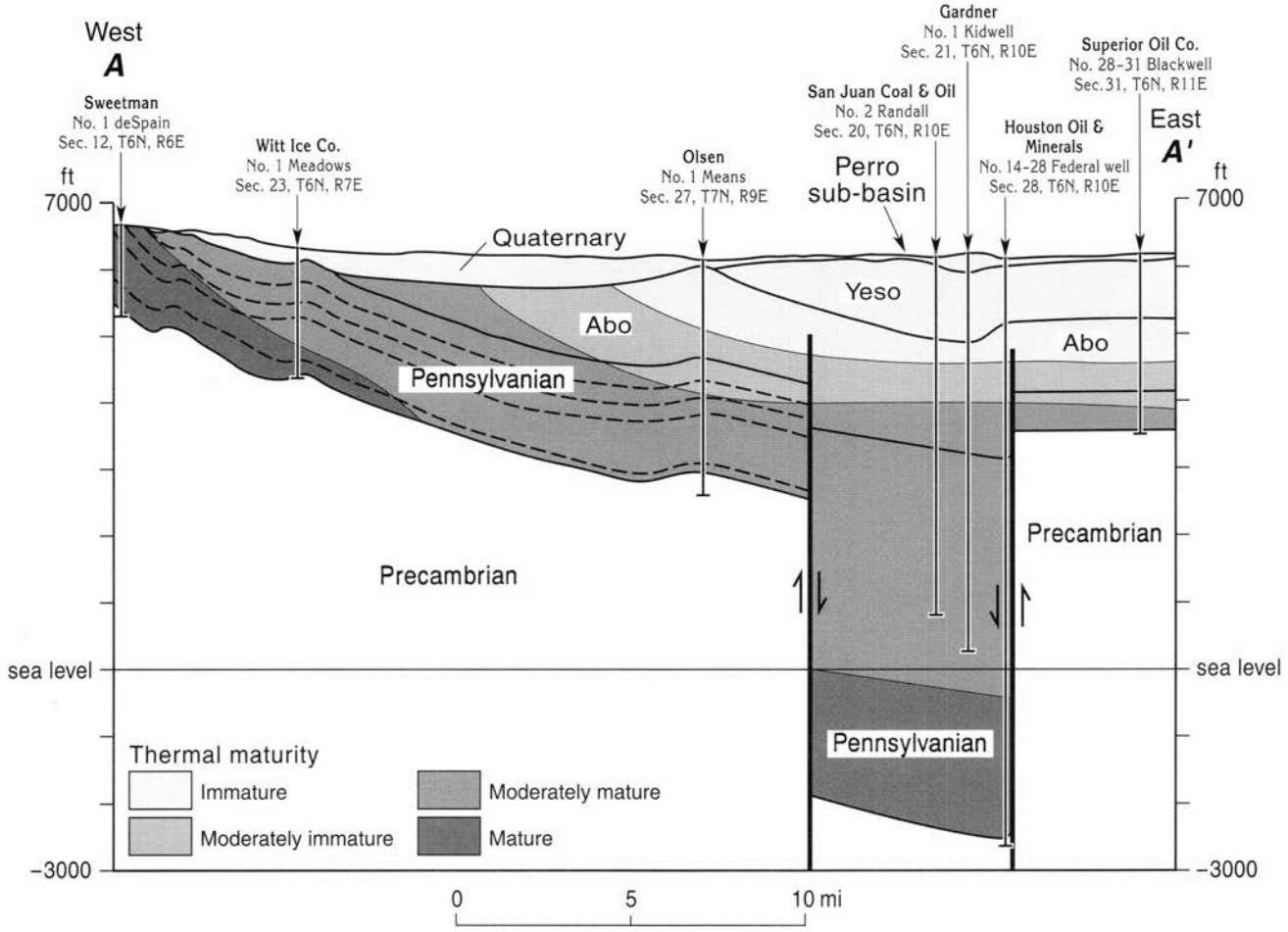

FIGURE 20—East–west structural cross section A–A' through Estancia Basin, showing thermal maturity of Paleozoic section.

Federal well, maximum TAI is 2.8, indicating that maturation has reached the upper part of the oil window, but the stage of peak oil generation has not been reached. The presence of erosional remnants of the San Andres Formation and Artesia Group (Permian), Chinle Group (Triassic), and Upper Cretaceous lithostratigraphic units indicates that a substantial, but unknown, thickness of Permian, Triassic, and Upper Cretaceous strata once covered the Estancia Basin but has been removed by erosion. If this is the case, then strata were once buried more deeply than they are at present, and thermal maturation will be greater than expected from present burial depth and present geothermal gradients. Kelley et al. (1992) concluded that thermal cooling in the region variably began during the early part of the Laramide orogeny, during Eocene erosion, and during early extension of the Rio Grande rift and/or waning of regional volcanism in the late Oligocene and early Miocene. If so, then maximum heating and approximate maximum hydrocarbon generation due to burial presumably occurred before these cooling events in the Tertiary. Perhaps maximum burial occurred during the Late Cretaceous with deposition of sediments in the Cretaceous interior seaway.

On the western shelf, thermal maturity of Pennsylvanian strata is not primarily depth dependent. In this area, thermal maturity increases westward (Figs. 19, 20) and for the most part is independent of present burial depth or paleo-burial depth. On the eastern part of the shelf, in the Virgle Landreth No. 1 Panhandle A, MAR Oil and Gas No. 1 Estes, and the Bar-S-Bar Ranch No. 1 Fee wells, the Pennsylvanian section is moderately mature, and the maximum TAI ranges from 2.2 to 2.3. Maturation increases to the west. On the western part of the shelf, in the James K. Anderson No. 1 Wishbone Federal, the Blue Quail Energy No. 1 Addison, and the Witt Ice No. 1 Meadows wells, the Pennsylvanian section is thermally mature, and the maximum TAI ranges from 2.6 to 3.2. In each well, thermal maturation increases with depth.

The cause of the westward increase in thermal maturation of Pennsylvanian strata is equivocal. A lack of correlation with present burial depth is obvious. A lack of correlation with paleo-burial depths can only be surmised but is still fairly well established. There is no indication within the sedimentary record that a large sedimentary pile existed over the western part of the basin during the late Paleozoic. If anything, thickness of the Paleozoic section increased to the east with proximity to the Pedernal uplift and decreased to the west with increasing distance from the sedimentary source area. Furthermore, regional depositional models and stratigraphic correlations for the Triassic (Lucas, 1991; Lucas et al., 1994), the Jurassic (Kocurek and Dott, 1983), and the Cretaceous (Bilodeau and Lindberg, 1983; Molenaar and Rice, 1988) indicate that no anomalously thick sedimentary pile was present

in the western Estancia Basin during the Mesozoic.

The most likely cause of the westward increase in thermal maturity of the Pennsylvanian section is a heating event associated with the Rio Grande rift. Contours of TAI (Fig. 19) are approximately parallel to the eastern boundary of the Albuquerque Basin segment of the rift and the mountain ranges that form the eastern boundary. This contour pattern is consistent with maturation from heat that emanated from the rift, rather than from heat associated with burial. Present-day heat flow in the rift basin is higher than present-day heat flow east and west of the rift (Reiter, 1986). This, in conjunction with volcanism associated with early-phase rifting (Chapin and Seager, 1975; Kelley et al., 1992), may have elevated temperatures in the western Estancia Basin, resulting in thermally mature petroleum source rocks in the oil window.

Permian

Abo and Bursum Formations (Wolfcampian)

The Abo and Bursum Formations contain no identified petroleum source rocks in the Estancia Basin. As discussed above, these stratigraphic units consist mostly of red shales and fine-grained sandstones and minor light-gray shales and limestones. The red and gray shales and limestones contain insufficient TOC to be source rocks. For all samples analyzed, maximum TOC was 0.37% (Table 4), which is below the 0.5% threshold value believed necessary for generation of hydrocarbons in commercial quantities. In most samples, TOC is less than 0.2%.

Yeso Formation (Leonardian)

The Yeso Formation does not appear to contain petroleum source rocks in the Estancia Basin. Only a few samples from the Yeso have been analyzed for source-rock parameters because of the limited areal extent and shallow depths of the Yeso. All samples analyzed contained less than 0.5% TOC (Table 4). Based on limited analyses of Yeso samples, it appears that this stratigraphic unit contains insufficient TOC to generate hydrocarbons in commercial quantities. Furthermore, the limited analyses indicate that maximum maturation is in the moderately mature stage of petroleum generation. The presence of thermally immature Abo in the MAR Oil and Gas No. 1 Estes well probably indicates a thermally immature Yeso throughout a large part of the Estancia Basin.

Post-Leonardian strata

Strata that overlie the Yeso Formation were not analyzed for source-rock parameters. The shallow depths of these strata virtually preclude their importance as source rocks. As previously discussed, many of these stratigraphic units are present only as erosional remnants at or near the surface. Furthermore, the lack of maturity of the underlying Abo and Yeso Formations suggests that these strata are thermally immature. The exception to this may be the Upper Cretaceous strata in the southern Espanola Basin; the discovery of oil by the Black Oil No. 1 Ferrill well suggests that the Upper Cretaceous may be thermally mature in the Espanola Basin and therefore indicates that strata in that basin were once buried more deeply than equivalent strata in the Estancia Basin.

Summary of petroleum potential

The Pennsylvanian section (Sandia Formation and Madera Group exclusive of Bursum Formation) of the Estancia Basin has the three fundamental ingredients for the entrapment of commercial quantities of hydrocarbons: reservoir rocks, thermally mature source rocks, and the setting for structural and/or stratigraphic traps. Any hydrocarbons present within the Perro sub-basin will probably be nonassociated gas; whereas, hydrocarbons present on the shelf will most likely be oil and associated gas.

In the Perro sub-basin, reservoirs are fine- to coarse-grained quartz arenites and subarkosic arenites. Porosities generally appear to be fairly low, so permeabilities will also probably be low. Traps may be either the stratigraphic types associated with nonmarine and marginal marine facies or, more probably, they will be the structural traps associated with deformation in strike-slip settings, which the Perro sub-basin appears to represent (see Harding and Lowell, 1979, for examples of these types of structural traps). Source rocks are thermally mature in the structurally lower parts of the sub-basin. Their content of primarily woody kerogens indicates that they have generated gas with only small amounts of liquid hydrocarbons. Several gas shows have been documented in the only well to drill to Precambrian, the Houston Oil and Minerals No. 14-28 Federal. This well was drilled very close to the master fault that forms the eastern margin of the Perro sub-basin. It is possible that the well intersected joints and ancillary faults associated with this master fault and that these fractures may have destroyed the integrity of hydrocarbon traps at the location of the well. If true, then traps may remain intact to the west within the interior of the Perro sub-basin.

On the shelf, reservoirs are mostly fine- to coarse-grained subarkosic arenites and quartz arenites. Reservoir quality is variable. Porosity ranges from 0% to as high as 16% and averages approximately 10% in most sandstones. Most of the limestones on the shelf have less than 5% porosity, have low permeability, and are poor reservoirs; however, algal grainstones and recrystallized lime mudstones appear locally to form good reservoirs.

Traps on the shelf may be either stratigraphic or structural. Localized stratigraphic traps may be present in high-porosity, high-energy carbonate grainstones, which form good reservoirs. The northeast-trending anticlines on the western flank of the basin are thought to form traps for CO2 gas at the now-abandoned Estancia fields. Other anticlines undoubtedly exist that have either not been mapped at the surface or remain hidden below the Quaternary sediments of the Estancia Valley. It is also conceivable that combination structural—stratigraphic traps were formed by updip pinchouts of sediments on the east-dipping western flank of the basin.

Thermally mature source rocks of both oil and gas are present on the shelf as gray to black shales. The presence of the most mature source rocks in the western, updip part of the shelf limits the most favorable exploratory opportunities to this area. It is not impossible that some-

what less mature source rocks that are thinly interbedded with reservoirs have generated commercial hydrocarbons in downdip areas to the east. Source rocks throughout the shelf of the Estancia Basin contain predominantly an oil-prone suite of algal, amorphous, and herbaceous kerogens; gas-prone woody kerogens and nongenerative inertinites form a subsidiary suite of kerogens and are not of primary consideration when evaluating petroleum potential.

The presence of CO2 accumulations at the Estancia fields almost certainly limits the opportunities for hydrocarbon exploration. The source of the CO2 is enigmatic; therefore, it is difficult to determine the parts of the basin that may be CO2 prone and the parts that may be hydrocarbon prone. Carbon dioxide shows, however, are limited to the area around the Estancia fields (Fig. 4). It appears that the remainder of the Estancia Basin is devoid of significant amounts of CO2; therefore, it would seem that most of the basin is hydrocarbon prone.

The Abo and Yeso Formations (Permian) have limited oil and gas potential. Although both formations contain reservoir rocks, they do not contain strata with either sufficient TOC or sufficient thermal maturity to be source rocks. It is possible, however, that hydrocarbons generated in the underlying Pennsylvanian section migrated vertically through faults into the Abo or Yeso sections. If so, then Yeso sandstones could be reservoirs for either oil or gas. The low-permeability Abo sandstones are possible reservoirs for gas but not for oil. In the Perro sub-basin, the Yeso bears a significant evaporite section that could act as a barrier to vertical migration and a seal for fractures and faults.

Pipelines

Should hydrocarbon gases be discovered in the basin, there is fairly ready access to major markets. Two major natural gas pipelines cross the southern part of the basin (Fig. 1). Construction of a gas-gathering system that could feed one or both of these pipelines should be relatively inexpensive. Also present is a pipeline that transports CO2 from the McElmo Dome CO2 field in southwestern Colorado to enhanced oil recovery projects in the Permian Basin. Depending upon market demands and pipeline capacity, any CO2 discoveries in the Estancia Basin could conceivably become economically viable projects.

References

Anderson, E. C., 1959, Carbon dioxide in New Mexico (1959): New Mexico Bureau of Mines and Mineral Resources, Circular 43,13 pp.

Armstrong, A. K., 1955, Preliminary observations on the Mississippian System of northern New Mexico: New Mexico Bureau of Mines and Mineral Resources, Circular 39,42 pp.

Armstrong, A. K., 1967, Biostratigraphy and carbonate facies of the Mississippian Arroyo Peñasco Formation, north-central New Mexico: New Mexico Bureau of Mines and Mineral Resources, Memoir 20,79 pp.

Armstrong, A. K., and Mamet, B. L., 1974, Biostratigraphy of the Arroyo Peñasco Group, Lower Carboniferous (Mississippian), north-central New Mexico; *in* Siemers, C. T., Woodward, L. A., and Callender, J. F (eds.), Ghost Ranch—central-northern New Mexico: New Mexico Geological Society, Guidebook 25, pp. 145-158.

Armstrong, A. K., Kottlowski, E E., Stewart, W. J., Mamet, B. L., Baltz, E. H., Jr., Siemers, W. T., and Thompson, S., III, 1979, The Mississippian and Pennsylvanian (Carboniferous) Systems in the United States—New Mexico: U.S. Geological Survey, Professional Paper 1110-W, 26 pp.

Armstrong, D. G., and Holcombe, R. J., 1982, Precambrian rocks of a portion of the Pedernal Highlands, Torrance County, New Mexico; *in* Grambling, J. A., and Wells, S. G. (eds.), Albuquerque country II: New Mexico Geological Society, Guidebook 33, pp. 203-210.

Bachhuber, F. W., 1982, Quaternary history of the Estancia Valley, central New Mexico; *in* Grambling, J. A., and Wells, S. G. (eds.), Albuquerque country II: New Mexico Geological Society, Guidebook 33, pp. 343-346.

Barker, C., 1980, Organic geochemistry in petroleum exploration: American Association of Petroleum Geologists, Continuing education course note series, no. 10,159 pp.

Barrow, R., and Keller, G. R., 1994, An integrated geophysical study of the Estancia Basin, central New Mexico; *in* Keller, G. R., and Cather, S. M., (eds.), Basins of the Rio Grande rift: structure, stratigraphy, and tectonic setting: Geological Society of America, Special Paper 291, pp. 171-186.

Bates, R. L., Wilpolt, R. H., MacAlpin, A. J., and Vorbe, G., 1947, Geology of the Gran Quivira quadrangle, New Mexico: New Mexico Bureau of Mines and Mineral Resources, Bulletin 26, 52 pp.

Bauer, P. W., and Williams, M. L., 1985, Structural relationships and mylonites in Proterozoic rocks of the northern Pedernal Hills, central New Mexico; *in* Lucas, S. G. (ed.), Santa Rosa-Tucumcari region: New Mexico Geological Society, Guidebook 36, pp. 141-145.

Beck, W. C., and Chapin, C. E., 1991, Structural data from the Joyita uplift: implications for ancestral Rocky Mountain deformation within central and southern New Mexico; *in* Barker, J. M., Kues, B. S., Austin, G. S., and Lucas, S. G. (eds.), Geology of the Sierra Blanca, Sacramento and Capitan Ranges, New Mexico: New Mexico Geological Society, Guidebook 42, pp. 183-190.

Beck, W. C., and Chapin, C. E., 1994, Structural and tectonic evolution of the Joyita Hills, central New Mexico: Implications of basement control on Rio Grande rift; *in* Keller, G. R., and Cather, S. M., (eds.), Basins of the Rio Grande rift: structure, stratigraphy, and tectonic setting: Geological Society of America, Special Paper 291, pp. 187- 205.

Bentz, L. M., 1992, Pecos Slope field U.S.A., Permian Basin, New Mexico; *in* Foster, N. H., and Beaumont, E. A. (comps.), Stratigraphic traps III: American Association of Petroleum Geologists, Treatise of petroleum geology, Atlas of oil and gas fields, pp. 129-153.

Bilodeau, W. L., and Lindberg, F A., 1983, Early Cretaceous tectonics and sedimentation in southern Arizona, southwestern New Mexico, and northern Sonora, Mexico; *in* Reynolds, M. W., and Dolly, E. D. (eds.), Mesozoic paleogeography of the west-central United States: Society of Economic Paleontologists and Mineralogists, Rocky Mountain Section, pp. 173-188.

Broadhead, R. F, 1984, Stratigraphically controlled gas production from Abo red beds (Permian), east-central New Mexico: New Mexico Bureau of Mines and Mineral Resources, Circular 183,35 pp.

Broadhead, R. F., 1994, Petroleum geology of the Estancia Basin, New Mexico: an exploration frontier (abs.): American

Association of Petroleum Geologists, Bulletin, v. 78, p. 493.
Brooks, J., Cornford, C., and Archer, R., 1987, The role of hydrocarbon source rocks in petroleum exploration; *in* Brooks, J., and Fleet, A. J. (eds.), Marine petroleum source rocks: Geological Society of London, Special Publication 26, pp. 17-46.
Chapin, C. E., 1971, The Rio Grande rift, part I: modifications and additions; *in* James, H. L. (ed.), Guidebook of the San Luis Basin, Colorado: New Mexico Geological Society, Guidebook 22, pp. 191-201.
Chapin, C. E., and Cather, S. M., 1981, Eocene tectonics and sedimentation in the Colorado Plateau-Rocky Mountain area: Arizona Geological Society, Digest, v. 14, pp. 173-198.
Chapin, C. E., and Seager, W. R., 1975, Evolution of the Rio Grande rift in Socorro and Las Cruces areas: New Mexico Geological Society, Guidebook 26, pp. 297-321.
Cordell, L., 1983, Composite residual total intensity aeromagnetic map of New Mexico: New Mexico State University, Energy Institute, Geothermal resources map of New Mexico, scale 1:500,000.
Cornford, C., 1984, Source rocks and hydrocarbons of the North Sea; *in* Glennie, K. W. (ed.), Introduction to the petroleum geology of the North Sea: Blackwell Scientific Publications, London, pp. 197-236.
Cornford, C., Morrow, J., Turrington, A., Miles, J. A., and Brooks, J., 1983, Some geological controls on oil composition in the North Sea; *in* Brooks, J. (ed.), Petroleum geochemistry and exploration of Europe: Geological Society of London, Special Publication. 12, pp. 175-194.
Dane, C. H., and Bachman, G. 0., 1965, Geologic map of New Mexico: U. S. Geological Survey, scale 1:500,000, 2 sheets.
Dow, W. G., 1978, Petroleum source-beds on continental slopes and rises: American Association of Petroleum Geologists, Bulletin, v. 62, pp. 1584-1606.
Foster, R. W., and Jensen, J. G., 1972, Carbon dioxide in northeastern New Mexico; *in* Kelley, V. C., and Trauger, F. D. (eds.), Guidebook of east-central New Mexico: New Mexico Geological Society, Guidebook 23, pp. 192-200.
Geochem Laboratories, Inc., 1980, Source rock evaluation reference manual: Geochem Laboratories, Inc., Houston, pages not consecutively numbered.
Gonzales, R. A., 1968, Petrography and structure of the Pedernal Hills, Torrance County, New Mexico: Unpublished MS thesis, University of New Mexico, Albuquerque, 78 pp.
Gonzales, R. A., and Woodward, L. A., 1972, Petrology and structure of Precambrian rocks of the Pedernal Hills, New Mexico; *in* Kelley, V. C., and Trauger, F. D. (eds.), Guidebook of east-central New Mexico: New Mexico Geological Society, Guidebook 23, pp. 144-147.
Harding, T. P., and Lowell, J. D., 1979, Structural styles, their plate-tectonic habitats, and hydrocarbon traps in petroleum provinces: American Association of Petroleum Geologists, Bulletin, v. 63, pp. 1016-1058.
Hatchell, W. 0., Blagbrough, J. W., and Hill, J. M., 1982, Stratigraphy and copper deposits of the Abo Formation, Abo Canyon area, central New Mexico; *in* Grambling, J. A., and Wells, S. G. (eds.), Albuquerque country II: New Mexico Geological Society, Guidebook 33, pp. 249-260.
Hawley, J. W., 1986, Environmental geology of the Keers Environmental, Inc. asbestos disposal site, Torrance County, New Mexico: New Mexico Bureau of Mines and Mineral Resources, Open-file Report 245, 12 pp.
Hunt, A., 1983, Plant fossils and lithostratigraphy of the Abo Formation (Lower Permian) in the Socorro area and plant biostratigraphy of Abo red beds in New Mexico; *in* Chapin, C. E. (ed.), Socorro region II: New Mexico Geological Society, Guidebook 34, pp. 157-163.
Hunt, J. M., 1979, Petroleum geochemistry and geology: W. H Freeman, San Francisco, 617 pp.
Hunter, J. C., and Ingersoll, R. V., 1981, Cañas Gypsum Member of Yeso Formation (Permian) in New Mexico: New Mexico Geology, v. 3, pp. 49-53.
Jarvie, D. M., 1991, Total organic carbon (TOC) analysis; *in* Merrill, R. K. (ed.), Source and migration processes and evaluation techniques: American Association of Petroleum Geologists, Treatise of petroleum geology Handbook of petroleum geology, pp. 113-118.
Johnpeer, G. D., Bobrow, D., Robinson-Cook, S., and Barrie, D., 1987a, Preliminary study for siting the superconducting super collider in New Mexico-an interim report on the northern Estancia Basin site: New Mexico Bureau of Mines and Mineral Resources, Open-file Report 257, 78 pp.
Johnpeer, G. D., Robinson-Cook, S., Bobrow, D., Kelliher, J., and McNeil, R., 1987b, Estancia Basin, New Mexico, superconducting super collider, v. 3-geology and tunneling: New Mexico Bureau of Mines and Mineral Resources, Open-file Report 258, 224 pp.
Keller, G. R., and Cordell, L., 1983, Bouguer gravity anomaly map of New Mexico: New Mexico State University, Energy Institute, Geothermal resources map of New Mexico, scale 1:500,000.
Kelley, S. A., Chapin, C. E., and Corrigan, J., 1992, Late Mesozoic to Cenozoic cooling histories of the flanks of the northern and central Rio Grande rift, Colorado and New Mexico: New Mexico Bureau of Mines and Mineral Resources, Bulletin 145, 39 pp.
Kelley, V. C., 1972, Geology of the Fort Sumner sheet, New Mexico: New Mexico Bureau of Mines and Mineral Resources, Bulletin 98, 55 pp.
Kelley, V. C., and Northrop, S. A., 1975, Geology of Sandia Mountains and vicinity, New Mexico: New Mexico Bureau of Mines and Mineral Resources, Memoir 29, 136 pp.
Kelley, V. C., and Wood, G. H., Jr., 1946, Geology of the Lucero uplift, Valencia, Socorro, and Bernalillo Counties, New Mexico: U.S. Geological Survey, Oil and Gas Investigations, Preliminary Map 47, scale 1 inch =1 mi.
Kocurek, G., and Dott, R. H., Jr., 1983, Jurassic paleogeography and paleoclimate of the central and southern Rocky Mountains region; *in* Reynolds, M. W., and Dolly, E. D. (eds.), Mesozoic paleogeography of the west-central United States: Society of Economic Paleontologists and Mineralogists, Rocky Mountain Section, pp. 101-116.
Kottlowski, F. E., 1963, Paleozoic and Mesozoic strata of southwestern and south-central New Mexico: New Mexico Bureau of Mines and Mineral Resources, Bulletin 79, 100 pp.
Kottlowski, F. E., 1985, Shoreline facies of the Yeso Formation in the northern Pedernal Hills; *in* Lucas, S. G. (ed.), Santa Rosa-Tucumcari region: New Mexico Geological Society, Guidebook 36, pp. 167-169.
Leythauser, D., Hageman, H. W., Hollerback, A., and Schafer, R. G., 1980, Hydrocarbon generation in source beds as a function of type and maturation of their organic matter: a mass balance approach: Proceedings of the 10th World Petroleum Congress, Bucharest, 1979, pp. 31-41.
Lucas, S. G., 1991, Correlation of Triassic strata of the Colorado Plateau and southern High Plains, New Mexico; *in* Julian, B., and Zidek, J. (eds.), Field guide to geologic excursions in New Mexico and adjacent areas of Texas and Colorado: New Mexico Bureau of Mines and Mineral Resources, Bulletin 137, pp. 47-56.
Lucas, S. G., Anderson, 0. J., and Hunt, A. P., 1994, Triassic stratigraphy and correlations, southern High Plains of New Mexico-Texas; *in* Ahlen, J., Peterson, J., and Bowsher, A. L. (eds.), Geologic activities in the 90's, Southwest Section of AAPG 1994, Ruidoso, New Mexico: New Mexico Bureau of Mines and Mineral Resources, Bulletin 150, pp. 105-126.
MacGregor, D. S., 1994, Coal-bearing strata as source rocks-a global overview; *in* Scott, A. C., and Fleet, A. J. (eds.), Coal and coal-bearing strata as oil-prone source rocks?: Geological Society of London, Special Publication 77, pp. 107-116.
Merrill, R. K., 1991, Preface to this volume; *in* Merrill, R. K. (ed.), Source rock and migration processes and evaluation techniques: American Association of Petroleum Geologists, Treatise of petroleum geology, Handbook of petroleum geology, pp. xiii-xvii.
Molenaar, C. M., and Rice, D. D., 1988, Cretaceous rocks of the

Western Interior Basin; *in* Sloss, L. L. (ed.), Sedimentary cover-North American craton, U.S.: Geological Society of America, Geology of North America, v. D-2, pp. 77-82.

Myers, D. A., 1967, Geologic map of the Torreon quadrangle, Torrance County, New Mexico: U.S. Geological Survey, Geologic Quadrangle Map GQ-639, scale 1:24,000.

Myers, D. A., 1969, Geologic map of the Escabosa quadrangle, Bernalillo County, New Mexico: U.S. Geological Survey, Geologic Quadrangle Map GQ-795, scale 1:24,000.

Myers, D. A., 1973, The upper Paleozoic Madera Group in the Manzano Mountains, New Mexico: U.S. Geological Survey, Bulletin 1372-F, 13 pp.

Myers, D. A., 1977, Geologic map of the Scholle quadrangle, Socorro, Valencia, and Torrance Counties, New Mexico: U.S. Geological Survey, Geologic Quadrangle Map GQ-1412, scale 1:24,000.

Myers, D. A., 1982, Stratigraphic summary of Pennsylvanian and Lower Permian rocks, Manzano Mountains, New Mexico: New Mexico Geological Society, Guidebook 33, pp. 233-237.

Myers, D. A., and McKay, E. J., 1970, Geologic map of the Mount Washington quadrangle, Bernalillo and Valencia Counties, New Mexico: U.S. Geological Survey, Geologic Quadrangle Map GQ-886, scale 1:24,000.

Myers, D. A., and McKay, E. J., 1971, Geologic map of the Bosque Peak quadrangle, Torrance, Valencia, and Bernalillo Counties, New Mexico: U.S. Geological Survey, Geologic Quadrangle Map GQ-948, scale 1:24,000.

Myers, D. A., and McKay, E. J., 1972, Geologic map of the Capilla Peak quadrangle, Torrance and Valencia Counties, New Mexico: U.S. Geological Survey, Geologic Quadrangle Map GQ-1008, scale 1:24,000.

Myers, D. A., McKay, E. J., and Sharps, J. A., 1981, Geologic map of the Becker quadrangle, Valencia and Socorro Counties, New Mexico: U.S. Geological Survey, Geologic Quadrangle Map GQ-1556, scale 1:24,000.

Needham, C. E., and Bates, R. L., 1943, Permian type sections in central New Mexico: Geological Society of America, Bulletin, v. 54, pp. 1653-1667.

Peters, K. E., 1986, Guidelines for evaluating petroleum source rock using programmed pyrolysis; American Association of Petroleum Geologists, Bulletin, v. 70, pp. 318-329.

Powell, T. G., and Boreham, C. J., 1994, Terrestrially sourced oils: where do they exist and what are our limits of knowledge?-A geochemical perspective; *in* Scott, A. C., and Fleet, A. J. (eds.), Coal and coal-bearing strata as oil-prone source rocks?: Geological Society of London, Special Publication 77, pp. 11-29.

Read, C. B., Wilpolt, R. H., Andrews, D. A., Summerson, C. H., and Wood, G. H., 1944, Geologic map and stratigraphic sections of Permian and Pennsylvanian rocks of parts of San Miguel, Santa Fe, Sandoval, Bernalillo, Torrance, and Valencia Counties, north-central New Mexico: U.S. Geological Survey, Oil and Gas Investigations, Preliminary Map 21, scale 1 inch = 3 mi.

Reiche, P., 1949, Geology of the Manzanita and north Manzano Mountains, New Mexico: Geological Society of America, Bulletin, v. 60, pp. 1183-1212.

Reiter, M. A., Eggleston, R. E., Broadwell, B. R., and Minier, J. D., 1986, Estimates of terrestrial heat flow from deep petroleum tests along the Rio Grande rift in central and southern New Mexico: Journal of Geophysical Research, v. 91, no. B6, pp. 6225-6245.

Russell, L. R., and Snelson, S., 1994, Structural style and tectonic evolution of the Albuquerque Basin segment of the Rio Grande rift, New Mexico, U.S.A.; *in* Landon, S. M. (ed.), Interior rift basins: American Association of Petroleum Geologists, Memoir 59, 205-258.

Sentfle, J. T., and Landis, C. R., 1991, Vitrinite reflectance as a tool to assess thermal maturity; *in* Merrill, R. K. (ed.), Source rock and migration processes and evaluation techniques: American Association of Petroleum Geologists, Treatise of petroleum geology, Handbook of petroleum geology, pp. 119-125.

Smith, R. E., 1957, Geology and ground-water resources of Torrance County, New Mexico: New Mexico Bureau of Mines and Mineral Resources, Ground-water Report 5, 186 pp.

Staplin, F L., 1969, Sedimentary organic matter, organic metamorphism and oil and gas occurrence: Bulletin of Canadian Petroleum Geology, v. 17, pp. 47-66.

Stark, J. T., 1956, Geology of the south Manzano Mountains, New Mexico: New Mexico Bureau of Mines and Mineral Resources, Bulletin 34, 49 pp.

Stark, J. T., and Dapples, E. C., 1946, Geology of the Los Pinos Mountains, New Mexico: Geological Society of America, Bulletin, v. 57, pp. 1121-1172.

Thompson, M. L., 1954, American Wolfcampian fusulinids: Kansas University, Paleontology Contributions No. 14, Protozoa, Article 5, 225 pp.

Tissot, B. P., and Welte, D. H., 1978, Petroleum formation and occurrence: A new approach to oil and gas exploration: Berlin, Springer-Verlag, 538 pp.

Titus, F. B., 1980, Ground water in the Sandia and northern Manzano Mountains, New Mexico: New Mexico Bureau of Mines and Mineral Resources, Hydrologic Report 5, 66 pp.

Tyson, R. V., 1987, The genesis and palynofacies characteristics of marine petroleum source rocks; *in* Brooks, J., and Fleet, A. J. (eds.), Marine petroleum source rocks: Geological Society of London, Special Publication 26, pp. 47-67.

White, R. R., 1994, Hydrology of the Estancia Basin, central New Mexico: U.S. Geological Survey, Water-resources Investigations, Report 93-4163, 83 pp.

Wilpolt, R. H., MacAlpin, A. J., Bates, R. L., and Vorbe, G., 1946, Geologic map and stratigraphic sections of Paleozoic rocks of Joyita Hills, Los Pinos Mountains, and northern Chupadera Mesa, Valencia, Torrance, and Socorro Counties, New Mexico: U.S. Geological Survey, Oil and Gas Investigations, Preliminary Map 61, scale 1 inch = 1 mi.

Winchester, D. E., 1933, The oil and gas resources of New Mexico: New Mexico Bureau of Mines and Mineral Resources, Bulletin 9, 223 pp.

Wood, G. H., and Northrop, S. A., 1946, Geology of the Nacimiento Mountains, San Pedro Mountain, and adjacent plateaus in parts of Sandoval and Rio Arriba Counties, New Mexico: U.S. Geological Survey, Oil and Gas Investigations, Map 57, scale 1 inch =1½mi.

Appendix

TABLE 1—Petroleum exploration wells in Estancia Basin and adjoining areas covered by this report. *Number* refers to numbered well locality in Figure 4.

Map no. (Fig. 4)	Operator	Well no. and lease	Location (section-township-range)	County	Total depth (ft)	Elevation (ft)
10	Simpson	No. 1 Simpson	17-1N-10E	Torrance	940	
11	Lubbock Machine Co.	No. 1 Colbough	12-1N-12E	Torrance	1137	6460
12	Rester	No. 1 Nalda	27-1N-15E	Torrance	3350	6396
13	Richard Laing	No. 1 Sanchez	23-2N-4E	Socorro	1182	5950
14	Richard Laing	No. 2 Sanchez	23-2N-4E	Socorro	400	
15	Richard Laing	No. 2A Sanchez	23-2N-4E	Socorro	800	
16	Blue Quail Energy	No. 1 Addison	13-2N-7E	Torrance	4284	6691
17	Blue Quail Energy	No. 1 Shoffner	10-2N-8E	Torrance	5839	6554
18	Blue Quail Energy	No. 1 Shaw	6-2N-9E	Torrance	4355	6610
19	Stevens Operating	No. 1 Hobbs	13-2N-10E	Torrance	1531	6352
20	Fraser	No. 1 Fraser	12-2N-13E	Torrance	1210	6245
21	Kimmons et al.	No. 1	8-2N-14E	Torrance		
22	Bruce Wilson	No. 1X Judd	6-3N-7E	Torrance	2840	6528
23	Abernathy & Jones (aka McAuley)	No. 1 Dean	28-3N-9E	Torrance	4117	6795
24	Hurley	No. 1 Gonce	13-3N-10E	Torrance	800	
25	C. O. Byrd	No. 1 Lammons	3-3N-12E	Torrance	678	
26	Stewart	No. 1 Lammons	3-3N-12E	Torrance	778	
27	Morrow	No. 1 Chavez	18-3N-13E	Torrance	390	
28	Minerman	No. 2 Permit	23-3N-13E	Torrance	742	
29	Associated Oil & Gas	No. 1 Luna Federal	25-3N-13E	Torrance	568	
31	Hall	No. 1 Pinon Wells	25-3N-13E	Torrance	400	
30	Ballard et al.	No. 1 Luna Federal	25-3N-13E	Torrance	568	
32	Pinos	No. 1 Anderson	28-3N-13E	Torrance	310	
33	Zero Corp. of Texas	No. 1 Bonds	25-3N-14E	Torrance		
34	Lang	No. 1 Whitlow	31-3N-15E	Torrance	1176	6287
35	Duran Dome Oil	No. 1 State	31-3N-15E	Torrance		
36	Rogers & Binns	No. 1 Hindi	31-3N-15E	Torrance	1201	6274
37	Corona-Tularosa	No. 1 Tularosa	35-3N-15E	Torrance		
38	Navajo Oil	No. 1 Bussed-McGarr	2-4N-6E	Torrance		
39	Mountainair Oil & Gas	No. 1 Veal	32-4N-7E	Torrance	3104	6540
40	Romero	No. 2 Shaw	13-4N-7E	Torrance	2840	6355
41	Romero	No. 1 Shaw	18-4N-8E	Torrance	2008	6350
42	RAF Enterprises	No. 1 Shaw	18-4N-8E	Torrance	2004	6350
43	Cimarron Energy	No. 3 Shaw	18-4N-8E	Torrance	600	6345
44	Eidal Manufacturing	No. 1 Mitchell	33-4N-8E	Torrance	3592	6351
45	Bluehall Oil Co.	No. 1 Kistler	7-4N-10E	Torrance	1780	6165
46	Jack Williams	No. 1 Harry Lammons	3-4N-12E	Torrance		
47	J. E. Williams	No. 1 Ashcroft	22-4N-12E	Torrance	450	
48	Rogers & Poyner	No. 2 Rogers Federal	26-4N-12E	Torrance	665	6100
49	SRI Production	No. 1 Kirkman State	28-4N-12E	Torrance	494	6367
50	Poyner & Rogers	No. 1 Federal	34-4N-12E	Torrance	643	6350
51	Navajo	No. 1 Manzano	36-5N-6E	Torrance	2147	6462
52	MAR Oil and Gas	No. 1 Estes	35-5N-8E	Torrance	2913	6178
53	Benz et al.	No. 1 Benz	18-5N-9E	Torrance	796	6095
54	Benz	No. 2 Benz	18-5N-9E	Torrance	570	6090
55	Powell Walters	No. 1 Formwalt	18-5N-11E	Torrance	1458	6193
56	Cacy	No. 1A Cacy	23-6N-5E	Torrance	955	7501
57	Overmier & Cacy	No. 1 Cacy	23-6N-5E	Torrance	575	7501
58	Leroy Bennett	No. 1 Aguayo Comanche	31-6N-5E	Torrance	1655	6043
59	Sweetman	No. 1 deSpain	12-6N-6E	Torrance	1343	7029
60	John Aday	No. 2 deSpain	12-6N-6E	Torrance	1900	6646
61	Estancia	No. 1 Munoz	5-6N-7E	Torrance	1346	6800
62	Meyers	No. 1 Milbourne	11-6N-7E	Torrance	1844	
63	Chief Oil & Gas	No. 1 Pace	12-6N-7E	Torrance	2062	
64	Wilson	No. 1A Pace	12-6N-7E	Torrance	2020	
65	Meyers	No. 1 Smith & Pace	12-6N-7E	Torrance	1910	6250
66	Witt Ice Co.	No. 1 Meadows	23-6N-7E	Torrance	2123	6310
67	Nelson	No. 1 Burns A	31-6N-8E	Torrance	2858	6252
68	Murphree & Bond	No. 1 Berkshire	19-6N-9E	Torrance	3268	6108
69	Gilbreath	No. 1 Berkshire	19-6N-9E	Torrance	2640	6102
70	Houston Oil & Minerals	No. 1 Berkshire Ranch	29-6N-9E	Torrance	2671	6095
71	San Juan Coal & Oil	No. 1 Randall	20-6N-10E	Torrance	320	
72	San Juan Coal & Oil	No. 2 Randall	20-6N-10E	Torrance	5321	6100
73	Gardner	No. 1 Kidwell	21-6N-10E	Torrance	5918	6158
74	Houston Oil & Minerals	No. 14-28 Federal	28-6N-10E	Torrance	8759	6115
75	Superior Oil Co.	No. 28-31 Blackwell	31-6N-11E	Torrance	2646	6136
76	Petrol	No. 1 State	1-6N-13E	Torrance	828	6310
77	Norton et al.	No. 1X Perez	18-6N-14E	Torrance	710	6284
78	Estancia Valley CO_2	No. 2 Kelley	1-7N-7E	Torrance	1415	6552

Table 1, continued.

Map no. (Fig. 4)	Operator	Well no. and lease	Location (section-township-range)	County	Total depth (ft)	Elevation (ft)
79	Estancia Valley CO_2	No. 2 DeHart	12-7N-7E	Torrance	1415	6526
80	Estancia Valley CO_2	No. 3 DeHart	12-7N-7E	Torrance	1264	6540
81	Estancia Valley CO_2	No. 4 DeHart	12-7N-7E	Torrance	1236	6548
82	Estancia Valley CO_2	No. 5 DeHart	12-7N-7E	Torrance	1258	6534
83	Estancia Valley CO_2	No. 1 Kellogg	12-7N-7E	Torrance	1268	6550
84	Estancia Valley CO_2	No. 1 Roland	12-7N-7E	Torrance	1359	6348
85	Estancia Valley CO_2	No. 2 Stubbs	12-7N-7E	Torrance		
86	Estancia Valley Gas & Ice	No. 4 Wilcox Dome	12-7N-7E	Torrance	1050+	
87	Sinoco Oil	No. 1 DeHart	12-7N-7E	Torrance	765	
88	Sinoco Oil	No. 2 DeHart	12-7N-7E	Torrance	1440	6368
89	Witt Ice & Gas Co.		12-7N-7E	Torrance	1270	
90	Witt Oil & Gas Co.	No. 3 DeHart	12-7N-7E	Torrance	1218	
91	Estancia Valley CO_2	No. 1 Kutchin	13-7N-7E	Torrance	1428	6644
92	Shinnock et al.	No. 1 Kutchin-Witt	13-7N-7E	Torrance	302	
93	Estancia	No. 1 Crawford	32-7N-7E	Torrance	1355	
94	Drice	No. 1 Garland	32-7N-7E	Torrance	2200	6505
95	Lee	No. 1 Milbourne	36-7N-7E	Torrance	2000	6315
96	Formwalt-Powell	No. 1 Norman	5-7N-8E	Torrance	230	6287
97	Formwalt-Powell	No. 2 Norman	5-7N-8E	Torrance	191	6290
98	Olsen	No. 1 Means	27-7N-9E	Torrance	3680	6107
99	San Juan Coal & Oil	No. 1 Minerman	32-7N-10E	Torrance	2647	6132
100	Pollard Brothers	No. 1 Sewell	28-8N-8E	Torrance	463	
101	Pollard Brothers	No. 1 Moore & Mead	30-8N-8E	Torrance	1025	
102	Woodson Exploration	No. 1 Meads	30-8N-8E	Torrance	645	
103	Williams	No. 1 Staplin	16-8N-10E	Torrance	1650	6350
104	Hatch Petroleum	No. 1	26-8N-11E	Torrance		
105	Toltec Oil Co.	No. 1 State	8-8N-13E	Torrance	1110	
106	Cardinal Oil Co.	No. 1 State	3-8N-14E	Torrance	2368	6235
107	Toltec Oil Co.	No. 2 State	8-8N-14E	Torrance	528	6590
108	Umbarger	No. 1 State	10-8N-14E	Torrance	2775	6280
109	Brock	No. 1 McClean	8-8N-15E	Torrance	1000?	
110	Forty-Eight Petroleum	No. 1 Greenfield	17-9N-8E	Torrance	2160	6335
111	Witt Ice Co.	No. 1 Cornett	32-9N-8E	Torrance	2402	6338
112	L. O. Hickerson	No. 2 Wright	12-10N-5E	Bernalillo	1510	6554
113	Peters, Siemens, & Boyds	No. 1 Wright	12-10N-5E	Bernalillo	1121	
114	Southern Union Production Co.	No. 1 Tijeras Canyon Unit	12-10N-5E	Bernalillo	1903	6493
115	Southern Union Production Co.	No. 2 Tijeras Canyon Unit	12-10N-5E	Bernalillo	1903	6543
116	Southern Union Production Co.	No. 3 Tijeras Canyon Unit	12-10N-5E	Bernalillo	2228	6618
117	Fisher & Wolcott	No. 1 Fisher	3-10N-7E	Santa Fe	980	7200
118	Forty-Eight Petroleum	No. 1 Fisher Hill	6-10N-7E	Santa Fe	2750	6960
119	Holmberg	No. 1 Cantwell	5-10N-9E	Santa Fe	812	
120	Kelsey	No. 2 State	22-10N-10E	Santa Fe		
121	Kelsey	No. 1 State	26-10N-10E	Santa Fe	1052	6638
122	Duke City	No. 1 State	29-10N-10E	Santa Fe	990	
123	Sanders	No. 1 State	32-10N-12E	San Miguel	3650	7025
124	Eastern Sandia Production	No. 1 Horton	32-11N-7E	Santa Fe	1930	6685
125	Eastern Sandia Production	No. 2 Horton	32-11N-7E	Santa Fe	2497	6705
126	Sage Corp.	No. 1 Horton	32-11N-7E	Santa Fe	1930	6685
127	Geologic Resources, Inc.	No. 1 Fullingim Strat Test	31-11N-8E	Santa Fe	2822	6480
128	Blackstone	No. 1 Neville	9-11N-11E	Santa Fe	1215	6820
129	Ramsey	No. 1 White Lake	28-11N-11E	Santa Fe	1058	6834
130	Newton Roberts	No. 1 McCune	22-11N-13E	San Miguel	3119	7000
131	Wood et al.	No. 1 Galisteo	7-12N-10E	Santa Fe	3500	
132	English, Byrd, & Frost	No. 1 Fullerton & Dobson	16-12N-10E	Santa Fe	3210	6420
133	Bar-S-Bar Ranch	No. 1 Fee	23-12N-10E	Santa Fe	4204	6497
134	Adkins	No. 1 Bashor	23-12N-11E	Santa Fe	977	7120
135	Kenneth Good	No. 2 Bustamante	27-12N-12E	San Miguel	3515	6580
136	Lubar Oil Co.	No. 1 Geronimo Gonzales	29-12N-14E	San Miguel	3226	6510
137	Black Oil	No. 1 Ferrill	1-13N-8E	Santa Fe	3696	5884
138	Black Oil	No. 5 Ferrill	1-13N-8E	Santa Fe	4252	5895
139	Black Oil	No. 6 Ferrill	1-13N-8E	Santa Fe	2390	5885
140	Black Oil	No. 3 Hazel	1-13N-8E	Santa Fe	3260	5915
141	Pelto Oil	No. 1 Ferrill	1-13N-8E	Santa Fe	3199	5982
142	Transocean Oil Co.	No. 1 McKee	4-13N-9E	Santa Fe	8128	5935
143	Black Oil	No. 1 Cash	5-13N-9E	Santa Fe	2600	5900
144	Black Oil	No. 1 McKee	5-13N-9E	Santa Fe	2800	5900
145	Colorado Plateau Geological Services	No. 2 Ferrill	5-13N-9E	Santa Fe	1610	5913
146	Pelto Oil	No. 1 McKee	5-13N-9E	Santa Fe	3100	5904
147	Colorado Plateau Geological Services	No. 1 Ferrill	7-13N-9E	Santa Fe	3192	6010
148	Eastland Oil Co.	No. 1 McKee	8-13N-9E	Santa Fe	2093	5980
149	Wood et al.	No. 2 Galisteo	29-13N-10E	Santa Fe	1540	
150	Toltec	No. 1 Pankey	2-13N-10E	Santa Fe	2165	6265

Table 1, continued.

Map no. (Fig. 4)	Operator	Well no. and lease	Location (section-township-range)	County	Total depth (ft)	Elevation (ft)
151	Lewis Drilling Co.	No. 1 Debra Federal	5-13N-13E	San Miguel	1605	7506
152	Cibola Petroleum	No. 1 Crow	9-13N-14E	San Miguel	755	
153	Charles W. Scott	No. 1 State	16-13N-14E	San Miguel	2859	6097
9	Rault Petroleum Corp.	No. 1 Taylor State	22-1S-15E	Lincoln	2494	5989
1	Skelly	No. 1 Goddard	22-2S-4E	Socorro	3386	5619
2	Chupadera Oil	No. 1	6-2S-6E	Socorro	350?	
3	Yates Petroleum Corp.	No. 1 McCaw Federal	23-2S-6E	Socorro	4450	6368
4	Basabe & Rupe Drilling Co.	No. 1 Ryberg	24-2S-14E	Lincoln	1320	
5	Mesa Petroleum Co.	No. 1 Chadwick State	2-2S-15E	Lincoln	2701	6011
6	B & B Oil & Gas Co.	No. 1 Garber Federal	23-2S-15E	Lincoln	570	5997
7	Duncan & Branin	No. 1 C. C. Franks	23-2S-15E	Lincoln	2140	
8	Malcom & Morrow	No. 1 C. C. Franks	23-2S-15E	Lincoln	2120	5920

TABLE 2—Petroleum exploration wells in Estancia Basin and adjoining areas covered by this report that have tested the Lower Permian, Pennsylvanian, and Precambrian sections or reported shows from these sections. **perf**, casing perforations; **DST**, drill stem test; **swbd**, swabbed; **SO**, slight oil; **SGCLW**, slight gas-cut load water; **VSWG**, very slight watery gas; **OCLW**, oil-cut load water; **GCSWTR**, gas-cut salt water; **MW**, muddy water; **HFW**, hole full of water; **SGCW**, slight gas-cut water; **SI**, shut in; **FP**, flowing pressure; **SIP**, shut-in pressure.

Operator	Lease name	Well no.	T	R	S	Top test (ft)	Base test (ft)	Strat. unit	Test	Pressure	Description	Times	FP	SIP
Yeso shows and tests														
Abernathy & Jones	Dean	1	3N	9E	28	1230		Yeso	samples		show oil & gas			
Morrow Bros.	Joe H. Chavez	1	3N	13E	18	134		Yeso			show gas			
Morrow Bros.	Joe H. Chavez	1	3N	13E	18	241	248	Yeso			show oil			
Duran Dome Oil	State	1	3N	15E	31	640	646	Yeso			show gas			
Duran Dome Oil	State	1	3N	15E	31	726	803	Yeso			show oil & gas			
Duran Dome Oil	State	1	3N	15E	31	847	854	Yeso			show oil & gas			
Duran Dome Oil	State	1	3N	15E	31	878	894	Yeso			show oil & gas			
Duran Dome Oil	State	1	3N	15E	31	932	940	Yeso			show gas			
Rogers & Poyner	Rogers Federal	2	4N	12E	26	150	155	Yeso			show gas			
Rogers & Poyner	Rogers Federal	2	4N	12E	26	170	175	Yeso			water			
Rogers & Poyner	Rogers Federal	2	4N	12E	26	320	322	Yeso			show gas with rainbow			
Poyner & Rogers	Federal	1	4N	12E	34	265		Yeso			water			
Poyner & Rogers	Federal	1	4N	12E	34	278		Yeso			water			
MAR Oil & Gas	Estes	1	5N	8E	35	145	157	Yeso			water			
MAR Oil & Gas	Estes	1	5N	8E	35	255	275	Yeso			water			
Benz et al.	Benz	1	5N	9E	18	549	554	Yeso	perf		swbd water			
Benz et al.	Benz	1	5N	9E	18	619	625	Yeso	perf		acid, swbd water			
Benz et al.	Benz	1	5N	9E	18	635	636	Yeso	perf		swbd SO & SGCLW			
Benz et al.	Benz	1	5N	9E	18	662	663	Yeso	perf		swbd VSWG & OCLW			
Benz et al.	Benz	1	5N	9E	18	774	774	Yeso	perf		swbd GCSWTR			
Superior Oil Co.	Blackwell	28-31	6N	11E	31	760	869	Yeso	DST	340	rec 500 ft MW	open 45 min SI 15 min	300	340
San Juan Coal & Oil	Minerman	1	7N	10E	32	825		Yeso			HFW			
San Juan Coal & Oil	Minerman	1	7N	10E	32	1428		Yeso			HFW			
San Juan Coal & Oil	Minerman	1	7N	10E	32	1655	1805	Yeso			show oil			
Toltec Oil Co.	State	1	8N	13E	8	745	762	Yeso			water			
J. H. Blackstone	Neville	1	11N	11E	9	1170		Yeso			show oil & gas			
Toltec Oil Co.	Pankey	1	13N	10E	2	890		Yeso			water			
Abo shows and tests														
Blue Quail Energy	Shaw	1	2N	9E	6	1607	2162	Abo	logs		crossover of porosity logs, numerous ss			
Bruce Wilson	Judd	1X	3N	7E	6	1628	1634	Abo	perf		swbd water			
Abernathy & Jones	Dean	1	3N	9E	28	2015	2035	Abo	samples		show oil			
Albert C. Lang	Whitlow	1	3N	15E	31	634	640	Abo	perf		HFW			
Albert C. Lang	Whitlow	1	3N	15E	31	707	713	Abo	perf		swbd dry			
Albert C. Lang	Whitlow	1	3N	15E	31	721.5	724.5	Abo	perf		swbd dry			
Albert C. Lang	Whitlow	1	3N	15E	31	730	737.5	Abo	perf		swbd fresh water			
Albert C. Lang	Whitlow	1	3N	15E	31	1060	1063	Abo	perf		HFW			
Albert C. Lang	Whitlow	1	3N	15E	31	1070.5	1073	Abo	perf		swbd fresh water			
Albert C. Lang	Whitlow	1	3N	15E	31	1132	1142	Abo	perf		swbd dry			
M. A. Romero	Sam Shaw	2	4N	7E	13	1696	1710	Abo	perf		acid, no details			
M. A. Romero	Sam Shaw	2	4N	7E	13	1781	1790	Abo	perf		acid, no details			
M. A. Romero	Sam Shaw	2	4N	7E	13	1816	1819	Abo	perf		acid, no details			
MAR Oil & Gas	Estes	1	5N	8E	35	376	393	Abo			water			
San Juan Coal & Oil	Randall	2	6N	10E	20	1895	1908	Abo			salt water			

Table 2, continued.

Operator	Lease name	Well no.	T	R	S	Top test (ft)	Base test (ft)	Strat. unit	Test	Pressure	Description	Times	FP	SIP
San Juan Coal & Oil	Minerman	1	7N	10E	32	2571	2598	Abo			show oil			
H. L. Williams	Staplin	1	8N	10E	16	860		Abo			HFW			
Pennsylvanian shows and tests														
Blue Quail Energy	Addison	1	2N	7E	13	3131	4214	Madera	logs		crossover of porosity logs, numerous ss			
Blue Quail Energy	Shaw	1	2N	9E	6	2934	4054	Madera	logs		crossover of porosity logs, numerous ss			
Bruce Wilson	Judd	1X	3N	7E	6	1876	1882	Madera	perf		swbd water			
Bruce Wilson	Judd	1X	3N	7E	6	2246	2252	Madera	perf		swbd water			
Bruce Wilson	Judd	1X	3N	7E	6	2440	2444	Madera	perf		swbd water			
Abernathy & Jones	Dean	1	3N	9E	28	3060	3095	Madera	samples		show oil			
Abernathy & Jones	Dean	1	3N	9E	28	3083	3104	Madera	perf		swbd dry, sqzd			
Abernathy & Jones	Dean	1	3N	9E	28	3165	3196	Madera	samples		show gas			
Navajo Oil	Manzano Structure	1	5N	6E	36	1104	1112	Madera			show oil			
Navajo Oil	Manzano Structure	1	5N	6E	36	1208	1218	Madera			show oil			
MAR Oil & Gas	Estes	1	5N	8E	35	2100	2110	Madera	perf		acid, swbd SGCW			
MAR Oil & Gas	Estes	1	5N	8E	35	2252	2258	Madera	perf		swbd SGCW w/CO_2			
Estancia Co.	Munoz	1	6N	7E	5	305	325	Madera			water			
Estancia Co.	Munoz	1	6N	7E	5	605	628	Madera			show oil & gas			
San Juan Coal & Oil	Randall	2	6N	10E	20	3297	3310	Madera			oil sand			
San Juan Coal & Oil	Randall	2	6N	10E	20	3485	3500	Madera			oil sand			
San Juan Coal & Oil	Randall	2	6N	10E	20	4600	4725	Madera			show oil			
Gardner Petroleum	Ed Kidwell	1	6N	10E	21	5467	5520	Madera	DST	0	rec 400 ft mud	open 1 hr	0	
Estancia Valley Dev.	Crawford	1	7N	7E	32	450		Madera			water			
Estancia Valley Dev.	Crawford	1	7N	7E	32	634		Madera			show CO_2			
Orville J. Lee	Milbourne	1	7N	7E	36	368		Madera			show oil & asphalt			
Formwalt-Powell	Norman	1	7N	8E	5	205	218	Madera	perf		acid, converted to water well			
Formwalt-Powell	Norman	2	7N	8E	5	116	159	Madera	perf		acid			
Forty-Eight Petroleum	Fisher Hill	1	10N	7E	6	875	900	Madera			show CO_2			
Forty-Eight Petroleum	Fisher Hill	1	10N	7E	6	1320		Madera			show gas, burned 10 ft above derrick floor			
Forty-Eight Petroleum	Fisher Hill	1	10N	7E	6	1630		Madera			show oil			
Forty-Eight Petroleum	Fisher Hill	1	10N	7E	6	1742	1746	Madera			oil rainbows in black shale			
Forty-Eight Petroleum	Fisher Hill	1	10N	7E	6	1850	1855	Madera			show oil			
Forty-Eight Petroleum	Fisher Hill	1	10N	7E	6	1905		Madera			show oil in ss			
Forty-Eight Petroleum	Fisher Hill	1	10N	7E	6	1950		Madera			show oil & gas			
Forty-Eight Petroleum	Fisher Hill	1	10N	7E	6	2000		Madera			show oil & gas			
Forty-Eight Petroleum	Fisher Hill	1	10N	7E	6	2200		Madera			rainbows of oil			
Forty-Eight Petroleum	Fisher Hill	1	10N	7E	6	2580		Madera			increase of gas			
Holmberg	Cantwell	1	10N	9E	5	600		Madera			show oil & gas in black lime			
Toltec Oil	Pankey	1	13N	10E	2	1865		Madera			water			
Toltec Oil	Pankey	1	13N	10E	2	1980		Madera			water			
Mountainair O & G	Veal	1	4N	7E	32	2190		Penn			show oil			
Mountainair O & G	Veal	1	4N	7E	32	2600		Penn			show oil			
Mountainair O & G	Veal	1	4N	7E	32	2835		Penn			show oil			
RAF Enterprises	Shaw	1	4N	8E	18	988	1260	Penn	perf		acid			
RAF Enterprises	Shaw	1	4N	8E	18	1325	1935	Penn	perf		sqzd			
Eidal Manufacturing	Mitchell	1	4N	8E	33	3460	3465	Penn			show gas			
MAR Oil & Gas	Estes	1	5N	8E	35	2582	2612	Sandia	perf		acid, swbd SGCW w/CO_2			
MAR Oil & Gas	Estes	1	5N	8E	35	2624	2646	Sandia	perf		acid, flowed CO_2 w/N_2			

Table 2, continued.

Operator	Lease name	Well no.	T	R	S	Top test (ft)	Base test (ft)	Strat. unit	Test	Pressure	Description	Times	FP	SIP
Precambrian shows and tests														
J. P. Stewart	Lammons	1	3N	12E	3	426	428	p€ schist			slight show oil			
Drice	Garland	1	7N	7E	32	1965		p€ schist			odor CO_2			
Orville J. Lee	Milbourne	1	7N	7E	36	1722		p€ schist			show CO_2			
Orville J. Lee	Milbourne	1	7N	7E	36	1769		p€ schist			show gas			
Orville J. Lee	Milbourne	1	7N	7E	36	1792	1813	p€ schist			show CO_2			
Kelsey Clients	State	2	10N	10E	22	867		p€ granite			show oil & gas			
Kelsey Clients	State	2	10N	10E	22	962		p€ granite			show oil & gas			

TABLE 4—Petroleum source-rock analyses in Estancia Basin and adjoining areas covered by this report. **ls**, limestone; **sh**, shale; **ss**, sandstone; **TOC**, total organic carbon as a weight percent of the rock; **TAI**, Thermal Alteration Index; **Am%**, percent amorphous kerogen; **Herb%**, percent herbaceous kerogen; **Inert%**, percent inertinitic kerogen. Wells marked with an asterisk are located either north or south of the area covered by this report but are included in this table because they provide control essential to interpretation and mapping of source rocks in the Estancia Basin.

Operator	Well & lease	Location (section-township-range)	Top depth (ft)	Bottom depth (ft)	Lithology	TOC	TAI	TMAX	Maturity	Algal %	Am %	Herb %	Woody %	Inert %
Analyses of Pennsylvanian strata														
Castle & Wigzell	1 Kelly Fed*	11-20N-9E	2500	2600	ls	0.82	2.6	439	mature	0	20	50	20	10
Castle & Wigzell	1 Kelly Fed*	11-20N-9E	2600	2695	ls	0.79	2.6	452	mature	0	27	45	18	18
Bar-S-Bar Ranch	1 Fee	23-12N-10E	1940	1990	ls	0.07	2.2	435	moderately mature	0	50	38	0	12
Virgle Landreth	1 Panhandle A*	23-4S-6E	2000	2020	sh	1.34	2.2	440	moderately mature	0	17	33	33	17
Virgle Landreth	1 Panhandle A*	23-4S-6E	2200	2300	sh	2.02	2.3	440	moderately mature	0	15	47	23	15
Transocean Oil Co.	1 McKee	4-13N-9E	6950	6970	ls (0.20), sh (0.80)	0.18	2.4	427	moderately mature	0	30	50	10	10
Transocean Oil Co.	1 McKee	4-13N-9E	7010	7030	ls (0.50), sh (0.50)	0.15	2.4	459	moderately mature	0	10	40	10	40
Transocean Oil Co.	1 McKee	4-13N-9E	7050	7070	ls (0.40), sh (0.60)	0.23	2.4	419	moderately mature	0	0	68	16	16
Transocean Oil Co.	1 McKee	4-13N-9E	7060	7080	ls (0.50), sh (0.50)	0.22	2.4	450	moderately mature	0	22	44	12	22
Transocean Oil Co.	1 McKee	4-13N-9E	7140	7150	ls (0.50), sh (0.50)	0.18	2.4	467	moderately mature	0	0	66	0	34
Transocean Oil Co.	1 McKee	4-13N-9E	7230	7240	ls (0.60), sh (0.40)	0.15	2.5	394	moderately mature	0	66	17	0	17
Transocean Oil Co.	1 McKee	4-13N-9E	7270	7290	ls (0.70), sh (0.30)	0.10	2.5	392	moderately mature	0	66	17	0	17
Transocean Oil Co.	1 McKee	4-13N-9E	7360	7380	ls (0.90), sh (0.10)	0.12	2.4	342	moderately mature	0	17	66	0	17
Transocean Oil Co.	1 McKee	4-13N-9E	7400	7420	ls (0.05), sh (0.95)	0.41	2.5	276	moderately mature	0	21	21	29	29
Transocean Oil Co.	1 McKee	4-13N-9E	7630	7650	ls (0.40), sh (0.60)	0.32	2.5	420	moderately mature	0	0	50	30	20
Transocean Oil Co.	1 McKee	4-13N-9E	7760	7780	ls (0.95), sh (0.05)	0.2	2.5	361	moderately mature	0	10	50	20	20
Sun	1 Bingham State*	23-5S-5E	1615	1650		0.13								
Sun	1 Bingham State*	23-5S-5E	1690	1720		0.95								
Sun	1 Bingham State*	23-5S-5E	2000	2030		0.07								
Sun	1 Bingham State*	23-5S-5E	2300	2330		0.01								
Sun	1 Bingham State*	23-5S-5E	2460	2490		0.11								
Sun	1 Bingham State*	23-5S-5E	2590	2620		0.10								
Sun	1 Bingham State*	23-5S-5E	2630	2660		0.11								
Virgle Landreth	1 Panhandle*	23-4S-6E	1820	1850		0.05								
Virgle Landreth	1 Panhandle*	23-4S-6E	1960	1990		0.11								
Virgle Landreth	1 Panhandle*	23-4S-6E	3020	3070		0.29								
Virgle Landreth	1 Panhandle*	23-4S-6E	3090	3130		0.19								
Virgle Landreth	1 Panhandle*	23-4S-6E	3280	3310		0.34								
Virgle Landreth	1 Panhandle*	23-4S-6E	3340	3380		0.20								
Virgle Landreth	1 Panhandle A*	28-4S-6E	1680	1720		0.04								
Virgle Landreth	1 Panhandle A*	28-4S-6E	1780	1820		0.07								
Virgle Landreth	1 Panhandle A*	28-4S-6E	2070	2110		0.01								
Virgle Landreth	1 Panhandle A*	28-4S-6E	2530	2570		0.21								
Virgle Landreth	1 Panhandle A*	28-4S-6E	2760	2790		0.36								

Table 4, continued.

Operator	Well & lease	Location (section-township-range)	Top depth (ft)	Bottom depth (ft)	Lithology	TOC	TAI	TMAX	Maturity	Algal %	Am %	Herb %	Woody %	Inert %
James K. Anderson	1 Wishbone Federal*	1-4S-3E	3000	3050	ls	0.13	2.3	436	moderately mature	0	11	44	11	34
James K. Anderson	1 Wishbone Federal*	1-4S-3E	3250	3300	ls (0.20), sh (0.80)	0.39	2.5	413	moderately mature	0	0	38	36	36
James K. Anderson	1 Wishbone Federal*	1-4S-3E	3350	3400	ls (0.20), sh (0.80)	0.50	2.5	274	moderately mature	0	0	28	36	36
James K. Anderson	1 Wishbone Federal*	1-4S-3E	3500	3550	ls	0.22	2.5	303	moderately mature	0	0	40	40	20
James K. Anderson	1 Wishbone Federal*	1-4S-3E	3800	3850	ls	0.30	2.5	262	moderately mature	0	0	36	36	28
James K. Anderson	1 Wishbone Federal*	1-4S-3E	3850	3900	ls	0.51	2.5	310	moderately mature	0	0	44	22	34
James K. Anderson	1 Wishbone Federal*	1-4S-3E	4000	4050	ls (0.40), sh (0.60)	0.38	2.5	426	moderately mature	0	0	40	30	30
James K. Anderson	1 Wishbone Federal*	1-4S-3E	4050	4100	ls (0.40), sh (0.60)	0.56	2.6	311	mature	0	0	36	28	36
James K. Anderson	1 Wishbone Federal*	1-4S-3E	4100	4150	ls (0.45), sh (0.55)	0.45	2.6	300	mature	0	8	26	33	33
James K. Anderson	1 Wishbone Federal*	1-4S-3E	4150	4200	ls (0.70), sh (0.30)	0.40	2.6	274	mature	0	8	33	26	33
James K. Anderson	1 Wishbone Federal*	1-4S-3E	4200	4250	ls (0.70), sh (0.30)	0.30	2.7	301	mature	0	8	33	33	26
James K. Anderson	1 Wishbone Federal*	1-4S-3E	4250	4300		0.36	2.7	355	mature	0	10	36	27	27
James K. Anderson	1 Wishbone Federal*	1-4S-3E	4300	4350	ls (0.90), sh (0.10)	0.24	2.7	308	mature	0	17	33	25	25
James K. Anderson	1 Wishbone Federal*	1-4S-3E	4350	4400	ls (0.70), sh (0.30)	0.32	2.7	259	mature	0	15	30	25	30
James K. Anderson	1 Wishbone Federal*	1-4S-3E	4400	4450	ls (0.55), sh (0.45)	0.37	2.7	274	mature	0	15	25	30	30
James K. Anderson	1 Wishbone Federal*	1-4S-3E	4450	4500	ls (0.25), sh (0.75)	1.59	2.8	527	mature	0	10	18	36	36
James K. Anderson	1 Wishbone Federal*	1-4S-3E	4550	4600	ls (0.10), sh (0.90)	2.08	2.8	535	mature	0	10	18	36	36
James K. Anderson	1 Wishbone Federal*	1-4S-3E	4600	4650	ls (0.40), sh (0.60)	1.07	2.8	418	mature	0	10	18	36	36
James K. Anderson	1 Wishbone Federal*	1-4S-3E	4650	4700	ls (0.10), sh (0.90)	0.77	2.8	358	mature	0	15	25	30	30
James K. Anderson	1 Wishbone Federal*	1-4S-3E	4700	4750	ss (0.30), sh (0.70)	0.56	2.8	296	mature	0	8	26	33	33
James K. Anderson	1 Wishbone Federal*	1-4S-3E	4750	4800	ss (0.30), sh (0.70)	0.49	2.8	274	mature	0	8	26	33	33
James K. Anderson	1 Wishbone Federal*	1-4S-3E	4800	4850	ss (0.30), sh (0.70)	0.55	2.8	345	mature	0	8	26	33	33
James K. Anderson	1 Wishbone Federal*	1-4S-3E	4850	4900	ss (0.30), sh (0.70)	0.42	2.8	240	mature	0	10	18	36	36
James K. Anderson	1 Wishbone Federal*	1-4S-3E	4900	4950	ss (0.40), sh (0.60)	0.29	2.8	217	mature	0	10	18	36	36
James K. Anderson	1 Wishbone Federal*	1-4S-3E	4950	4996	ss (0.20), ls (0.40), sh (0.40)	0.23	2.8	207	mature	0	8	33	26	33
Superior	28-31 Blackwell	31-6N-11E	2000	2100		0.11		269						
Superior	28-31 Blackwell	31-6N-11E	2100	2200		0.11		339						

Table 4, continued.

Operator	Well & lease	Location (section-township-range)	Top depth (ft)	Bottom depth (ft)	Lithology	TOC	TAI	TMAX	Maturity	Algal %	Am %	Herb %	Woody %	Inert %
Superior	28-31 Blackwell	31-6N-11E	2200	2300		0.11		292						
Superior	28-31 Blackwell	31-6N-11E	2300	2400		0.23		384						
Superior	28-31 Blackwell	31-6N-11E	2400	2500		0.50		321						
Superior	28-31 Blackwell	31-6N-11E	2500	2600		0.79		417						
Witt Ice Co.	1 Meadows	23-6N-7E	335	357	ls	0.05	2.5	437	moderately mature	0	50	26	12	12
Witt Ice Co.	1 Meadows	23-6N-7E	855	865	ls	0.08	2.5	355	moderately mature	0	57	28	0	15
Witt Ice Co.	1 Meadows	23-6N-7E	990	1050	sh	0.46	2.5	381	moderately mature	0	10	18	36	36
Witt Ice Co.	1 Meadows	23-6N-7E	1155	1200	sh	0.40	2.5	410	moderately mature	0	34	44	11	11
Witt Ice Co.	1 Meadows	23-6N-7E	1264	1300	ls	0.60	2.5	440	moderately mature	0	68	16	0	16
Witt Ice Co.	1 Meadows	23-6N-7E	1668	1729	sh	0.75	2.6	374	mature	0	8	26	33	33
Olsen	1 Means	27-7N-9E	1500	1600		0.12		258						
Olsen	1 Means	27-7N-9E	1600	1700		0.12		266						
Olsen	1 Means	27-7N-9E	1700	1800		0.14		247						
Olsen	1 Means	27-7N-9E	1800	1900		0.14		348						
Olsen	1 Means	27-7N-9E	1900	2000		0.15		270						
Olsen	1 Means	27-7N-9E	2000	2100		0.11		270						
Olsen	1 Means	27-7N-9E	2100	2200		0.21		334						
Olsen	1 Means	27-7N-9E	2200	2300		0.18		272						
Olsen	1 Means	27-7N-9E	2300	2400		0.24		255						
Olsen	1 Means	27-7N-9E	2400	2500		0.22		250						
Olsen	1 Means	27-7N-9E	2500	2600		0.25		263						
Olsen	1 Means	27-7N-9E	2600	2700		0.26		253						
Olsen	1 Means	27-7N-9E	2700	2800		0.39		318						
Olsen	1 Means	27-7N-9E	2800	2900		0.39		272						
Olsen	1 Means	27-7N-9E	2900	3000		0.20		272						
Olsen	1 Means	27-7N-9E	3000	3100		0.22		484						
Olsen	1 Means	27-7N-9E	3100	3200		0.61		243						
Gardner Petroleum	1 Kidwell	21-6N-10E	3000	3100		0.26		270						
Gardner Petroleum	1 Kidwell	21-6N-10E	3100	3200		0.19		243						
Gardner Petroleum	1 Kidwell	21-6N-10E	3200	3300		0.41		230						
Gardner Petroleum	1 Kidwell	21-6N-10E	3300	3400		0.21		225						
Gardner Petroleum	1 Kidwell	21-6N-10E	3400	3500		0.39		357						
Gardner Petroleum	1 Kidwell	21-6N-10E	3500	3600		0.31		304						
Gardner Petroleum	1 Kidwell	21-6N-10E	3600	3700		0.47		238						
Gardner Petroleum	1 Kidwell	21-6N-10E	3700	3800		0.29		224						
Gardner Petroleum	1 Kidwell	21-6N-10E	3800	3900		0.37		336						
Gardner Petroleum	1 Kidwell	21-6N-10E	3900	4000		0.29		275						
Gardner Petroleum	1 Kidwell	21-6N-10E	4000	4100		0.35		275						
Gardner Petroleum	1 Kidwell	21-6N-10E	4100	4200		0.25		275						
Gardner Petroleum	1 Kidwell	21-6N-10E	4200	4300		0.30		275						
Gardner Petroleum	1 Kidwell	21-6N-10E	4300	4400		0.41		246						
Gardner Petroleum	1 Kidwell	21-6N-10E	4400	4500		0.35		317						
Gardner Petroleum	1 Kidwell	21-6N-10E	4500	4600		0.31		271						
Gardner Petroleum	1 Kidwell	21-6N-10E	4600	4700		0.29		273						
Gardner Petroleum	1 Kidwell	21-6N-10E	4700	4800		0.23		339						
Gardner Petroleum	1 Kidwell	21-6N-10E	4800	4900		0.54		361						
Gardner Petroleum	1 Kidwell	21-6N-10E	4900	5000		0.67		331						
Gardner Petroleum	1 Kidwell	21-6N-10E	5000	5100		0.27		332						

Table 4, continued.

Operator	Well & lease	Location (section-township-range)	Top depth (ft)	Bottom depth (ft)	Lithology	TOC	TAI	TMAX	Maturity	Algal %	Am %	Herb %	Woody %	Inert %
Gardner Petroleum	1 Kidwell	21-6N-10E	5100	5200		0.31		273						
Gardner Petroleum	1 Kidwell	21-6N-10E	5200	5300		0.31		274						
Gardner Petroleum	1 Kidwell	21-6N-10E	5300	5400		0.44		296						
Gardner Petroleum	1 Kidwell	21-6N-10E	5400	5500		0.50		345						
Gardner Petroleum	1 Kidwell	21-6N-10E	5500	5600		0.22		264						
Gardner Petroleum	1 Kidwell	21-6N-10E	5600	5700		0.39		226						
Gardner Petroleum	1 Kidwell	21-6N-10E	5700	5800		0.50		267						
Gardner Petroleum	1 Kidwell	21-6N-10E	5800	5900		0.36		339						
Gardner Petroleum	1 Kidwell	21-6N-10E	5900	6000		0.31		348						
Houston Oil & Minerals	14-28 Federal	28-6N-10E	5190	5270	sh	0.12		371						
Houston Oil & Minerals	14-28 Federal	28-6N-10E	5560	5610	ss (0.40), sh (0.60)	0.1		260						
Houston Oil & Minerals	14-28 Federal	28-6N-10E	5700	5750	ss (0.40), sh (0.60)	0.4		296						
Houston Oil & Minerals	14-28 Federal	28-6N-10E	5940	6000	sh (0.50), anhy (0.50)	0.22		265						
Houston Oil & Minerals	14-28 Federal	28-6N-10E	6300	6340	ss (0.50), sh (0.50)	0.14		418						
Houston Oil & Minerals	14-28 Federal	28-6N-10E	6510	6550	ss (0.30), sh (0.70)	1.73		420						
Houston Oil & Minerals	14-28 Federal	28-6N-10E	6840	6880	slst	0.12		428						
Houston Oil & Minerals	14-28 Federal	28-6N-10E	7200	7260	ss, slst	0.63		364						
Houston Oil & Minerals	14-28 Federal	28-6N-10E	7310	7380	ss, slst	0.33		384						
Houston Oil & Minerals	14-28 Federal	28-6N-10E	7590	7640	ss, slst	0.58		375						
Houston Oil & Minerals	14-28 Federal	28-6N-10E	7900	7970	ss, slst	0.38		289						
Houston Oil & Minerals	14-28 Federal	28-6N-10E	8140	8220	slst	0.47		312						
Houston Oil & Minerals	14-28 Federal	28-6N-10E	8330	8380	ss (0.40), sh (0.60)	0.86		408						
Houston Oil & Minerals	14-28 Federal	28-6N-10E	8500	8590	ss (0.40), sh (0.60)	0.58		323						
Blue Quail Energy	1 Addison	13-2N-7E	3250	3300	sh	0.13	3.0	233	mature	0	0	36	28	36
Blue Quail Energy	1 Addison	13-2N-7E	3500	3550	sh	0.16	3.0	245	mature	0	0	36	28	36
Blue Quail Energy	1 Addison	13-2N-7E	3750	3800	sh	0.13	3.2	267	mature	0	9	33	25	33
Blue Quail Energy	1 Addison	13-2N-7E	3900	3950	sh	0.52	3.2	482	mature	0	0	36	28	36
Blue Quail Energy	1 Addison	13-2N-7E	4230	4280	sh	0.96	2.4	475	moderately mature	0	16	41	16	27
MAR Oil & Gas	1 Estes	35-5N-8E	1460	1550	sh	0.17	1.9	270	moderately immature	0	0	44	12	44
MAR Oil & Gas	1 Estes	35-5N-8E	1950	2030	sh	0.12	2.2	257	moderately mature	0	0	46	27	27
MAR Oil & Gas	1 Estes	35-5N-8E	2090	2150	ls	0.04	2.2	194	moderately mature	0	57	43	0	0
MAR Oil & Gas	1 Estes	35-5N-8E	2110	2160	ls	0.83	2.2	460	moderately mature	0	9	25	33	33
MAR Oil & Gas	1 Estes	35-5N-8E	2450	2550	ls	0.14	2.3	338	moderately mature	0	44	44	0	12
MAR Oil & Gas	1 Estes	35-5N-8E	2700	2770	ls	0.79	2.3	426	moderately mature	0	0	28	36	36
Analyses of Abo Formation (Permian: Wolfcampian)														
Sun	1 Bingham State*	23-5S-5E	1120	1140		0.07								
Sun	1 Bingham State*	23-5S-5E	1140	1160		0.07								
Sun	1 Bingham State*	23-5S-5E	1240	1270		0.13								
Virgle Landreth	1 Panhandle*	23-4S-6E	1120	1160		0.13								

Table 4, continued.

Operator	Well & lease	Location (section-township-range)	Top depth (ft)	Bottom depth (ft)	Lithology	TOC	TAI	TMAX	Maturity	Algal %	Am %	Herb %	Woody %	Inert %
Virgle Landreth	1 Panhandle*	23-4S-6E	1220	1260		0.08								
Virgle Landreth	1 Panhandle*	23-4S-6E	1390	1430		0.04								
Virgle Landreth	1 Panhandle*	23-4S-6E	1570	1610		0.10								
Virgle Landreth	1 Panhandle A*	28-4S-6E	900	930		0.19								
Virgle Landreth	1 Panhandle A*	28-4S-6E	980	1010		0.22								
Virgle Landreth	1 Panhandle A*	28-4S-6E	1230	1270		0.06								
Virgle Landreth	1 Panhandle A*	28-4S-6E	1510	1540		0.07								
Superior	28-31 Blackwell	31-6N-11E	970	1000		0.09		320						
Superior	28-31 Blackwell	31-6N-11E	1000	1100		0.08		324						
Superior	28-31 Blackwell	31-6N-11E	1100	1200		0.17		321						
Superior	28-31 Blackwell	31-6N-11E	1200	1300		0.11		330						
Superior	28-31 Blackwell	31-6N-11E	1300	1400		0.11		388						
Superior	28-31 Blackwell	31-6N-11E	1400	1500		0.12		269						
Superior	28-31 Blackwell	31-6N-11E	1500	1600		0.14		269						
Superior	28-31 Blackwell	31-6N-11E	1600	1700		0.06		269						
Superior	28-31 Blackwell	31-6N-11E	1700	1800		0.10		269						
Superior	28-31 Blackwell	31-6N-11E	1800	1900		0.07		268						
Superior	28-31 Blackwell	31-6N-11E	1900	2000		0.11		268						
Olsen	1 Means	27-7N-9E	300	400		0.11		343						
Olsen	1 Means	27-7N-9E	400	500		0.11		263						
Olsen	1 Means	27-7N-9E	500	600		0.11		263						
Olsen	1 Means	27-7N-9E	600	700		0.15		251						
Olsen	1 Means	27-7N-9E	700	800		0.60		281						
Olsen	1 Means	27-7N-9E	800	900		0.05		235						
Olsen	1 Means	27-7N-9E	900	1000		0.05		223						
Olsen	1 Means	27-7N-9E	1000	1100		0.06		269						
Olsen	1 Means	27-7N-9E	1100	1200		0.10		309						
Olsen	1 Means	27-7N-9E	1200	1300		0.16		220						
Olsen	1 Means	27-7N-9E	1300	1400		0.13		254						
Olsen	1 Means	27-7N-9E	1400	1500		0.16		253						
Gardner Petroleum	1 Kidwell	21-6N-10E	1300	1400		0.14		270						
Gardner Petroleum	1 Kidwell	21-6N-10E	1400	1500		0.17		259						
Gardner Petroleum	1 Kidwell	21-6N-10E	1500	1600		0.16		224						
Gardner Petroleum	1 Kidwell	21-6N-10E	1600	1700		0.12		224						
Gardner Petroleum	1 Kidwell	21-6N-10E	1700	1800		0.12		221						
Gardner Petroleum	1 Kidwell	21-6N-10E	1800	1900		0.12		222						
Gardner Petroleum	1 Kidwell	21-6N-10E	1900	2000		0.17		270						
Gardner Petroleum	1 Kidwell	21-6N-10E	2000	2100		0.17		300						
Gardner Petroleum	1 Kidwell	21-6N-10E	2100	2200		0.14		325						
Gardner Petroleum	1 Kidwell	21-6N-10E	2200	2300		0.12		272						
Gardner Petroleum	1 Kidwell	21-6N-10E	2300	2400		0.14		271						
Gardner Petroleum	1 Kidwell	21-6N-10E	2400	2500		0.18		272						
Gardner Petroleum	1 Kidwell	21-6N-10E	2500	2600		0.40		291						
Gardner Petroleum	1 Kidwell	21-6N-10E	2600	2700		0.33		363						
Gardner Petroleum	1 Kidwell	21-6N-10E	2700	2800		0.37		272						
Gardner Petroleum	1 Kidwell	21-6N-10E	2800	2900		0.21		281						
Gardner Petroleum	1 Kidwell	21-6N-10E	2900	3000		0.20		275						

Table 4, continued.

Operator	Well & lease	Location (section-township-range)	Top depth (ft)	Bottom depth (ft)	Lithology	TOC	TAI	TMAX	Maturity	Algal %	Am %	Herb %	Woody %	Inert %
Blue Quail Energy	1 Addison	13-2N-7E	1850	1900	sh	0.03	2.5	228	moderately mature	0	28	57	0	15
Blue Quail Energy	1 Addison	13-2N-7E	2850	2900	sh	0.09	2.9	273	mature	0	0	36	28	36
MAR Oil & Gas	1 Estes	35-5N-8E	530	600	sh	0.09	1.5	294	immature	0	14	57	0	29
MAR Oil & Gas	1 Estes	35-5N-8E	900	1000	sh	0.07	1.6	270	immature	0	14	57	0	29
Analyses of Yeso Formation (Permian: Leonardian)														
Transocean Oil Co.	1 McKee	4-13N-9E	5600	5610	ds (0.20), sh (0.80)	0.30	2.4	414	moderately mature	0	36	28	18	18
Transocean Oil Co.	1 McKee	4-13N-9E	5610	5620	ds (0.20), sh (0.80)	0.35	2.4	410	moderately mature	0	28	56	0	16
Virgle Landreth	1 Panhandle A*	23-4S-6E	530	550		0.29								
Gardner Petroleum	1 Kidwell	21-6N-10E	1280	1300		0.14		228						
Blue Quail Energy	1 Addison	13-2N-7E	950	980	sh	0.05	2.4	309	moderately mature	0	25	50	0	25
Blue Quail Energy	1 Addison	13-2N-7E	1220	1240	ls	0.11	2.4	265	moderately mature	0	22	44	12	22
Blue Quail Energy	1 Addison	13-2N-7E	1400	1450	sh	0.04	2.4	343	moderately mature	0	0	72	0	28

Index

(Italics denotes discussion.)

Selected conversion factors*

TO CONVERT	MULTIPLY BY	TO OBTAIN
Length		
inches, in	2.540	centimeters, cm
feet, ft	3.048×10^{-1}	meters, m
yards, yds	9.144×10^{-1}	m
statute miles, mi	1.609	kilometers, km
fathoms	1.829	m
angstroms, Å	1.0×10^{-8}	cm
Å	1.0×10^{-4}	micrometers, µm
Area		
in^2	6.452	cm^2
ft^2	9.29×10^{-2}	m^2
yds^2	8.361×10^{-1}	m^2
mi^2	2.590	km^2
acres	4.047×10^{3}	m^2
acres	4.047×10^{-1}	hectares, ha
Volume (wet and dry)		
in^3	1.639×10^{1}	cm^3
ft^3	2.832×10^{-2}	m^3
yds^3	7.646×10^{-1}	m^3
fluid ounces	2.957×10^{-2}	liters, l *or* L
quarts	9.463×10^{-1}	l
U.S. gallons, gal	3.785	l
U.S. gal	3.785×10^{-3}	m^3
acre-ft	1.234×10^{3}	m^3
barrels (oil), bbl	1.589×10^{-1}	m^3
Weight, mass		
ounces avoirdupois, avdp	2.8349×10^{1}	grams, gr
troy ounces, oz	3.1103×10^{1}	gr
pounds, lb	4.536×10^{-1}	kilograms, kg
long tons	1.016	metric tons, mt
short tons	9.078×10^{-1}	mt
oz mt^{-1}	3.43×10^{1}	parts per million, ppm
Velocity		
ft sec^{-1} (= ft/sec)	3.048×10^{-1}	m sec^{-1} (= m/sec)
mi hr^{-1}	1.6093	km hr^{-1}
mi hr^{-1}	4.470×10^{-1}	m sec^{-1}

TO CONVERT	MULTIPLY BY	TO OBTAIN
Pressure stress		
lb in^{-2} (= lb/in^2), psi	7.03×10^{-2}	kg cm^{-2} (= kg/cm^2)
lb in^{-2}	6.804×10^{-2}	atmospheres, atm
lb in^{-2}	6.895×10^{3}	newtons (N)/m^2, N m^{-2}
atm	1.0333	kg cm^{-2}
atm	7.6×10^{2}	mm of Hg (at 0° C)
inches of Hg (at 0° C)	3.453×10^{-2}	kg cm^{-2}
bars, b	1.020	kg cm^{-2}
b	1.0×10^{6}	dynes cm^{-2}
b	9.869×10^{-1}	atm
b	1.0×10^{-1}	megapascals, MPa
Density		
lb in^{-3} (= lb/in^3)	2.768×10^{1}	gr cm^{-3} (= gr/cm^3)
Viscosity		
poises	1.0	gr cm^{-1} sec^{-1} *or* dynes cm^{-2}
Discharge		
U.S. gal min^{-1}, gpm	6.308×10^{-2}	l sec^{-1}
gpm	6.308×10^{-5}	m^3 sec^{-1}
ft^3 sec^{-1}	2.832×10^{-2}	m^3 sec^{-1}
Hydraulic conductivity		
U.S. gal day^{-1} ft^{-2}	4.720×10^{-7}	m sec^{-1}
Permeability		
darcies	9.870×10^{-13}	m^2
Transmissivity		
U.S. gal day^{-1} ft^{-1}	1.438×10^{-7}	m^2 sec^{-1}
U.S. gal min^{-1} ft^{-1}	2.072×10^{-1}	l sec^{-1} m^{-1}
Magnetic field intensity		
gausses	1.0×10^{5}	gammas
Energy, heat		
British thermal units, BTU	2.52×10^{-1}	calories, cal
BTU	1.0758×10^{2}	kilogram-meters, kgm
BTU lb^{-1}	5.56×10^{-1}	cal kg^{-1}
Temperature		
°C + 273	1.0	°K (Kelvin)
°C + 17.78	1.8	°F (Fahrenheit)
°F – 32	5/9	°C (Celsius)

Divide by the factor number to reverse conversions.
Exponents: for example 4.047×10^{3} (see acres) = 4,047; 9.29×10^{-2} (see ft^2) = 0.0929.

Editors: Jane Love
Nancy Gilson

Drafter: Rebecca J. Titus

Typeface: Palatino

Presswork: 40 inch Komori
Four Color Offset

Binding: Saddlestitched with softbound cover

Paper: Cover on 12-pt. Kivar Text
on 70-lb White Matte

Ink: Cover—PMS 320, 4-color process
Text—Black

Quantity: 1,000